SKB

TECHNICAL REPORT 97-06

ÄSPÖ HRL – Geoscientific evaluation 1997/5

Models based on site characterization 1986–1995

Ingvar Rhén (ed.)[1], Gunnar Gustafson[2], Roy Stanfors[3], Peter Wikberg[4]

1 VBB Viak, Göteborg
2 VBB Viak/CTH, Göteborg
3 RS Consulting, Lund
4 SKB, Stockholm

October 1997

SVENSK KÄRNBRÄNSLEHANTERING AB
SWEDISH NUCLEAR FUEL AND WASTE MANAGEMENT CO
P.O.BOX 5864 S-102 40 STOCKHOLM SWEDEN
PHONE +46 8 459 84 00
FAX +46 8 661 57 19

ÄSPÖ HRL - GEOSCIENTIFIC EVALUATION 1997/5

MODELS BASED ON SITE CHARACTERIZATION 1986-1995

Ingvar Rhén (ed.)[1], Gunnar Gustafson[2], Roy Stanfors[3], Peter Wikberg[4]

1 VBB Viak, Göteborg
2 VBB Viak/CTH, Göteborg
3 RS Consulting, Lund
4 SKB, Stockholm

October 1997

Information on SKB technical reports from1977-1978 (TR 121), 1979 (TR 79-28), 1980 (TR 80-26), 1981 (TR 81-17), 1982 (TR 82-28), 1983 (TR 83-77), 1984 (TR 85-01), 1985 (TR 85-20), 1986 (TR 86-31), 1987 (TR 87-33), 1988 (TR 88-32), 1989 (TR 89-40), 1990 (TR 90-46), 1991 (TR 91-64), 1992 (TR 92-46), 1993 (TR 93-34), 1994 (TR 94-33), 1995 (TR 95-37) and 1996 (TR 96-25) is available through SKB.

ÄSPÖ HRL

GEOSCIENTIFIC EVALUATION 1997/5

MODELS BASED ON SITE CHARACTERIZATION 1986-1995

Ingvar Rhén (ed), VBB Viak, Göteborg
Gunnar Gustafson, VBB Viak/CTH, Göteborg
Roy Stanfors, RS Consulting, Lund
Peter Wikberg, SKB, Stockholm

October 1997

Keywords: site characterization, Äspö geological model, mechanical stability model, hydrochemistry model, hydrogeological model, transport of solutes model, conceptual models.

FOREWORD

The booklet *Äspö Hard Rock Laboratory - 10 years of research*, available from SKB, provides the reader with a popular review of the achievements. This report is No. 5 of six Technical Reports summarizing the pre-investigation and construction phase of the Äspö Hard Rock Laboratory.

The reports are:

1 Stanfors R, Erlström M, Markström I.
Äspö HRL - Geoscientific evaluation 1997/1.
Overview of site characterization 1986-1995
SKB TR 97-02.

2 Rhén I (ed), Bäckblom (ed), Gustafson G, Stanfors R, Wikberg P.
Äspö HRL - Geoscientific evaluation 1997/2.
Results from pre-investigations and detailed site characterization.
Summary report.
SKB TR 97-03.

3 Stanfors R, Olsson P, Stille H .
Äspö HRL - Geoscientific evaluation 1997/3.
Results from pre-investigations and detailed site characterization.
Comparison of predictions and observations.
Geology and Mechanical stability.
SKB TR 97-04.

4 Rhén I, Gustafson G, Wikberg P.
Äspö HRL - Geoscientific evaluation 1997/4.
Results from pre-investigations and detailed site characterization.
Comparison of predictions and observations.
Hydrogeology, Groundwater chemistry and Transport of solutes.
SKB TR 97-05.

5 Rhén I (ed), Gustafson G, Stanfors R, Wikberg P.
Äspö HRL - Geoscientific evaluation 1997/5.
Models based on site characterization 1986-1995.
SKB TR 97-06.

6 Almén K-E (ed), Olsson P, Rhén I, Stanfors R, Wikberg P.
Äspö Hard Rock Laboratory.
Feasibility and usefulness of site investigation methods.
Experience from the pre-investigation phase.
SKB TR 94-24.

The background and objectives of the project are presented in a background report to SKB R&D Programme 1989 (Hard Rock Laboratory), which contains a detailed description of the HRL project.

The purpose of this report, No. 5, is to present the new models of the Äspö HRL, the concepts and some comments on how the models have developed based on data from the pre-investigation and construction phases of Äspö HRL. Parts of the geological and hydrogeological models in *Report 5* are based on results from the SKB Palaeohydrogeological programme, and these results are also presented in reports concerning that programme. An overview of all the investigations performed is summarized in *Report 1*. The evaluation of the pre-investigation is presented in *Reports 2-4*. *Report 6* outlines the usefulness and feasibility of pre-investigation methods.

October 1997

Ingvar Rhén Gunnar Gustafson Roy Stanfors

Peter Wikberg

ABSTRACT

The pre-investigations for the Äspö Hard Rock Laboratory were started in 1986 and involved extensive field measurements, aimed at characterizing the rock formations with regard to geology, geohydrology, hydrochemistry and rock mechanics.

Predictions for the excavation phase were made prior to excavation of the laboratory which was started in the autumn of 1990. The predictions concern five key issues: lithology and geological structures, groundwater flow, hydrochemistry, transport of solutes and mechanical stability.

During 1996 the results from the pre-investigations and the excavation of the Äspö Hard Rock Laboratory were evaluated and were compiled in geological, mechanical stability, geohydrological, groundwater chemical and transport-of-solutes models. The model concepts and the models of 1996 are presented in this report. The model developments from the pre-investigation phase up to the models made 1996 are also presented briefly.

ABSTRACT (in Swedish)

Förundersökningarna för Äspölaboratoriet startade 1986 med syfte att karakterisera berget geologiskt, hydrogeologiskt, grundvattenkemiskt och bergmekaniskt.

Innan byggandet av Äspölaboratoriet startade hösten 1990 gjordes prediktioner för byggfasen av laboratoriet avseende fem huvudfrågor: litologi, geologiska strukturer, grundvattenflöde, grundvattenkemi, transport av lösta ämnen och mekanisk stabilitet.

Under 1996 har resultaten från förundersökningarna och byggfasen av Äspölaboratoriet utvärderats och sammanfattats i geologiska, bergmekaniska, geohydrologiska, grundvattenkemiska modeller samt modeller för transport av lösta ämnen. I denna rapport presenteras de koncept som modellerna baseras på samt de nya modellerna.Vidare presenteras kortfattat modellutvecklingen från förundersökningfasen fram till modellerna upprättade 1996.

CONTENTS

SUMMARY

MODELS ON REGIONAL SCALE

Investigations

For the geological-structural model, comprising one lithological and one structural model, airborne geophysical (magnetic, electromagnetic and radiometric) measurements were interpreted and lineament interpretation of terrain models was used to identify the major fracture zones and their extent. Some of the indicated fracture zones were also characterized by means of surface mapping, petrophysical measurement of rock samples and ground geophysics (gravity, refraction seismics, etc.).

Sources of preliminary geohydrological data were the water well archive at the Swedish Geological Survey (SGU), hydraulic tests performed in a few boreholes on the island of Ävrö and geohydrological investigations performed on the Simpevarp peninsula in conjunction with the construction of the power plants and the CLAB facility. During investigations for the Äspö HRL hydraulic tests in boreholes were performed in the Äspö, Hålö, Ävrö and Laxemar areas.

To obtain water chemistry information data from the water well archive for the whole of Kalmar County was compiled.

Lithological model

The main rocks in the Äspö area belong to the vast region of Småland-Värmland intrusions (or Trans-Scandinavian Granite-Porphyry Belt).

A number of massifs of basic rocks elongated E-W have been indicated by positive magnetic and gravity anomalies. Fine-grained irregular bodies and xenoliths of greenstone (old volcanites) were found as remnants within the granite mass.

Some circular/semi-circular structures in the area investigated are interpreted as granite diapirs. They are all represented by a more or less round, non-magnetic pattern and negative Bouger gravity anomalies. The Götemar and Uthammar anorogenic granites are two of these structures which have been interpreted as true diapirs.

Fine-grained greyish-red granite is common in the whole area. On and near Äspö, which has been mapped in detail, the fine-grained granite occurs both in smaller massifs and in dikes in the older rock.

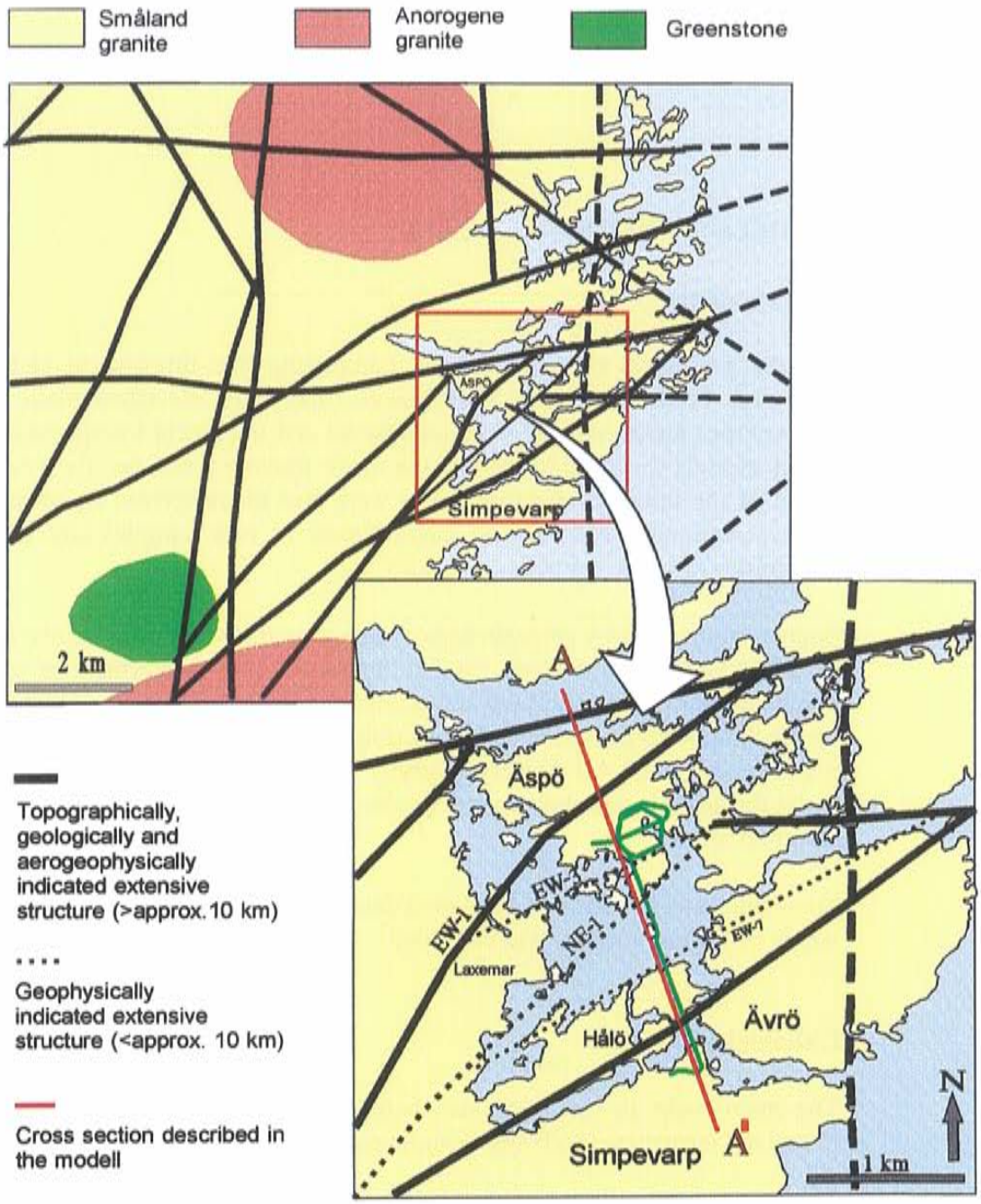

Figure 1. *Regional structural model of the Äspö area A-A': vertical section in Figures 2, 3 and 4.*

Structural model - Major discontinuities (major fracture zones)

Information from all geological and geophysical investigations support a tectonic picture dominated by one almost orthogonal system of major structures trending N-S and E-W and one trending NW and NE, all extending more than 10 km. They often coincide with some hundred-metre-wide low-magnetic zones with a central more intense fracture zone up to some tens of metres wide. *Figure 1.*

The structures trending E-W are mostly vertical or with a moderately low dip. A major structure trending NE-SW across the island of Äspö, is indicated by mylonites in outcrops and boreholes. According to a general interpretation most of the structures trending NE-SW are older than the systems trending N-S and E-W. Most of the structures trending N-S are probably younger than the ones trending E-W.

The depth of most of the major structures is estimated to be at least 1500 m to several kilometres.

MODELS ON A SITE SCALE

Investigations

The site scale model covers some 1 km^2 of Äspö island. The framework for the site scale modelling was the existing regional scale model. Refinement of the site scale model was mainly done during the siting stage and the site description stage when extensive investigation data were gathered. Further detailing of the site scale model was done during the prediction stage, based on results from further deep borehole investigations. The final refinement was based on data from tunnel documentation after excavation.

Lithological model

Four main rock types - Äspö diorite, Småland (Ävrö) granite, greenstone and fine-grained granite make up most of the rock mass in the Äspö tunnel area (see *Figure 2*). Äspö diorite and Småland (Ävrö) granite are two varieties of the country rock called "Småland granite". Rocks belonging to the Äspö diorite group are by far the most common within the Äspö area, both on the surface and in the tunnel. The rocks are usually grey to reddish grey, medium-grained, and contain more or less scattered, large crystals of potassium feldspar. Granodiorites and quartz monzonites are most common, but there are also some tonalites, quartz diorites and quartz monzonites included in this group. Age determination gave a well defined age of 1804 ±3 million years for the Äspö diorite.

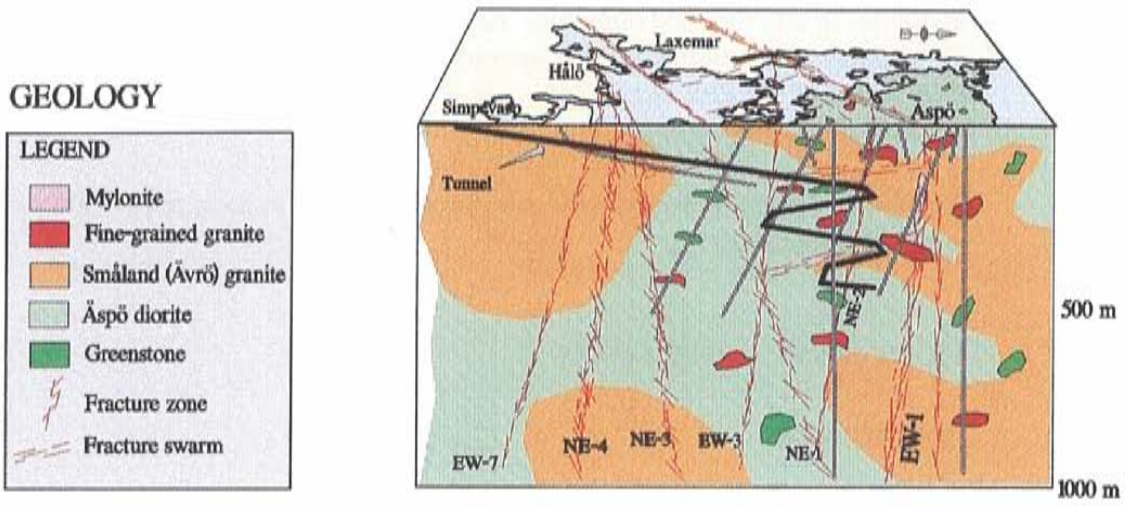

Figure 2. *Lithological Model 96 showing domains of Äspö diorite and Småland (Ävrö) granite with inclusions of fine-grained granites, greenstone and mylonite The structural model shows major fracture zones (width > 5 m) and fracture swarms. Cored boreholes near the vertical section A-A´ are coloured grey. EW-7 etc is the fracture zone ID. Vertical section A-A´ shown in Figure 1.*

Macroscopically, the Småland (Ävrö) granite differs from the previous group in its brighter, sometimes distinctly more reddish colour. The amount of potassium feldspar phenocrysts is lower and the crystals are much more irregularly distributed. In many places the Småland (Ävrö) granite can be seen to cut the Äspö diorite, which implies that the former is younger. The age difference between the two groups is probably very small. The Småland (Ävrö) granite - which is exposed on Ävrö south of Äspö and on Äspö over the southern part of the spiral probably extends northwards folded beneath the Äspö diorite.

The greenstones - fine-grained (probably of volcanic origin) and medium to coarse-grained greenstone (diorites to gabbros) are easily distinguished from the granitoid rocks by their very dark, greenish or greyish black colour. As a rule they occur as minor inclusions or irregular, often elongated bodies within the granitoids and dioritoids following the common E-W foliation trend within the area. Except the smallest inclusions, the greenstones are often intensely penetrated by fine-grained, granitic material.

Fine-grained granites occur rather frequently, both on the surface of the island of Äspö and its surroundings, as well as in the tunnel. From the surface mapping it is clear that many of the granites occur as dikes. The dike character is sometimes not very clear because of strong deformation in the fine-grained granites, which has obscured contacts.

The brittle deformation has caused a joint pattern in the fine-grained granites, often characterized by many short joints lying closely together, which divide the rock into small blocks. This is quite different from the pattern in the medium to coarse-grained granitoids where joints are much more widely spaced. No significant difference has been found between the joint patterns on outcrops surface and in the tunnel.

Most of the greenstone has the character of inclusions but dikes are also mapped mostly trending EW to the NE. All the rock mass is veined by fine-grained granite but the number of veins in the Småland (Ävrö) granite in the tunnel is sparse compared with the number of veins and dikes in the Äspö diorite. Most of the dikes of fine-grained granite trending NE confirm the idea that the fine-grained granite is closely related to the Småland (Ävrö) granite which is obviously younger than the Äspö diorite.

Structural model

The geological-structural model describes the geometrical distribution and character of discontinuities in a rock volume. Discontinuity is the general term for any mechanical feature in a rock mass having zero or low tensile strength. It is the collective term for most fractures, weak schistosity planes, weakness (fracture) zones and faults. During pre-investigation and tunnel mapping of the Äspö HRL discontinuities were divided into **fracture zones** (major and minor) and small scale **fractures** in the rock mass between fracture zones.

An almost vertical, penetrating foliation trending NE-ENE is the most dominant structural element in the 1700-1800 million year old Äspö granitoids and seems to be the oldest sign of the ductile deformation related to the sub-horizontal NNW-SSE compression. This deformation is also marked by the orientation of mafic sheets often back-veined by two or three generations of fine-grained granites.

Strong foliation and mylonites are common in the Äspö shear zone - where more than 10-metre-long bodies of mylonite occur trending E-W and dipping steeply to the north. Regional evidence suggests that the E-W trending mylonites are older than those trending NE. The first brittle faults probably developed in the region in response to the emplacement of younger granites. These faults and older ductile zones were reactivated several times. Fracture zones on Äspö have a wide range of orientations and styles and most of them reactivate older structures. The style of each fracture zone tends to depend on the nature of any older structure being reactivated, such as EW gneissic zones, mylonites trending NE or E-W and gently dipping alteration zones. Fracture zones trending N, NE or E-W on Äspö normally had ductile precursors whereas those trending NW apparently did not.

EW-7 was estimated to trend almost parallel to the main lineament trending ENE-NE and geophysical anomalies in the Hålö-Äspö area. Only one branch of EW-7 was indicated in borehole (KBH02). In the tunnel EW-7 consists of

one set of fractures trending NNE - which are the most conductive structures - and one fracture set trending WNW.

NE-4 was indicated during pre-investigations by geophysical methods (ground magnetics and seismic refraction) and borehole data (KBH02) and estimated to consist of three branches trending NE. The dominating rock type in the zone - which is found to consist of two more or less continuous branches - is Småland (Ävrö) granite with inclusions of mylonite and greenstone.

NE-3 was indicated by ground magnetics and seismic refraction and confirmed in borehole KBH02 in the pre-investigation phase. After excavation, NE-3 was found to be approximately 49 m wide in the tunnel. Fine-grained granite is the dominating rock type with some intersections of Småland (Ävrö) granite and greenstone.

NE-1 was clearly indicated by geophysics and several boreholes in the pre-investigations and was estimated to be composed of three branches. All three branches are connected to a rather complex rock mass with Äspö diorite, fine-grained granite and greenstone. The two southernmost branches, trending NE and dipping NW, can be described as highly fractured and more or less water-bearing. The northern NW-dipping branch, which is approximately 28 m wide in the tunnel, is the most intense part of NE-1 and highly water-bearing.

The fracture zone EW-3 was very well indicated topographically, and geophysically (magnetic, seismic and electric) and in core boreholes KAS06 and KAS07 during the pre-investigations and estimated to be approximately 10 m wide. In the tunnel EW-3 is found to be approximately 14 m wide and consisting of a 2-3 m wide crushed central section connected to a contact between Äspö diorite and fine-grained granite.

According to the prediction fracture zone NE-2, trending NE/ENE, should be regarded as the southern part of the main Äspö Shear zone and was expected to follow a somewhat winding course. The dip of NE-2 was estimated to change from steeply northwards in the NE part to steeply southeast in the SW part of the zone and to be only moderately hydraulically conductive. The southwestern part of the zone NE-2 was judged to be 'probable'. In the tunnel NE-2 has been demonstrated to be a 'minor' fracture zone dipping to the SE.

The fracture zone EW-1 was early indicated by the airborne geophysical survey and the lineament interpretation. Ground geophysical investigation confirmed the extent of EW-1 in more detail. In the first drilling campaign a cored borehole (KAS04) - inclined at 60° to the SE crossed the zone. EW-1 is very well indicated topographically (50-100 m wide depression in the ground extending many hundreds of metres), geophysically (low-magnetic and low-resistivity zone 200-300 m wide), geologically (outcrops in a trench with mylonites and crushed sections) and in boreholes (mylonites and many highly fractured and altered sections in drill cores). Fracture zone EW-1 can be regarded as a part of the about 300 m wide low-magnetic zone (Äspö shear zone), trending NE, which divides Äspö into two main blocks.

Gently dipping (<35°) fracture zones (GDF) on the surface of Äspö were first described by and interpreted as superficial stress-relief to the surface exaggerated by the retreating Quaternary ice sheets. Further studies of the surface geology revealed the presence of three gentle thrusts on Äspö striking E-W and dipping N all of which appeared to be associated with early gently dipping gneiss zones, thrusts and high fault scarps. Interpretations based on seismic reflections suggested the presence of gently dipping fracture zones with a 90-133 m spacing at depth. Two well defined gently dipping minor fracture zones were found in the tunnel. The first one intersects the tunnel at chainage 220 m. It consists of anastomosing fractures striking NW and dipping 25°SW with a spacing of less than 10 cm. The width of the zone is 0.5 m. The second and most prominent gently dipping fracture zone appears at chainage 1744 m down to 1850 m. Intense fracturing trending NE and dipping 32°SE, subparallel to the tunnel for almost a hundred metres.

A number of minor fracture zones striking approximately NNW to NNE have been mapped on outcrops in Äspö. More or less extensive, they seem to branch out in an en-échelon pattern across the island. Only a few of them are topographically significant but normally too narrow to be geologically unambiguously indicated. All these minor fracture zones were described under the designation 'NNW' in the predictions. The different sub-zones, expected to be 0.1-5 m wide, in the system 'NNW' were predicted to be 'possible-probable' and their predicted position in the tunnel very approximate. The mapping underground found several indications of minor fracture zones, generally not wider than 1 m. The water-bearing minor fracture zone NNW-4W is an example of a minor fracture zone which is indicated in the tunnel by three intersections at 2020 m, 2120 and 2914 m, with 5-10 cm wide fractures in this metre-wide section of cataclastic granite filled by grout.

Thorough analyses of the small scale fractures in the rock mass at Äspö have been made. The data base consists of more than ten thousand fracture observations. A special study with the main aim of synthesizing the structural geology of water-bearing fractures has been made. Most fractures mapped at the Äspö HRL (all fractures >1 m in the tunnel except fractures in 'fracture zones') fall into four clusters. Three are steep and strike NS, NNW and WNW; a fourth cluster is subhorizontal. The array of fractures coated with the mineral assemblage chlorite-calcite can be represented by the same four sets. Most of the mapped fractures containing water are arranged into a single intense cluster of steep fractures striking WNW. A succession of fracture fillings of decreasing age has been proposed and includes: quartz, epidote, red staining, chlorite, Fe-oxy-hydroxides and calcite. The arrays of mineralized fractures differ considerably with mineral infilling. Younger arrays are more complex due to the superposition of new fracture sets and reactivation of old sets. Repeated and sequential reactivation of the same faults has been demonstrated by superposition of different mineral coatings. Fractures trace lengths are log-normally distributed in all rock types. Fracture trace lengths do not vary with rock type. Mapped waterbearing fractures generally have coatings enriched in epidote, quartz and Fe-oxides. Fractures with injected grout are steep, strike WNW and generally longer than other fractures.

Hydraulic conductor domains

The geometry of the hydraulic conductor domains is mainly defined by the major fracture zones described above. The minor fracture zones in the 'NNW-system' are also important conductors. A few hydraulic conductor domains were also added to the model in order to explain some of the responses obtained in the interference tests. A simplified model of the hydraulic conductor domains was made by fitting planes to the observations at the surface and in the boreholes.

The evaluated transmissivities are generally in the range 10^{-6}-10^{-4} m^2/s with a median of about 10^{-5} m^2/s. The greatest transmissivities for these larger features are for the hydraulic conductor domains below the Baltic Sea and for the minor fracture zone NNW-4. The largest transmissivity is approximately $3 \cdot 10^{-4}$ m^2/s for hydraulic conductor domain NE-1.

Hydraulic rock mass domain

The Äspö area is divided into five groups of Site hydraulic Rock mass Domains (SRD) with different hydraulic properties:

- SRD 1: Northern part of Äspö , bounded to the south by the Northern part of EW-1
- SRD 2 : Volume bounded by the northern and southern parts of EW-1.
- SRD 3 :Southern part of Äspö bounded to the north by the southern part of EW-1 and to the south by EW-3.
- SRD 4 : South of EW-3.
- SRD 5: A Fine-grained granite domain in the middle of the tunnel spiral at a depth of about 350 m.

Outside Äspö, SRD1-4 are assumed to be valid within an area bounded by EW-7 to the south and some 100 m outside Äspö to the west, north and east.

The data based on the injection tests with 3 m packer interval show that the estimated median hydraulic conductivity for the rock mass, where data for the deterministic hydraulic conductors were excluded, is highest in within the discontinuity EW-1 (data from KAS04) and lowest on the southern part of Äspö. The tests on the test scales 3, 30 and 100 m do not indicate a decreasing hydraulic conductivity with depth in the interval 0 - 500 m. Below level -600 m the hydraulic conductivity decreases on southern Äspö, but the result is only based on one borehole that is vertical. If the data from the 1700 m deep cored borehole KLX02 is included in the analysis the hydraulic conductivity seems to decrease below a depth of -600 m below sea level.

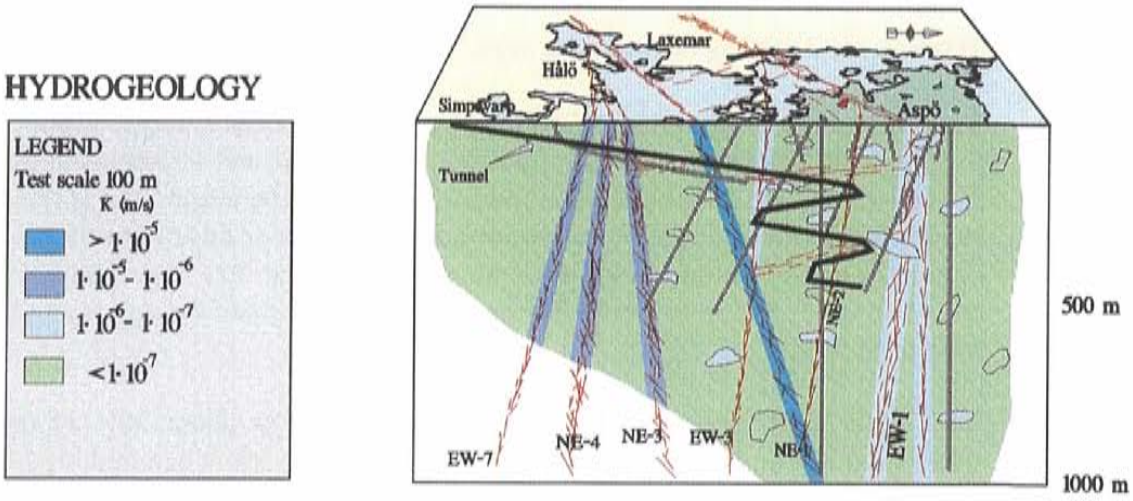

Figure 3. *Hydrogeological Model 96 showing the hydraulic conductivity of the major fracture zones and a typical range of hydraulic conductivity for the rock mass between the fracture zones. Widths of zones shown in figure are only approximate. Cored boreholes near the vertical section A-A´ are coloured grey. Inclusions of fine-grained granites, greenstone and mylonite are indicated in the figure (see Figure 2 for details concerning the lithology). Vertical section A-A´ is shown in Figure 1.*

An investigation of the structural geology of water-bearing fractures was made in the tunnel. It was found that the entire fracture system consists of four main sets. The mapped water-bearing fractures and the fractures filled with grout (from the pre-grouting ahead of the tunnel face) are dominated by a subvertical fracture set striking WNW-NW. The N-S and NNW subvertical sets are also present but these subvertical sets are less pronounced compared to the entire fracture set. The mapped grout-filled fractures should be a good indicator of the water conducting fractures, as the grouting was performed generally 5-15 m ahead of the tunnel face where the rock mass should be fairly undisturbed. This indicates that the hydraulic properties of the rock mass is probably anisotropic. Hydraulic tests in probe holes drilled along the tunnel during excavation indicate that subvertical fractures striking approximately WNW and N-S are more transmissive than the others. It is believed that, on a larger scale, the WNW and N-S fracture sets form the hydraulic conductors called "NNW".

Occasionally single water conducting fractures in the hydraulic rock mass domains can be very transmissive and cause high flow rates into drilled boreholes.

Hydraulic tests were performed in different test scales (length of tested borehole section). The results show that the evaluated effective hydraulic conducivities are dependent of the test scales.

Hydrological setting of the Äspö area

The land surface of Äspö is slightly undulating, with a maximum height of about 14 m, giving small drainage basins with some peatlands and sediments in the topographic lows. There are no perennial streams on the island. The surface water is drained to the sea by the peatlands, sediments or directly to the sea. The annual mean precipitation and temperature of the area are about 650 mm/year, and 6.5°C respectively. The annual sea level fluctuations are generally within ±0.5 m.

The water table elevation above the mean sea level is about 30% of the elevation of the topography above mean sea level, within a few hundred metres from the coast line. During the construction of the tunnel the elevation of the water table decreased, mainly on southern Äspö. The minimum water table elevation in 1995 was about 100 m below sea level.

Mechanical stability model

Based on the results from rock stress measurements in three boreholes on Äspö, the laboratory testing on core samples and geological pre-investigations a rock mechanics evaluation was made for the Äspö HRL. During excavation of the tunnel a number of overcoring rock stress measurements were made underground. Complementary laboratory tests of rock samples from the tunnel were also made.

During the site investigation phase, rock stress measurements were made in surface boreholes KAS02, KAS03 and KAS05. KAS02 and KAS05 were drilled almost vertically, within and below the rock volume later enveloped by the ramp loops. KAS03 is also near-vertical, but located some 500 m to the north-west of the ramp area. The surface borehole measurements employed both hydraulic fracturing and overcoring.

Concurrent with the excavation of the access ramp, overcoring measurements were made in a series of 12-18 m long, near-horizontal boreholes drilled from suitable locations along the ramp. The main objective was to evaluate predictions made prior to excavation. An additional objective was to provide background data required to establish stress ranges on a site scale.

The measurements prove a dominating NW-SE orientation of the maximum horizontal stress (σ_H), which corresponds to the prediction. The measurements made in the tunnel proved the presence of a considerably higher stress level than was anticipated, based on the measurements made in the deep surface boreholes. The estimated mean K_o-value, (K_o is the ratio between the maximum horizontal stress (σ_H) and the theoretical vertical stress (σ_V)) for all boreholes is 2.9, with the average for individual boreholes ranging between 1.7 and 4.0. Single measurements in the individual boreholes varied between 1.5 and 4.0. The maximum horizontal stress component proved to be significantly higher for the measurements made in the tunnel.

Since parts of the tunnel were located at a very considerable depth there was a possible risk of rock burst. Rock burst usually occurs at great depth where rock stresses are high, but it may also be observed at smaller depths under some conditions. Rock stress problems with frequent rock burst are very difficult to foresee with certainty.

It was predicted that no rock burst to just minor rock burst should occur and if rock burst should occur it would only be of minor intensity, like spalling and mainly connected to greenstone. However, the strength of the rock based on the laboratory testing has shown itself to be a little stronger than predicted. An updated prediction should thus indicate that minor spalling may occur both in the greenstone and diorite at depths greater than 400 m. No rock burst was observed during the tunnelling operation. Occasional cracking was heard after excavation and some tendency to spalling was noted. The rock burst problem was thus less than expected from the updated prediction. The result emphasises the difficulties of foreseeing rock burst activity.

Hydrochemical models

To obtain water chemical information data from the water well archive from the whole of Kalmar County was compiled at the start of the investigations.

The compilation of data showed a correlation between high bicarbonate content of the water and a thick soil cover on top of the bedrock. Another important correlation was that the salinity of the water increased with decreasing distance from the shore line. All other correlations were of low significance. Based on this the Äspö site groundwater could be expected to be saline. This was confirmed on a semi-regional scale, were data obtained from shallow, 100 m deep, boreholes drilled at Äspö, Laxemar and Ävrö, indicated a higher salinity at Äspö.

Site scale investigations included samples from sections isolated by packers in the deep cored boreholes on Äspö. Most of the sampling was done in the first three boreholes which penetrated the northern and the southern part of the island and intersected the Äspö shear zone in the middle of the island.

The objective of the models developed during the pre-investigation phase was to obtain an understanding of the complex nature of the Äspö site. From a hydrochemical point of view there was one specific situation which favoured the evaluation. The very large range of salinity, from surface freshwater with less than 100 mg/l of chloride to 12000 mg/l of chloride at a depth of 860 m. The large contrasts in salinity have unravelled many important features of the hydrogeochemical conditions.

On the average there was a linear increase in salinity with depth, with an increase of 1000 mg/l for each approximately 100 m. However, despite the linear increase in salinity, different water types could be distinguished. Glacial meltwater could be identified due to its very low oxygen-18 value, modern and

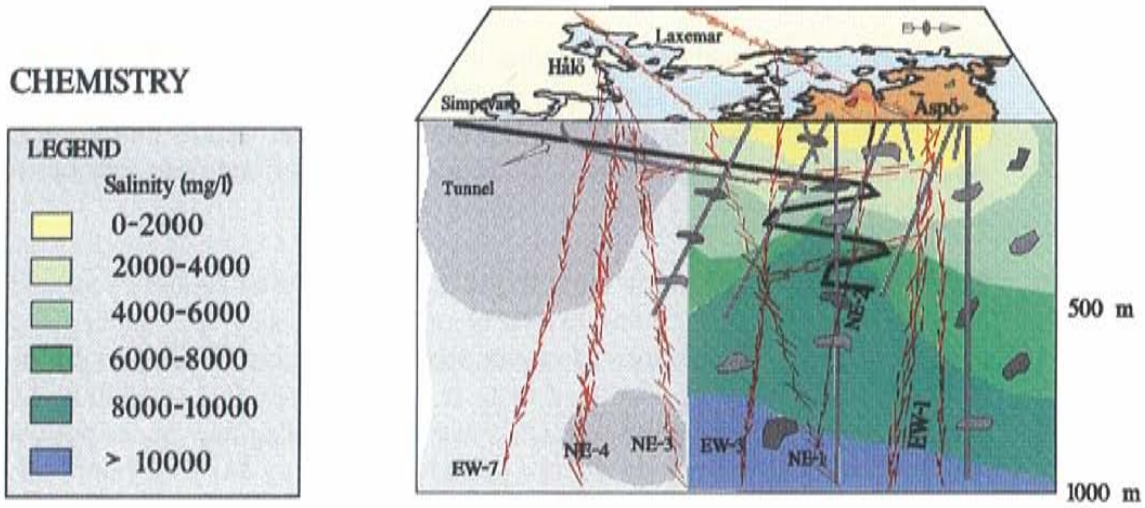

Figure 4. *Hydrochemical Model 96 showing the distribution of saline water in the Äspö area based on 3D interpolation of observations in borehole sections, the Baltic sea and the composition of the recharge on Äspö. Cored boreholes near the vertical section A-A´ are coloured grey. Inclusions of fine-grained granites, greenstone and mylonite are indicated in the figure (see Figure 2 for details concerning the lithology). Vertical section A-A´ is shown in Figure 1.*

old Baltic Sea water and meteoric freshwater were also distinguished based on their ratios of major components. At depths of more than 500 m the water has not been affected by the different stages of the Baltic Sea evolution since the last glaciation. This indicates that the water has been stagnant in the past 10 000 years, and probably for much longer time.

The sampled groundwater is in general reducing at depths exceeding a few tens of metres. However, in exceptional cases oxidizing conditions may prevail down to 100 m. Oxygen-rich surface water is rapidly becoming anoxic as it percolates into the rock due to microbial activity.

Bacterial activity has warranted several studies to fully understand the redox processes. It has been found that bacteria are important for establishing high dissolved iron and bicarbonate concentrations and that bacterial reduction of iron (III) minerals and sulphate increase the reducing capacity of the groundwater. The effects of bacteria on the hydrochemistry had not been accounted for in the modelling work made prior to construction of the laboratory.

Important improvements in the groundwater chemical modelling

During the evaluation and modelling of the Äspö data a systematic development of the modelling approaches has been made. Statistical multivariate procedures have been used to evaluate the data which have been collected. For the spatial predictions of the mixing process multivariate principal component

analyses, linear regression methods, kriging and neural networks have been tested.

The most important modelling development has been the ability to differentiate between waters of different origin, not only in relation to the saline and non-saline waters but also in relation to the previously prevailing conditions, i.e. the different phases of the Baltic Sea evolution since last glaciation. Identification of the sources and the mixing-mass-balance calculations have significantly shifted the hydrochemical modelling from a non-reproducible expert based task to a more reproducible expert-computer based one.

Methods and models have been developed for identifying the different sources of groundwater (end members) at the Äspö site and how groundwater at specific locations in the rock mass can be quantified as a mixture of end members. The present hydrochemistry model of Äspö incorporates the anticipated conditions prevailing since the latest glaciation. For this model mixing of groundwater of different origin and composition, calcite saturation, redox properties, groundwater/rock interaction and biological activity are important processes to describe and understand.

The Multivariate Mixing and Mass balance calculation code is abbreviated M3.

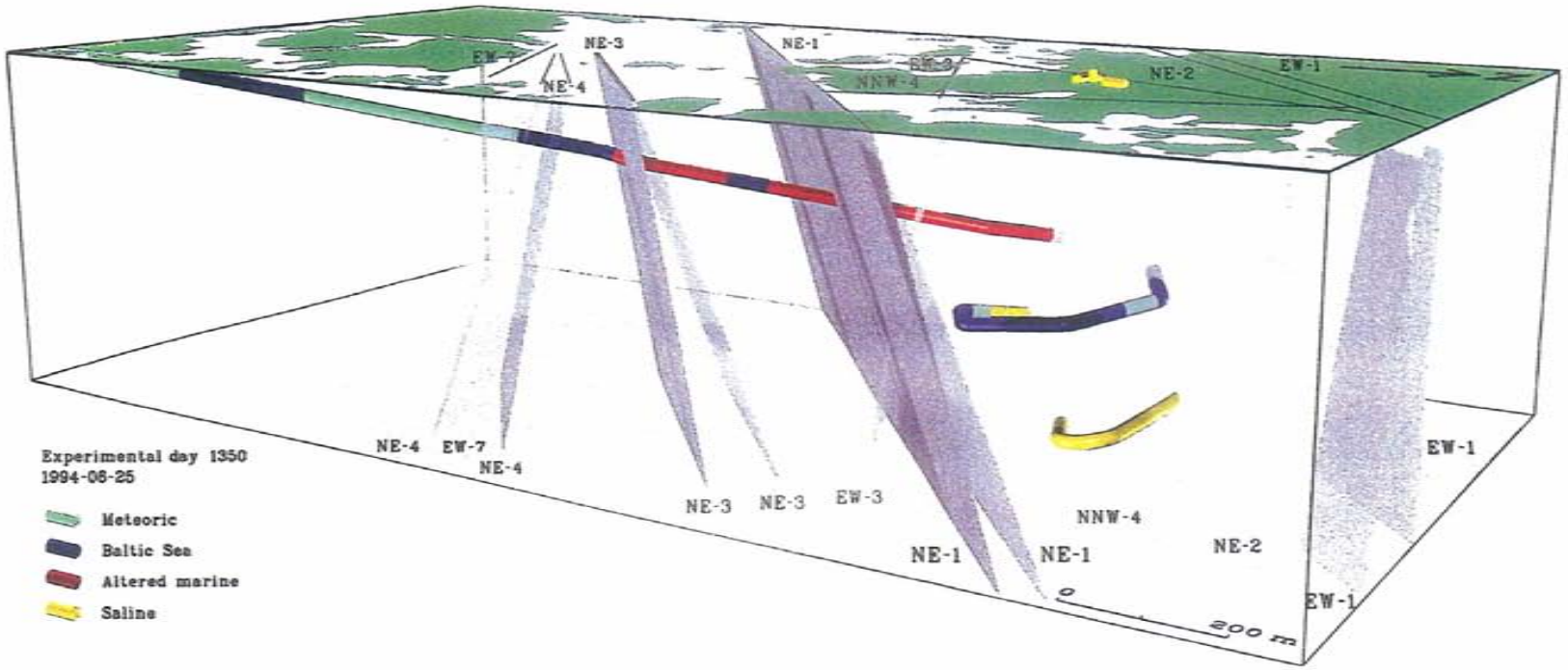

Figure 5. *Hydrochemical model 1996, presenting the dominating groundwater types as a function of the inflow to the tunnel. See Section 7.6.2 for a comprehensive discussion.*

1 INTRODUCTION

1.1 ÄSPÖ HARD ROCK LABORATORY (Äspö HRL)

The Äspö Hard Rock Laboratory (HRL) constitutes an important part of the work of developing a deep repository and developing and testing methods for investigating and licensing a suitable site. The plan to build an underground rock laboratory was presented in *R&D Programme 86 /1986/* and was received very positively by the reviewing bodies. In the autumn of 1986, SKB initiated the field work for the siting of the underground laboratory in the Simpevarp area of the municipality of Oskarshamn. At the end of 1988, SKB arrived at a decision in principle to site the laboratory on southern Äspö, about 2 km north of the Oskarshamn Nuclear Power Station (see *Figure 1-1)*. After regulatory review and approval, construction work on the facility was commenced in the autumn of 1990.

The Äspö HRL has been designed to meet the projected needs of the planned research, development and demonstration activities. The underground part takes the form of a tunnel from the Simpevarp peninsula to the southern part of the island of Äspö (see *Figure 1-2)*. Below Äspö, the tunnel runs in two turns down to a depth of 450 m (see *Figure 1-3)*. The total length of the tunnel is 3600 m. The first part of the tunnel was excavated using the drill-and-blast technique. The last 400 metres were excavated by a tunnel boring machine (TBM) with a diameter of 5 metres. The underground excavations are connected to the surface facilities by a hoist shaft and two ventilation shafts. The Äspö Research Village with offices, stores and hoist and ventilation building is located at the surface, (see *Figure 1-4*).

The work at the Äspö HRL was divided into three phases: the pre-investigation phase, the construction phase and the operating phase. The **pre-investigation phase**, 1986–1990, involved siting the Äspö HRL. The natural conditions in the bedrock were described and predictions made with respect to the geohydrological and other conditions that would be observed during the construction phase */Gustafson et al, 1991/*. Planning for the construction and operating phases was also carried out.

During the **construction phase**, 1990–1995, extensive investigations, tests and experiments were carried out in parallel with the civil engineering activities, mainly to check the reliability of the pre-investigations. The tunnel was excavated to a depth of 450 m and construction of the Äspö Research Village was completed. The Äspö Research Village was taken into service during the summer of 1994. The underground civil engineering works were mostly completed in the summer of 1995.

The **operating phase** began in 1995. A programme for these studies is presented in *RD&D Programme 95 /1995/*.

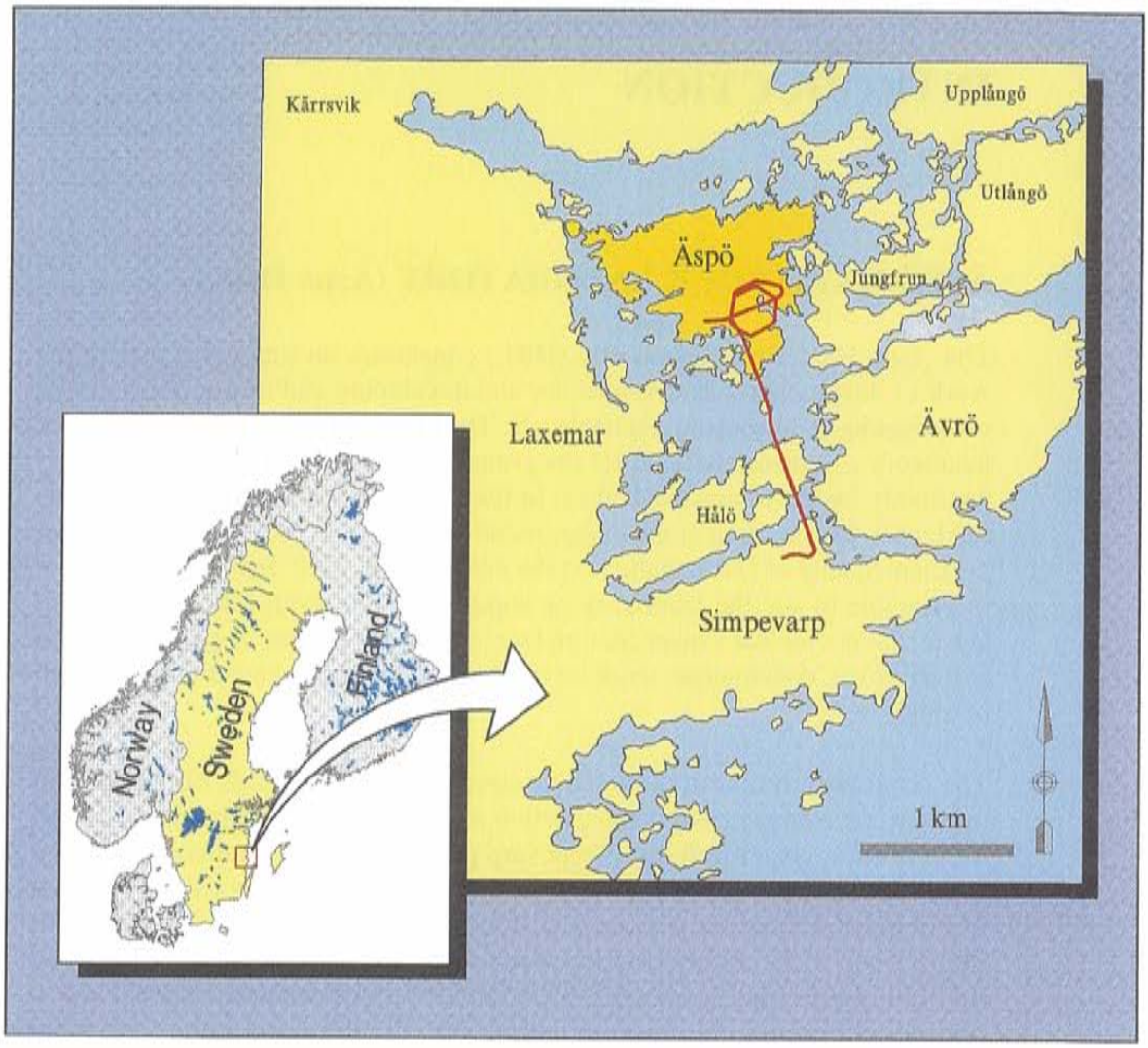

Figure 1-1. *Location of the Äspö Hard Rock Laboratory.*

Figure 1-2. *Overview of the area around the Äspö HRL.*

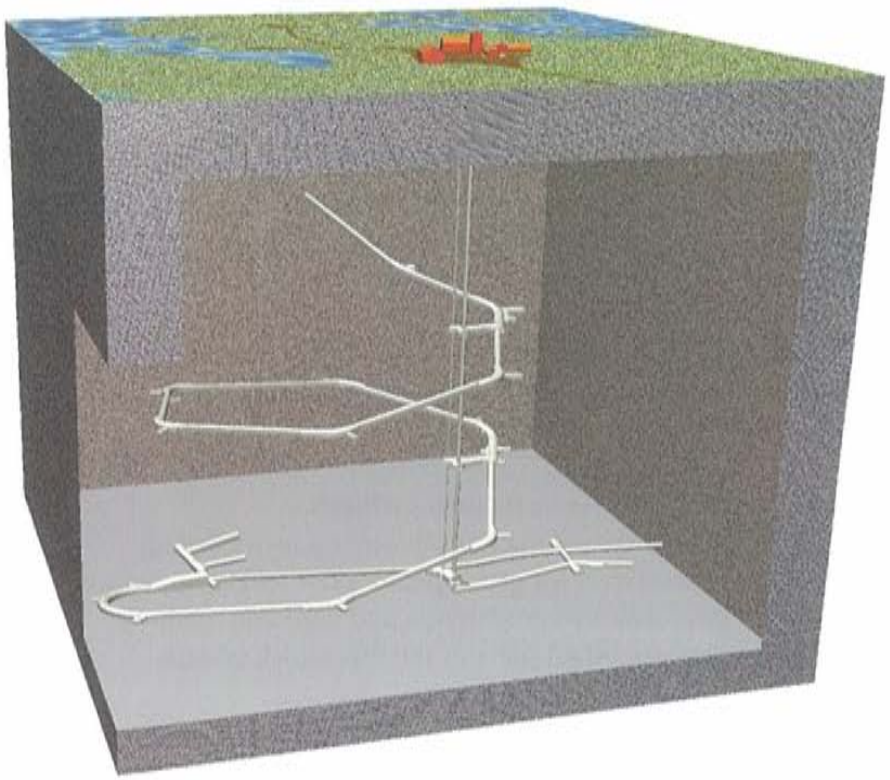

Figure 1-3. *General layout of the Äspö HRL. The total length of the tunnel is 3600 m. The first part of the tunnel was excavated using the drill-and-blast technique. The last 400 metres were excavated by a Tunnel Boring Machine (TBM) with a diameter of 5 metres. The underground excavations are connected to the Äspö Research Village, containing offices, stores, hoist and ventilation building, by a hoist shaft and two ventilation shafts.*

Figure 1-4. *Bird's-eye view of the Äspö Research Village.*

1.2 OVERALL GOALS OF THE ÄSPÖ PROJECT

One of the basic motives for SKB's decision to build the Äspö HRL was to provide an opportunity for research, development and demonstration in a realistic and undisturbed rock environment down to the depth planned for a future deep repository.

To meet the overall schedule for SKB's RD&D work, the following (here abbreviated) stage goals were set up in *R&D-Programme 89 /1989/* for the activities at the Äspö HRL.

1 Verify pre-investigation methods.
2 Finalize detailed characterization methodology.
3 Test models for groundwater flow and radionuclide migration.
4 Demonstrate construction and handling methods.
5 Test important parts of the repository system.

In the planning and design of activities to be performed at the Äspö HRL during the operating phase, priority is being given to projects which aim to:

- increase scientific understanding of the deep repository's safety margins,
- develop and test technology which reduces costs and simplifies the repository concept without sacrificing high quality and safety, and
- demonstrate technology that will be used for the deposition of spent nuclear fuel and other long-lived waste.

The start of the operating phase has motivated a revision and focusing of the goals of the Äspö HRL, based on the experience gained to date. For the operating phase, the stage goals have been worded as follows, */R&D-Programme 95 /1995/*:

1 Verify pre-investigation methods
Demonstrate that investigations at the ground surface and in boreholes provide sufficient data on essential safety-related properties of the rock at repository level.

2 Finalize detailed characterization methodology
Refine and verify the methods and the technology needed for characterization of the rock in the detailed characterization of a site.

3 Test models for description of the barrier function of the rock
Refine and at repository depth test methods and models for describing groundwater flow, radionuclide migration and chemical conditions during the repository's operating period and after closure.

4 Demonstrate the technology for and function of important parts of the repository system
Test, investigate and demonstrate on a full scale different components of importance for the long-term safety of a deep repository system and show that high quality can be achieved in the design, construction and operation of system components.

that high quality can be achieved in the design, construction and operation of system components.

The four reports mentioned in the foreword mainly address the first and, to some extent, the second of the above stage goals.

The Äspö HRL comprises an important part of the work being pursued within SKB's RD&D-Programme.

1.3 AIM OF THIS REPORT

The purpose of this report, No. 5, is to present the 1996 model of the Äspö HRL, the concepts behind it and some comments on how the model has developed based on data from the pre-investigation and construction phases of Äspö HRL.

The intended readers are mainly the scientists working at Äspö HRL. By reading this report one should get a good insight in the properties of the rock mass and with help of *Report No 1, Stanfors et al /1997a/*, an introduction of what data and reports that are available. The reports summarizes the knowledge up to 1996 and the models are referred to *"Model 96"* in this and other reports.

The report is also intended to be used by modellers who intend to model groundwater flow at Äspö. The report should provide much of the information needed except for geometric information concerning topography, tunnel layout etc.

The report is independent from *Reports No 2, 3 and 4* in this series */Stanfors et al, 1997b, Rhén et al, 1997a and 1997b/*. These reports concern the evaluation of the methods and methodology used for the site characterization.

In this report, *No 5, Chapter 2* presents briefly how the model has developed during the pre-investigation and the construction phases.

Chapter 3 presents the concepts used for the models presented in the following chapters. The detailed descriptions of the models are presented in six chapters:

- 4 Geological model
- 5 Mechanical stability model
- 6 Geohydrological model
- 7 Hydro chemical model
- 8 Transport of solutes model

1.4 COORDINATE SYSTEM

For various reasons a number of coordinate systems have been used during the pre-investigation and construction phases.

At Äspö four different coordinate systems are used. The systems are rotated relative to one another and have different North directions. Within the Äspö Project all geological information on the orientation of structures is given relative to magnetic North. This reference direction is generally used in this report. Geographic North is also used occasionally as a reference direction, but for practical purposes this is the same as magnetic North, considering the accuracy in orientation that can be obtained for geological features.

Location of drifts and boreholes are always given in the local Äspö coordinate system.

The relative orientation between the four coordinate systems are:

- RAK-38 North is 11.819 degrees East of Äspö local North map system.
- Geographic North is 11.119 degrees East of Äspö local North.
- Magnetic North is approximately 12 degrees East of Äspö local North (1985-1990).

The coordinate transformation between the RAK-38 and local Äspö systems is according to the equations below:

$$X_{RAK\text{-}38} = 6367978.295 + 0.978799\,(X_{Äspö} - 7484.309) + 0.204822\,(Y_{Äspö} - 1956.68)$$

$$Y_{RAK\text{-}38} = 1551210.173 - 0.204822\,(X_{Äspö} - 7484.309) + 0.978799\,(Y_{Äspö} - 1956.68)$$

$$(6360251.890,\ 1550827.928)_{RAK\text{-}38} = (0,0)_{Äspö}$$

The length correction between the systems is as follows:

$$L_{RAK\text{-}38} = 0.999999852 \bullet L_{Äspö}$$

2 DEVELOPMENT OF MODELS OF THE ÄSPÖ SITE

2.1 INTRODUCTION

During pre-investigations for the Äspö site the analyses of the data were frequently summarized in different kinds of models after each pre-investigation stage. Development of these models is the described in *Wikberg et al, 1991.* Details of the previous models, the characterization work and investigation methods are found in *Gustafson et al /1988/, Gustafson et al /1989/, Stanfors et al /1991/, Almén and Zellman /1991/* and *Wikberg et al /1991/.* Predictions made for the construction phase were presented in *Gustafson et al /1991/.* Details of the present model made after the construction phase, *Model 96*, is presented in *Chapters 3 to 8* in this report. The main modelling concepts for the previous models */Gustafson et al /1988/, Gustafson et al /1989/* and *Wikberg et al /1991/* are summarized in *Table 2-1*, last in this chapter. The aim of this chapter is to briefly present the pre-investigation models and *Model 96.*

The pre-investigations were divided into three stages:

- siting stage
- site description stage
- prediction stage

The siting stage included mostly regional investigations and some more detailed semi-regional investigations covering some potential sites around the Simpevarp peninsula. The site description and the prediction stages both focused on the Äspö island and the Äspö-Hålö area, see *Figure 2-1.* The prediction stage investigations were performed in two steps, mainly because the planned tunnel entrance was moved from Äspö to the Simpevarp peninsula during this stage. Simplified models for the stages are presented in a number of figures and the models are briefly described in *Section 2.2 to 2.4.* Present models are briefly described in *Section 2.5.*

2.2 REGIONAL MODELS (1986-1987)

Most investigations for the regional scale were performed during 1986-1987. A few supplementary investigations were also performed during the construction phase of the Äspö HRL.

Geology

The bedrock model on the regional scale, based on interpretation of geological field investigations and geophysics, shows that the area is mainly of granitic composition.

Lineament interpretation, structural mapping and geophysical investigations show the structural framework of Äspö island comprising ENE to NE trending regional lineaments close to the island but also N to NW trending lineaments outside the figure area, see *Figure 2-1*. According to aeromagnetic indications these are estimated to be about 100 to 300 metres wide zones of low magnetic intensity extending over 5 to 30 km along strike.

Geohydrology

A source for preliminary geohydrological data was the water well archive at the Swedish Geological Survey (SGU). Data used for the preliminary analysis covered a larger area than shown in *Figure 2-1*. At this stage there were also two other sources for information: hydraulic tests performed in a few boreholes on the Ävrö island and geohydrological investigations performed on the Simpevarp peninsula in connection with the construction of the power plants and the CLAB facility.

The data from the SGU Well Archive showed that the median of the specific capacity measured in the wells was about the same for wells close to Äspö compared to the entire area. These wells were about 60 m deep and were mainly drilled in Småland (Ävrö) granite. The hydraulic conductivity of different rock types were compared. It was noted that younger granites of type Götemar and Uthammar granite were more conductive and that gabbro or diorite were less conductive in comparison with the Småland (Ävrö) granite. The data from Ävrö indicted that the hydraulic conductivity decreased with depth.

Hydrochemistry

Chemical data from the Water Well Archive at the SGU were compiled for the entire Kalmar County. A statistical treatment of these data showed that the salinity increased towards the coast of the Baltic Sea. The Äspö groundwater could therefore be expected to be saline.

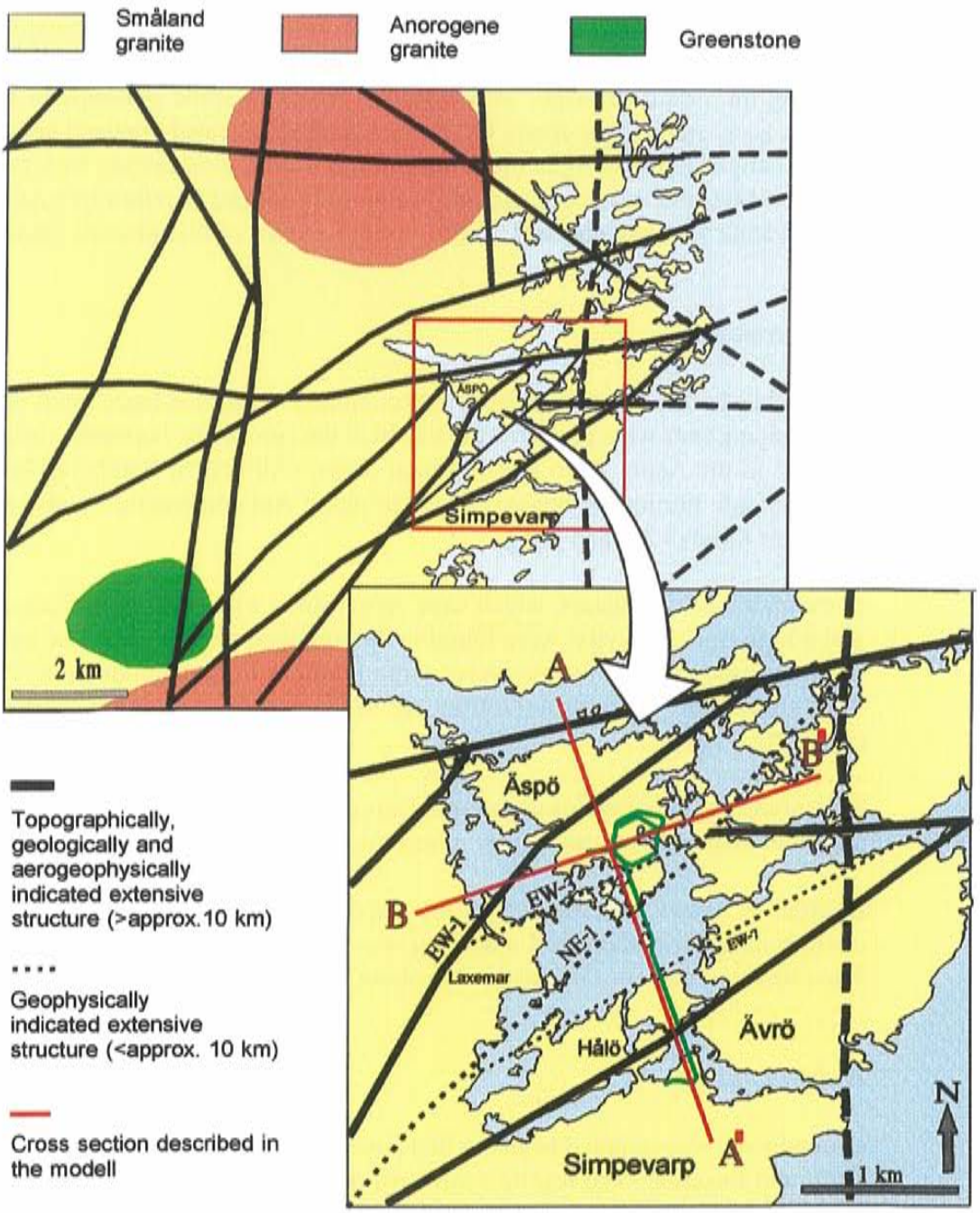

Figure 2-1. *Regional outline structural model of the Äspö area. A-A´: vertical section in Figures 2-2--2-5, 2-7. B-B´: vertical section in Figure 2-6.*

2.3 SEMI REGIONAL SCALE

2.3.1 Modelling stage 1 (1986-1987)

Geology

Aeromagnetic anomalies compared with results from the digital terrain models clearly indicated a some hundred metres wide fracture zone trending NE crossing the island of Äspö. Mylonite was found in some outcrops in the fracture zone (Äspö shear-zone). Overview mapping indicated Småland granite (later changed to the designation 'Äspö diorite') as the dominating rock type on Äspö. Metavolcanic rocks and greenstone were noticed as minor inclusions in the granite which often is intruded by irregular veins of fine-grained granite.

Geohydrology

The surface hydrology of the region was compiled to provide basic input data and pumping tests were performed in the 26 of the percussion boreholes drilled in 1987 in the Äspö, Ävrö and Laxemar areas. (All drilled boreholes from surface made during the pre-investigation phase and construction phase are shown in *Figures 2-3* and *2-4*.)

Some hydraulic conductors, which were very distinct with a few open fractures and a high transmissivity, were found in the Småland granite area. The areas of greenstone and greenstone lenses were found to be less conductive. The Äspö shear-zone, crossing Äspö from NE to SW was found to be moderately conductive.

Measurements in boreholes situated in Laxemar, Äspö and Ävrö showed that the groundwater level was closely related to the ground surface level.

In order to assess the influence of the Äspö HRL on the groundwater flow conditions generic numerical modeling was made of two layout alternatives. The estimated radius of influence was about 2 km.

Hydrochemistry

Groundwater was sampled from the first percussion drilled boreholes at Äspö, Ävrö and Laxemar. The results confirmed the assumptions that saline water was found at shallow depth (<100 m). However, it was also clear that at Äspö the saline water was more close to the surface than at both Laxemar and Ävrö. The reasons for this could be found in the facts that Äspö has a lower topography and as an island surrounded by the sea on all sides.

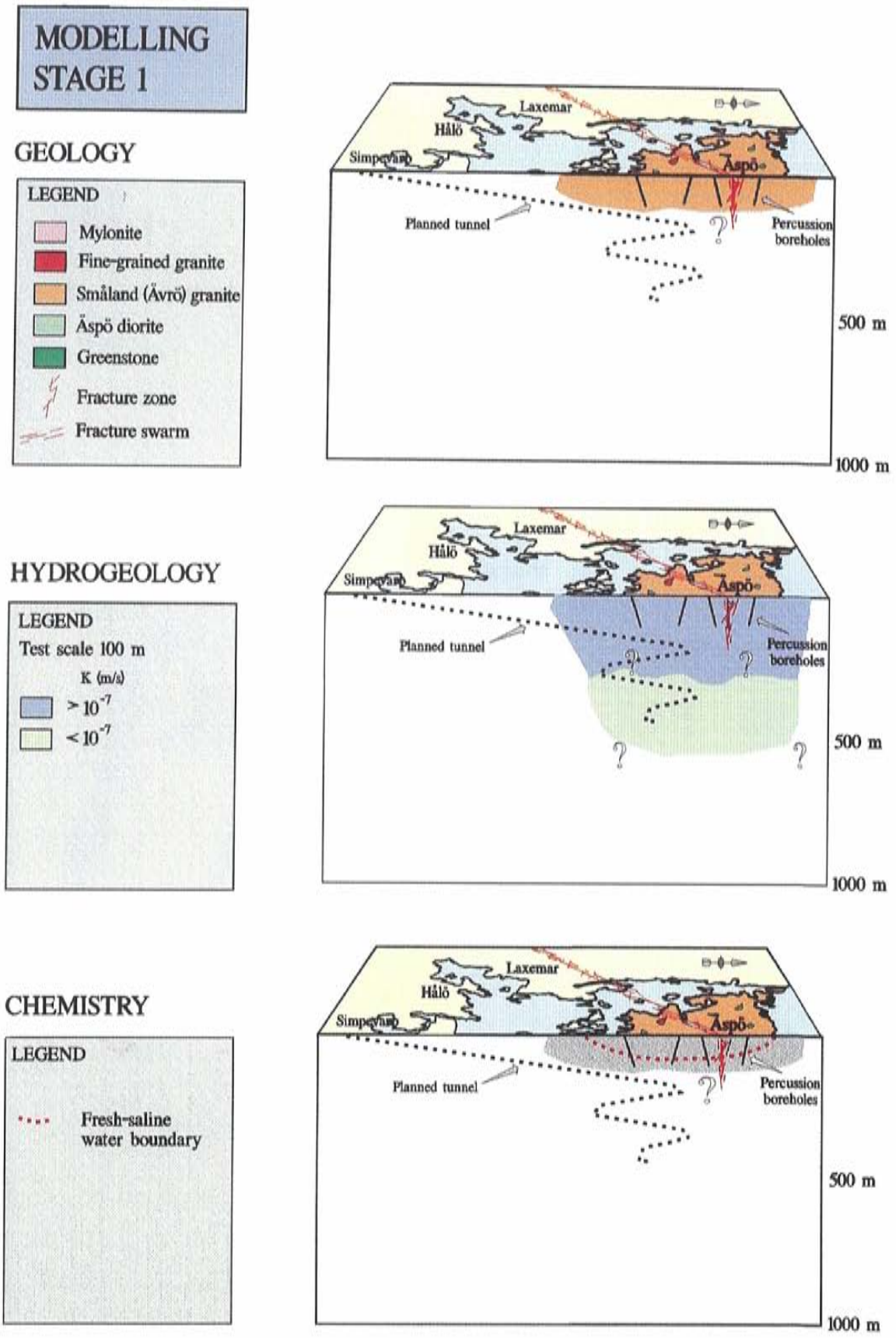

Figure 2-2. *Investigation stage 1. Vertical section A-A'.*

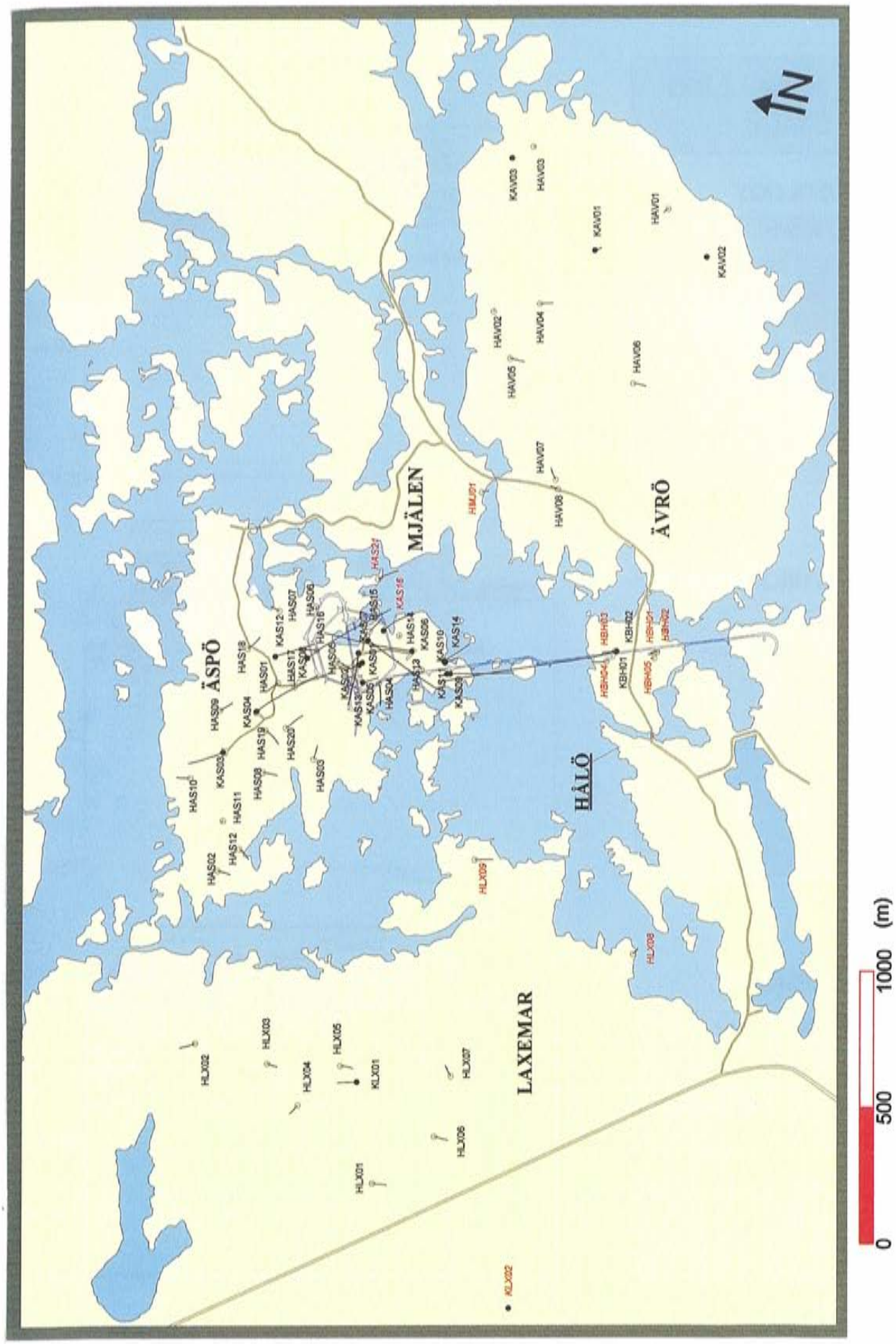

Figure 2-3. *Plan of the boreholes. Boreholes with a black label were drilled before construction of the Äspö HRL and boreholes with a red label were drilled during the construction of the Äspö HRL. Filled circles: Cored boreholes. Un-filled circles: Percussion boreholes.*

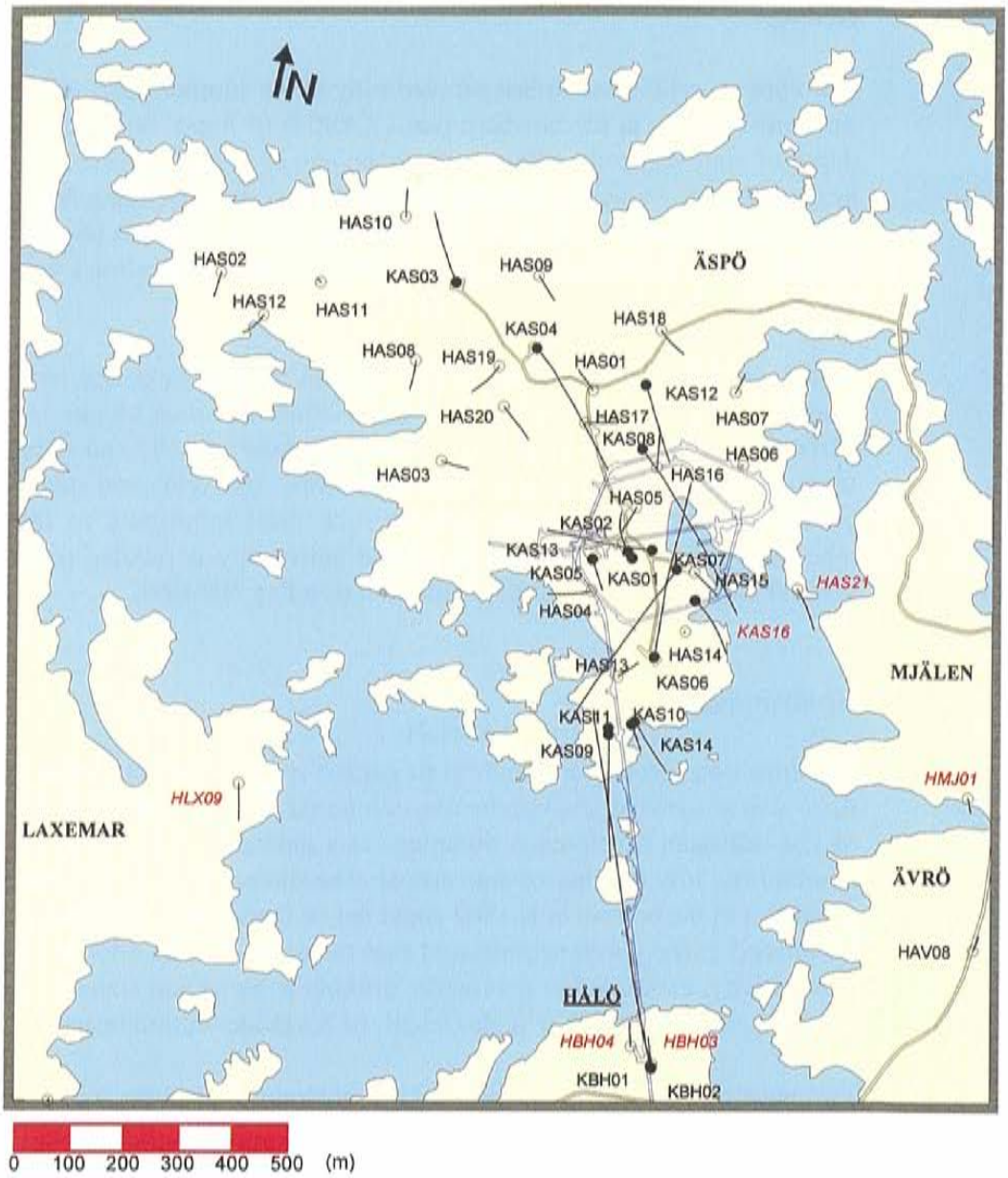

Figure 2-4. *Plan of the boreholes. Boreholes with a black label were drilled before construction of the Äspö HRL and boreholes with a red label were drilled during the construction of the Äspö HRL. Filled circles: Cored boreholes. Un-filled circles: Percussion boreholes.*

2.4 SITE SCALE

2.4.1 Modelling stage 2 (1987-1988)

Geology

One cored borehole was drilled sub-vertically in the southern part (KAS02) and one subvertically in the northern part (KAS03) of Äspö, both boreholes to a depth of approximately 1000 m. The main aim of a third borehole (KAS04) – inclined 60°SE – was to cross the indicated shear-zone trending NE in central Äspö, see *Figure 2-5*. One cored borehole was also drilled to a depth of 700 m in Laxemar as a reference hole and another five percussion holes were drilled on Äspö.

Based on these investigations the geological model comprises two granitic blocks that are divided by a mylonitic shear-zone. The rock blocks are built up of the varieties of Småland granite - Småland (Ävrö) granite and Äspö diorite. Irregular inclusions of fine-grained greenstone and veins and dikes of fine-grained granite intruding the granitic rock mass contribute to lithological inhomogeneity. The dominant structural anisotropy is parallel to an almost vertical more or less penetrating foliation trending NE-ENE.

Geohydrology

The injection tests with 3 and 30 m packer spacing indicated that Southern Äspö was somewhat less conductive compared to Northern Äspö. Evaluation of the transient interference pumping tests indicated a few larger hydraulic conductors, low dipping or subvertical. The direction of a very transmissive conductor in the bottom of KAS02 could not be determined. The hydraulic tests performed in the corehole indicated that measures for the effective hydraulic conductivity, estimated as geometric, arithmetic mean and standard deviation were dependent of the test scale (length of borehole section tested).

Two numerical models of the regional groundwater flow were set up. These 3-dimensional models were used to assess the area of influence from the laboratory, which was shown to be 1-2 km. A generic study of the behaviour of the saline water front in a fractured rock was simulated by a stochastic continuum model. It was shown that salinity interface below an island can be quite irregular if the hydraulic conductivity is stochastically distributed.

Hydrochemistry

In the two rock blocks the groundwater salinity increased gradually by depth. The increase was roughly linear and somewhat different in the two boreholes. This suggested a more stagnant situation in the southern rock block. The gradual increase in salinity implied that the origin of the water could be mixing between freshwater, relict and modern Baltic Sea water and pre-glacial water.

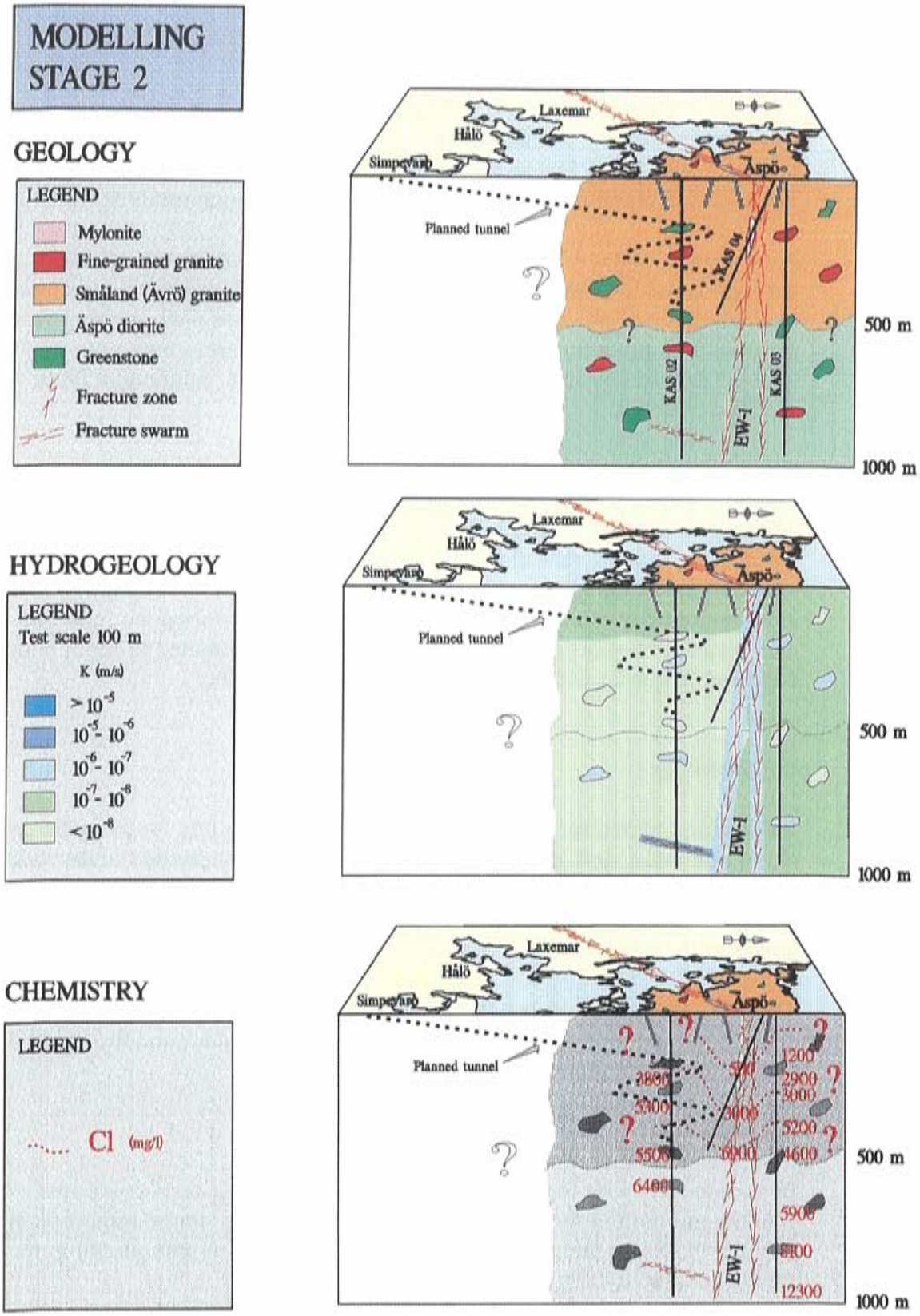

Figure 2-5. Investigation stage 2. Vertical section A-A'.

2.4.2 Modelling stage 3 (1988-1989)

Geology

The four additional cored boreholes, KAS05-08, were directed towards indicated zones of geological and hydraulic importance on southern Äspö, see *Figure 2-6*. They were drilled to a vertical depth of approximately 500 m.

A geological field study was done in order to obtain information to make a description of the lithological distribution and petrological and structural characteristics of the different rocks on Äspö. Very detailed mapping was performed along cleaned trenches across the island. Data concerning 4500 mapped fractures – such as orientation, length, aperture and fracture filling – was also presented.

The main aim of a detailed geophysical investigation was to indicate fracture zones on Äspö, using mainly geomagnetic, geoelectric and seismic methods. The major fracture zones NE-1, EW-3 and NE-2 were indicated in a number of boreholes. Seismic reflection investigation identified two sub-horizontal anomalies situated at depths of from 300 to 500 metres and 950 to 1150 metres along both profiles characterized by several rather short and irregular reflectors. The seismic reflectors could only to some extent be correlated to zones with increased frequency of low-dipping fractures in drill cores.

Geohydrology

Short term interference tests and a long term pumping test, by pumping an entire bore hole, were made to find out the hydraulic connections in the rock mass. Several important hydraulic features were identified. Their approximate extent, strike, dip, position and transmissivities were given. The approximate strikes of the conductive features were NW, ENE, NE and NNW.

The lithological units of hydrogeological importance were considered to be Äspö diorite (lowest hydraulic conductivity), Småland granite and fine-grained granite (highest hydraulic conductivity).

Hydrochemistry

In conjunction with the hydraulic interference pumping tests conducted in KAS06 and HAS13 the groundwater was analysed in a similar manner as in KAS02-04. Some information, but of lower quality, was also gained in the samples collected during drilling of all other boreholes.

The results of samples and analyses from newly drilled boreholes and all previous analyses were co-evaluated by a multivariate procedure called principal component analyses. Despite the continuous increase in salinity with depth there are four distinctly different classes, see *Figure 2-6*. The classes were later found to be resulting from the episodic events affecting the ground- water system under Äspö in the time span since last glaciation.

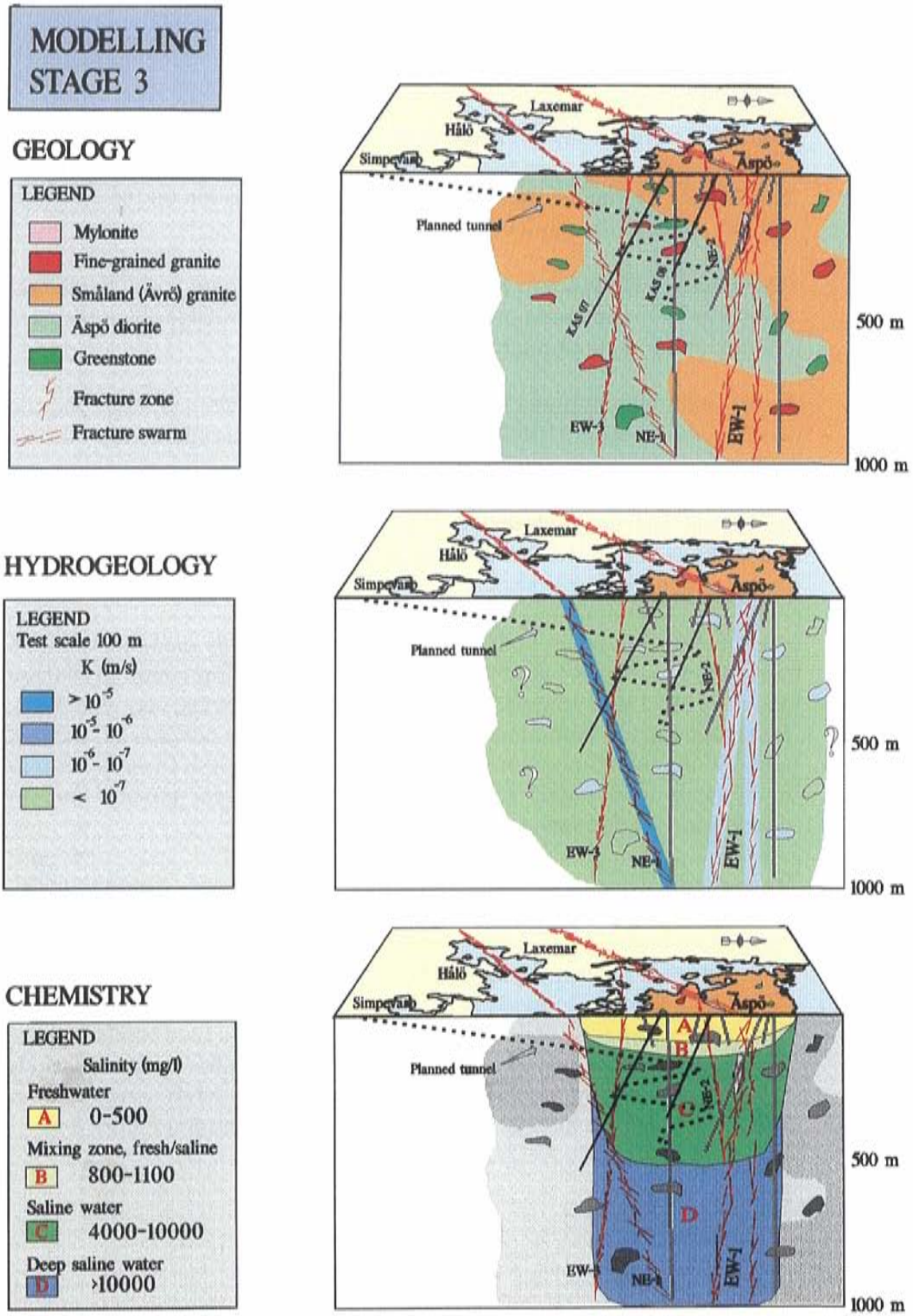

Figure 2-6. *Investigation stage 3. Vertical section A-A´. Geology (N-S section).*

2.4.3 Modelling stage 4 (1989-1990)

Geology

Due to the change in layout, in which the entrance to the tunnel was moved to the Simpevarp area, a complementary drilling programme was carried out. KAS09, 10, 11 and 14 were drilled to provide information on the indicated fracture zones to the south of Äspö.

The percussion boreholes, HAS18, 19, 20 and two more cored boreholes, KAS12 and 13 were drilled in order to improve the knowledge about the main fracture zones on southern Äspö.

Geophysical investigations in the sea area between Hålö and Äspö and the inclined core borehole KBH02 parallel to the planned tunnel gave very valuable information to the final modelling work, especially concerning orientation and character of the major fracture zones EW-7, NE-4, NE-3 and NE-1. Detailed geological and geophysical investigations combined with hydrotesting in boreholes indicated the 'NNW system' of minor fracture zones supposed to connect the major water-bearing NE trending fracture zones.

Cored boreholes KAS09, KAS11 and KAS14 were mainly sited to investigate the fracture zones EW-5 and NE-1 bordering on Äspö to the south. In all these boreholes NE-1 was very well indicated (increased fracturing, clay alteration). Borehole radar and Vertical Seismic Profiling results also confirmed the extent and NW dip of NE-1, and the fracture zone NE-1 was also found to be very hydraulically conductive. Concerning EW-5 there were possible but no unambiguous indications in these boreholes.

Evaluation of all pre-investigation data resulted in a geologic-structural model. A N-S vertical section almost parallel to the tunnel is presented in *Figure 2-7*.

The geological pre-investigations were concentrated to the access tunnel and the spiral tunnel area in southern Äspö. Due to the main NE to ENE trend of the major fracture zones and the ENE foliation most of the core boreholes have a N to NW direction. Only one core borehole (KAS13) has an approximately E-W direction mainly in order to cross estimated minor NNW-structures. An E-W vertical section through the shaft position is presented in *Figure 2-8*.

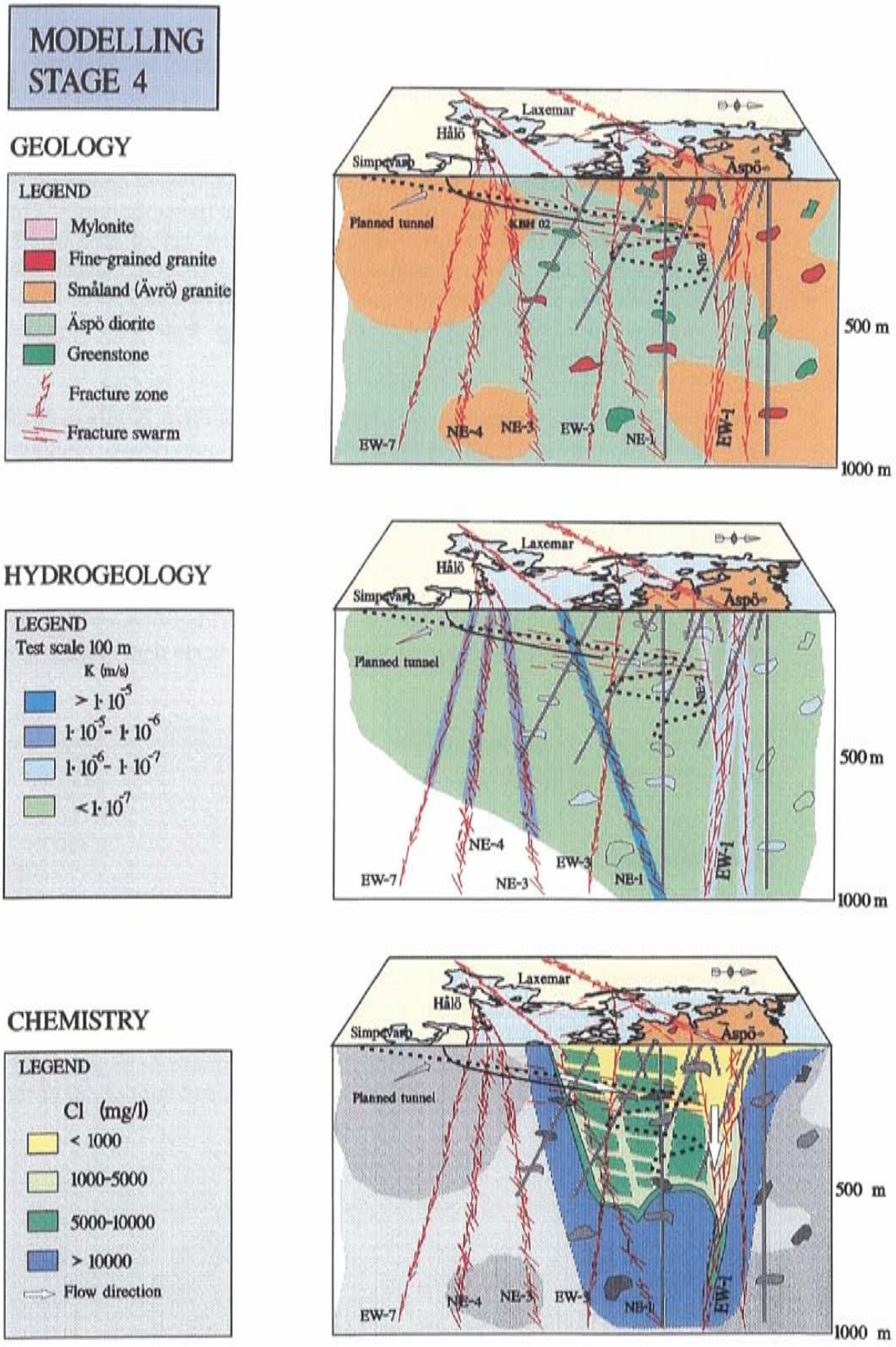

Figure 2-7. Investigation stage 4. Vertical section A-A´.

Geohydrology

The geohydrological investigations were focused on the deep cored boreholes in which short pumping tests and flow logging of the entire boreholes were performed.

15 main hydraulic conductors on Äspö and south of Äspö were described in detail with approximate extent, strike, dip, position and transmissivities. The main strikes were as in the stage 3, except for a new set of EW to NE structures. All these new structures were found to the south of Äspö, which was quite natural because all the investigations were focused on that part of Äspö. South of NE-1, in KBH02, only a few airlift pumping tests with long test sections were performed.

Five different rock mass domains were identified. Two of them, Northern Äspö and Äspö shear zone were approximately the same as previously. Southern Äspö was divided into two parts and the area south of Äspö was new. The depth dependency of the hydraulic conductivity was updated and the standard deviation of the hydraulic conductivity was calculated using data from the new hydraulic tests. The scale dependency of the hydraulic conductivity and standard deviation of the hydraulic conductivity were also updated. The hydraulic conductivity did not show any clear depth dependency and the standard deviation seemed to decrease with depth. The scale dependency was approximately as in the stage 2.

Using a numerical model for the Äspö island the groundwater recharge was estimated to be 3 mm/year.

Hydrochemistry

At this stage additional data was obtained only from samples collected during drilling. A closer examination of the data indicated that the water extracted from low conductive sections in the rock mass was more saline than the water from the surrounding more conductive rock and fracture systems */Smellie and Laaksoharju, 1992/*. However, the data from sampling during drilling was of low quality and therefore the conceptual groundwater model in *Figure 2-7* is more qualitative than quantitative. There is not evidence to support all of the details in the figure.

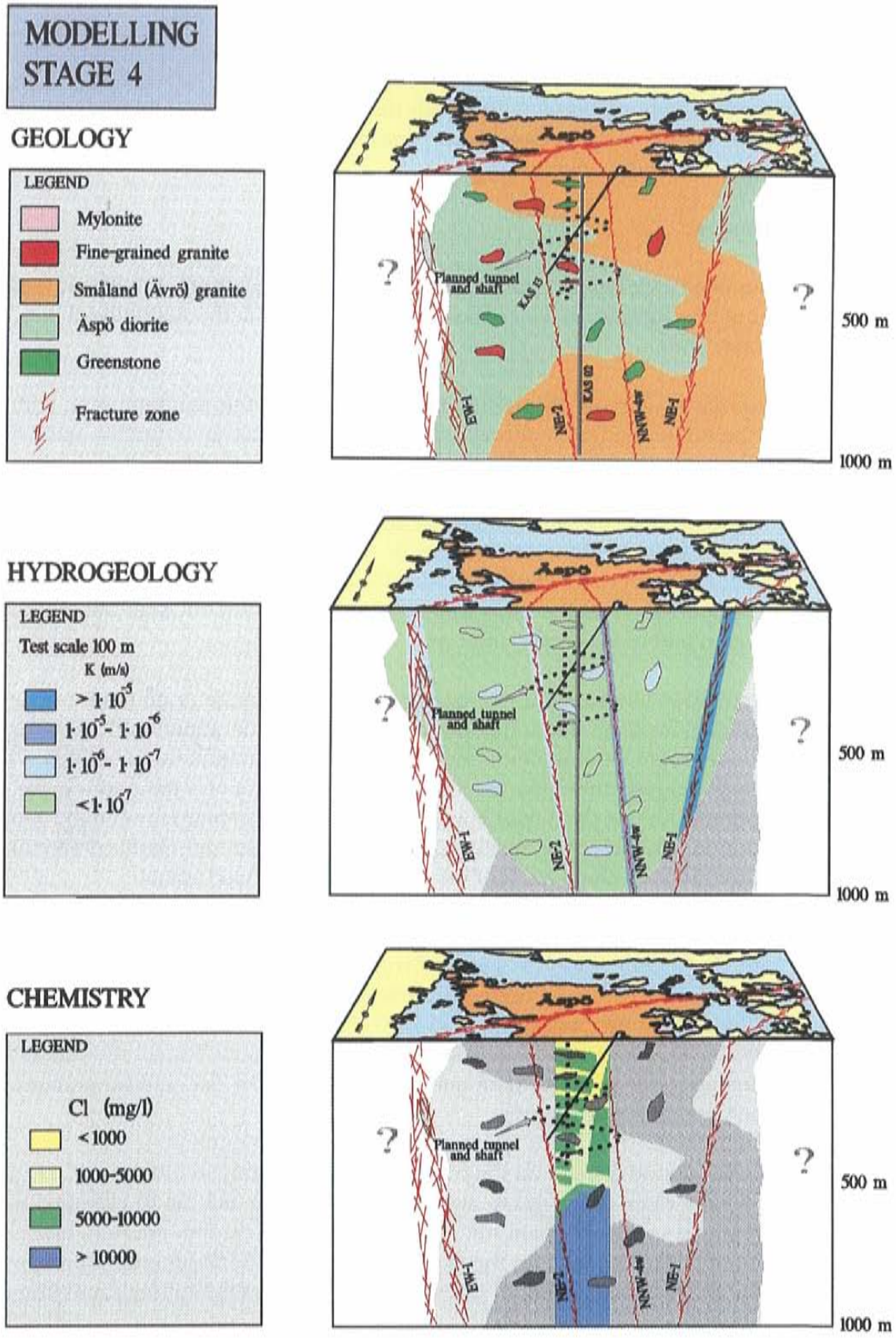

Figure 2-8. Investigation stage 4.Vertical section B-B´.

2.5 MODELS 96

The following models presented is a comprehensive result of modelling work based on data collected during both the pre-investigation and construction phase. Details of the models 96 are presented in *Chapter 4* to *8*.

Lithology

Four main rock types - Äspö diorite, Småland (Ävrö) granite, greenstone and fine-grained granite make up most of the rock mass in the Äspö tunnel area. *(Figure 2-9)*.

Äspö diorite is by far the most common rock type within the Äspö area, both on the surface and in the tunnel. During the first surface investigation most of the bedrock on Äspö was mapped as 'Småland granite'. After more detailed studies from the surface and the tunnel the designation 'Småland granite' was changed to 'Äspö diorite'. Usually the the Äspö diorite is grey to reddish grey, medium-grained, and contain more or less scattered, large crystals of K-feldspar. A variety called Småland (Ävrö) granite being more like a real granite in composition is found especially on the southern part of Äspö and in the northern part of the tunnel spiral area.

Macroscopically Småland (Ävrö) granite differs from the Äspö diorite in its brighter, sometimes distinctly more reddish colour. The amount of K-feldspar phenocrysts are lower and the crystals are much more irregularly distributed. In many places one can see that the Småland (Ävrö) granite cuts the Äspö diorite, which implies that the former is younger. The age difference between the two groups is probably very small. Together Äspö diorite and Småland (Ävrö) granite make up about 80 % of the rock mass in the Äspö tunnel.

Greenstones (about 5 % of the rock mass) is a fine-grained to medium-coarse-grained rock and is easily distinguished from the granitoid rocks by a very dark, greenish or greyish black colour. As a rule greenstone occur as minor inclusions or irregular, often elongated bodies within the granitoids and dioritoids following the common E-W foliation trend within the area. Except the smallest inclusions, greenstone is often intensely penetrated by fine-grained granites, which has obscured contacts.

The fine-grained granites vary in colour from reddish grey to distinct red. They are in most cases rich in quartz and potassium feldspar and can be classified as true granites. From the field studies it is obvious that the fine-grained granites all seem to be younger than the more coarse-grained Småland granite groups. There are also observations of dikes of fine-grained granite cutting each other.

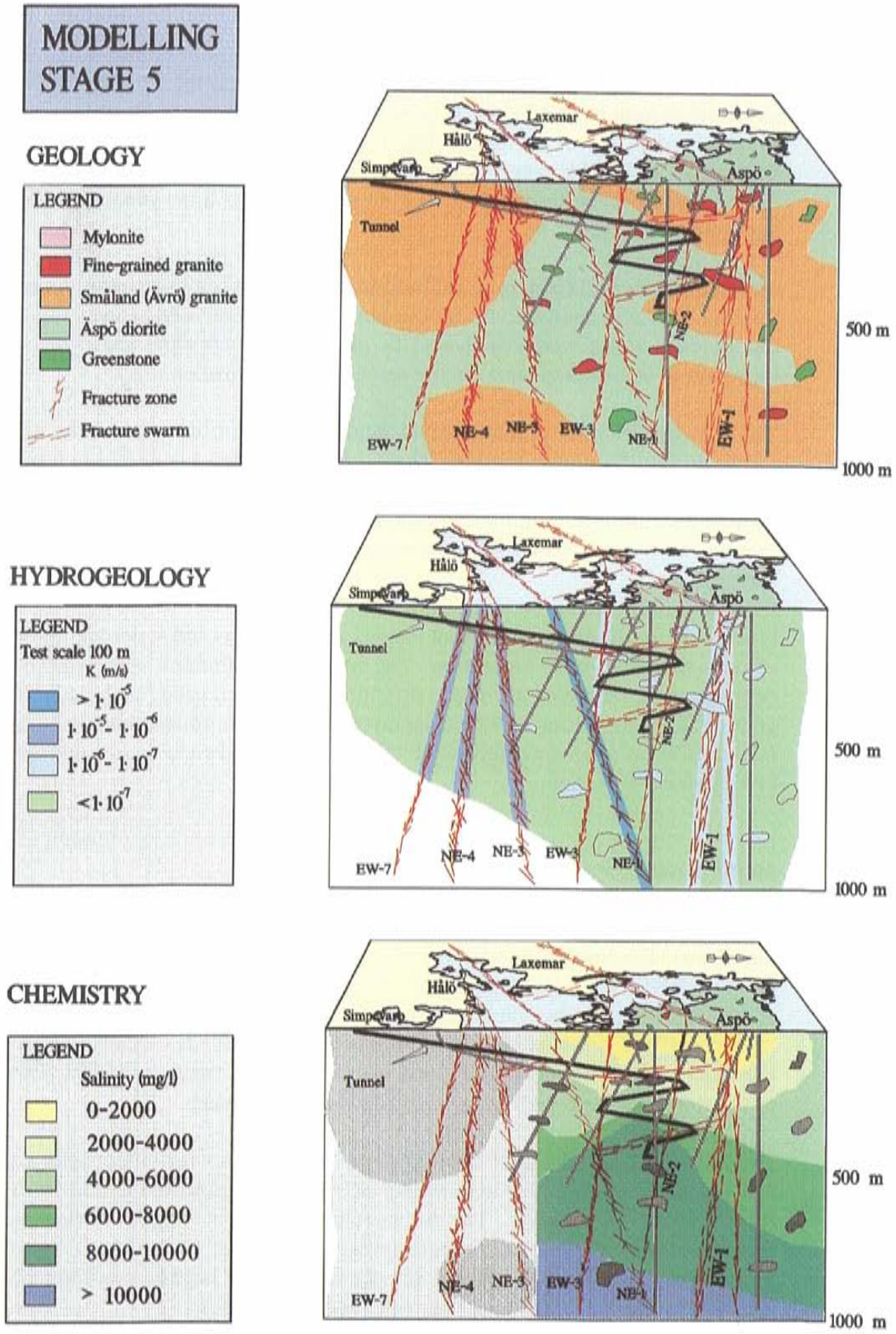

Figure 2-9. Outline of Model 96.

Structural development

A NE-ENE trending almost vertical, penetrating foliation is the most dominant structural element in the 1700-1800 million years old Äspö granitoids and seems to be the oldest sign of the ductile deformation related to the sub-horizontal NNW-SSE compression. This deformation is also marked by the orientation of mafic sheets often back veined by two or three generations of fine-grained granites.

Intensified strain formed in the amphibolite-facies are marked by gneissic zones trending NE-ENE, dipping to the N. Elevated to a higher structural level, these old gneissic zones were reactivated as mylonitic NE-trending shear-zones especially in central Äspö in a ductile-semiductile deformation phase.

The first brittle faults probably developed in the region in response to the emplacement of younger granites. These faults and older ductile zones were activated several times. The rock mass became increasingly brittle as it was uplifted and unroofed about 1000 million years ago. Parts of the epidotic vein system reactivated and its fractures were later filled by chlorite, zeolite and carbonate.

Fracture zones on Äspö have a wide range of orientations and styles and most of them reactivate older structures. The style of each fracture zone tends to depend on the nature of any older structure being reactivated, such as E-W gneissic zones and NE or E-W trending mylonites. Fracture zones trending N-S, NE or E-W on Äspö normally had ductile precursors whereas those trending NW apparently did not.

Major fracture zones

The *Figure 2-10* illustrates the most important fracture zones in the Äspö tunnel area. The fracture zone EW-7 was estimated to trend almost parallel to the main ENE-NE trending lineament and geophysical anomalies in the Hålö-Äspö area. Only one branch of EW-7 was indicated in borehole (KBH02). In the tunnel EW-7 consists of one set of fractures trending NNE - which here are the most conductive structures - and one fracture set trending WNW. The dominating rock type in the zone is Småland (Ävrö) granite.

NE-4 was indicated during pre-investigations by geophysics (ground magnetics and seismic refraction) and borehole data (KBH02) and estimated to consist of three branches trending NE. The dominating rock type in the zone - which is found to consist of two more or less continuous branches - is Småland (Ävrö) granite with inclusions of mylonite and greenstone. The northernmost branch is clearly connected to the mylonite, which is partly crushed.

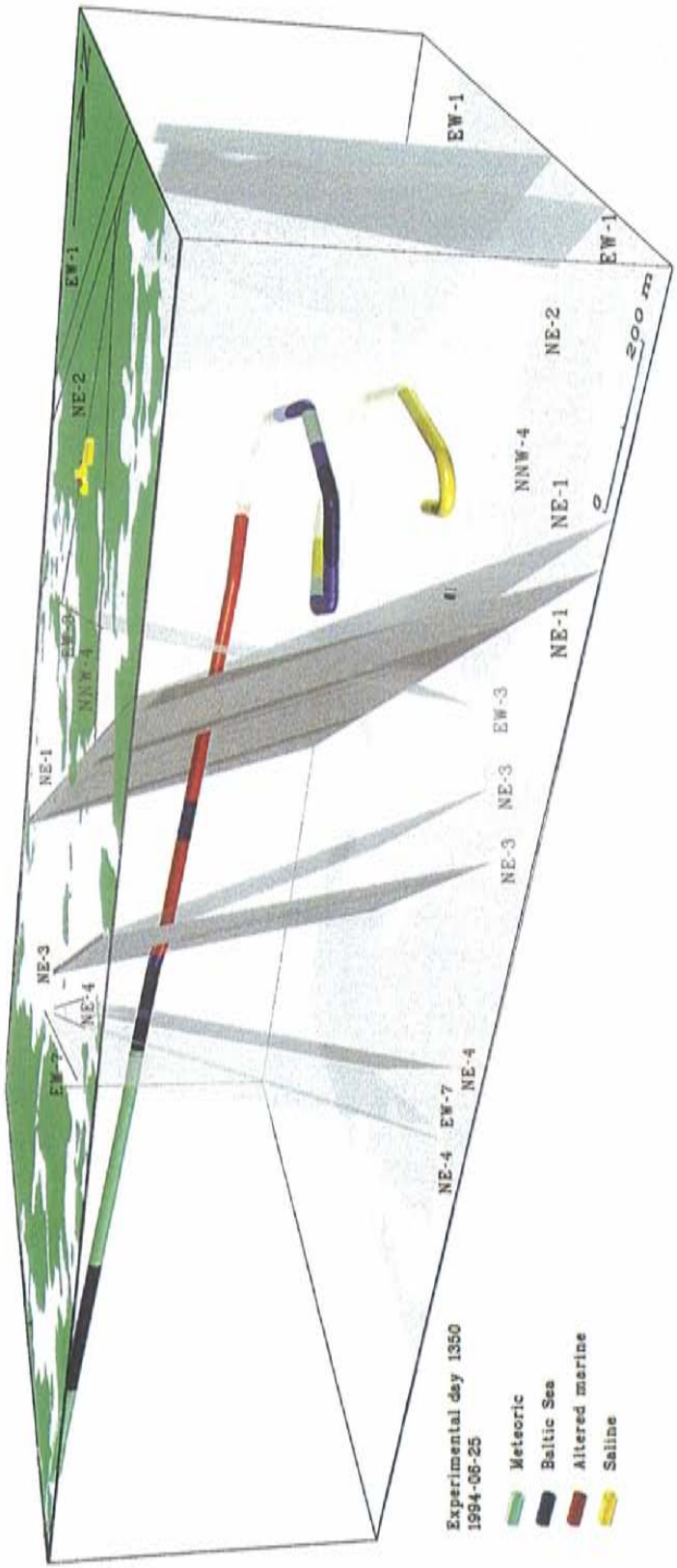

Figure 2-10. *Outline of model 96. Perspective view of the main structures, and dominating groundwater types flowing into the tunnel.*

NE-3 was indicated by ground magnetics and seismic refraction and confirmed in borehole KBH02 in the pre-investigation phase. After excavation, NE-3 was found to be approximately 49 m wide in the tunnel. Fine-grained granite is the dominating rock type with some intersections of Småland (Ävrö) granite and greenstone. Fracture spacing is mostly 5-20 cm but crushed parts are found locally. Although the zone itself dips steeply towards the NNW, as indicated by geophysics, its constituent fractures are steep and strike E-W and N-S. Their coatings are typically chloritic and calcitic. NE-3 possibly consists of several sub-parallel strands, that strike about N50°-70°E, of which two have been determined to dip about 70°N and 80°N respectively.

Fracture zone NE-1 was clearly indicated by geophysics and several boreholes in the pre-investigations and was predicted to be composed of three branches. All three branches are connected to a rather complex rock mass with Äspö diorite, fine-grained granite and greenstone. The two southernmost branches, trending NE and dipping NW, can be described as highly fractured and more or less water-bearing. The northern branch, which is approximately 28 m wide in the tunnel, is the most intense part of NE-1 and highly water-bearing. The central approximately 8 m wide - part of this branch, trending N50°E and dipping 75°N, with open, centimetre wide fractures and cavities and partly clay-altered rock, is surrounded by 10 to 15 m wide sections of more or less fractured rock. The fracture array consists of three sets; one is steep and strikes WNW, one is sub-horizontal and a third strikes ENE and dips moderately towards the NNW. The latter contain long faults (N75°E, dip 50°NNW) with gouge and has been used to determine the local orientation of NE-1.

The fracture zone EW-3 was very well indicated topographically, and geophysically (magnetic, seismic and electric) and in core boreholes KAS06 and KAS07 during the pre-investigations and estimated to be approximately 10 m wide. In the tunnel EW-3 is found to be approximately 14 m wide and consisiting of a 2-3 m wide crushed central section connected to a contact between Äspö diorite and fine-grained granite.

According to the earlier evaluation fracture zone NE-2 trending NE/ENE, should be regarded as the southern part of the main Äspö Shear zone and was expected to follow a somewhat winding course. The brittle deformation of this zone probably is greatly influenced by the formed ductile shearing and mylonitization. The dip of NE-2 was estimated to change from steeply northwards in the NE to steeply southeast in the SW part of the zone and to be only moderately hydraulically conductive. A probable interpretation of NE-2 is that tunnel intersections of minor fracture zones at about 1602 m, 1844 m and 2480 m represent one or two branches of NE-2. Measured strikes vary between N15°E and N36°E and measured dips cluster around 65°-82°S. However, the width of the most intensively foliated portion of the mylonite varies between 1 and 5 m. An estimated southeastern dip of NE-2 is supported by the fact that there is no indications of fractured mylonites in the cored boreholes KA1754A and KA1751A, drilled from the tunnel spiral.

EW-1 was early indicated by the initial airborne geophysical survey and the lineament interpretation. Ground geophysical investigation confirmed the more

detailed extension of the EW-1. In the first drilling campaign a cored borehole (KAS04) - inclined 60°SE crossed the zone.

The fracture zone EW-1 is very well documented topographically (50-200 m wide depression in the ground extending many hundred metres), geophysically (low-magnetic and low-resistivity zone 200-300 m wide), geologically (outcrops in trench with mylonites and crushed sections) and in boreholes (mylonites and many highly fractured and altered sections in drill cores). EW-1 is also indicated by VSP and radar. EW-1 is not crossed by the tunnel but the cored borehole KA1755A, drilled sub-horizontally from the tunnel through the zone at 300 m depth, mainly support the initial model of EW-1 as a complex fracture zone comprising steeply dipping branches in an inhomogeneous rock mass. Two branches are indicated in the core. The rather wide mylonites in the surface trench are found again as narrow veins in the core but the volcanite at surface is not found again in the core *(Figure 4-26)*.

Gently dipping fracture zones

Interpretations based on geological surface observations and seismic reflections suggested the presence of gently dipping fracture zones with approximately 100 m spacing at depth assuming similar spacing for the sub-horizontal fracture zones as steep ones. In the predictions prior to excavation gently dipping fracture zones, EW-5 were specified to intersect the access ramp at a depth of between 0 m and about 300 m and EW-X at greater depth (300-500 m) in the tunnel spiral. These gently dipping fracture zones were predicted as 'Possible' geologically.

Structural mapping in the vertical elevator shafts did not reveal any sub-horizontal fracture zones or gently dipping gneiss zones but a few gently dipping fracture zones with a width of less than 1 m were found in the tunnel.

Minor fracture zones

A great number of approximately NNW to NNE-striking narrow (dm - a few metres wide) fracture zones have been mapped on outcrops in Äspö. Only a few of them are topographically significant but normally too narrow to be geologically unambiguously indicated. VSP and borehole information support the notion of steep, mostly easterly dips. All these fracture zones were described under the designation "NNW" in the predictions. The different zones in the system NNW were predicted to be "possible" and their predicted position in the tunnel very approximate. The widths were expected to be 0.1-5 m.

The mapping underground indicated several minor fracture zones. These are generally not wider than 1 m. Most consists of a single or up to a handful of faults that generally contain gouge. The host rock is generally mylonitized near faults.

The water-bearing minor fracture zone NNW-4W makes an example of a fracture zone which is indicated in the tunnel by three intersections at 2020 m,

2120 m and 2914 m. 5-10 cm wide fractures in this metre-wide section of cataclastic granite were filled by grout.

Except for NNW-4W it is not possible to find persistent "minor fracture zones" in the tunnel according to the definition given in the prediction based on surface indications. One reason for this may be the tendency of most fracture zones to be narrower at depth, than what could be expected from surface indication in form of fractured and weathered rock.

Combined results from tunnel mapping and drilling show a characteristic structural pattern of WNW-NE-trending fracture zones and steeply dipping fractures (fracture swarms).

Hydraulic conductor domains

The geometry of the hydraulic conductor domains is mainly defined by the major fracture zones described above. The minor fracture zones in the 'NNW-system' are also important conductors. A few hydraulic conductor domains were also added to the model in order to explain some of the responses obtained in the interference tests. A simplified model of the hydraulic conductor domains was made by fitting planes to the observations at the surface and in the boreholes.

The evaluated transmissivities are generally in the range 10^{-6}-10^{-4} m^2/s with a median of about 10^{-5} m^2/s. The greatest transmissivities for these larger features are for the hydraulic conductor domains below the Baltic Sea and for the minor fracture zone NNW-4. The largest transmissivity is approximately $3 \cdot 10^{-4}$ m^2/s for hydraulic conductor domain NE-1.

Hydraulic rock mass domain

Hydraulic rock mass domains are geometrically defined volumes in space with properties different from surrounding domains (rock mass and conductors). They may either be defined by lithological domains or purely by interpretation of results from hydraulic tests.

The Äspö area is divided into five groups of Site hydraulic Rock mass Domains (SRD) with different hydraulic properties :

- SRD 1: Northern part of Äspö , bounded to the South by Northern part of EW-1
- SRD 2 : Volume bounded by Northern and Southern part of EW-1.
- SRD 3 :Southern part of Äspö bounded to the North by South part of EW-1 and to the South by EW-3.
- SRD 4 : South of EW-3.

- SRD 5: A Fine-grained granite domain in the middle of the tunnel spiral at about 350 m depth.

Outside Äspö SRD1-4 is assumed to be valid within an area bounded by EW-7 to the South and some 100 m outside Äspö to the West, North and East.

The data based on the injection tests with 3 m packer interval shows that the estimated median hydraulic conductivity for the rock mass, where data for the deterministic hydraulic conductors were excluded, is highest in within the discontinuity EW-1 (data from KAS04) and lowest in the southern part of Äspö. The tests on the test scales 3, 30 and 100 m do not indicate a decreasing hydraulic conductivity in the 0 - 500 m depth interval. Below the 600 m depth the hydraulic conductivity decreases on southern Äspö, but the result is only based on one vertical borehole. If the data from the 1700 m deep cored borehole KLX02 are included in the analysis the hydraulic conductivity seem to decrease below a depth of 600 m below sea level.

An investigation of the structural geology of water-bearing fractures was made in the tunnel. It was found that the entire fracture system consists of four main sets. The mapped water-bearing fractures and the fractures filled with grout in the tunnel (from the pre-grouting ahead of the tunnel face) are dominated by a subvertical fracture set striking WNW. This fracture set also has the highest frequency of all fracture sets. N-S, NNW subvertical sets and a subhorizontal set are also present but these sets are less pronounced. The mapped grout-filled fractures should be a good indicator of the water conducting fractures, as the grouting was performed generally 5-15 m ahead of the tunnel face where the rock mass should be fairly undisturbed. This indicates that the hydraulic properties of the rock mass is probably anisotropic. Hydraulic tests in probe holes drilled along the tunnel during excavation indicate that subvertical fractures striking approximately WNW and N-S are more transmissive than the others. It is believed that the WNW-NW and N-S fracture sets on a larger scale forms the hydraulic conductor domains called "NNW".

Occasionally single water conducting fractures in the hydraulic rock mass domains can be very transmissive and cause high flow rates into drilled boreholes.

Hydraulic tests were performed in different scales (length of tested borehole section). The results show that the evaluated effective hydraulic conductivities are dependent of the test scales.

Hydrological setting of the Äspö area

The land surface of Äspö is slightly undulating, with a maximum height of about 14 m, giving small drainage basins with some peatlands and sediments in the topographic lows. There are no perennial streams on the island. The surface water is drained to the sea by the peatlands, sediments or directly to the sea. The annual mean precipitation and temperature of the area are about 650 mm/year, and 6.5 °C respectively. The annual sea level fluctuations are generally within ±0.5 m.

The water table elevation above the mean sea level is about 30% of the elevation of the topography above mean sea level, within a few hundred metres from the coast line. During the construction of the tunnel the elevation of the water table decreased, mainly on southern Äspö. The minimum water table elevation in 1995 was about 100 m below sea level.

Hydrochemistry

The detailed information of the hydrochemical properties along the tunnel gave a more detailed picture of the variability in the data of the site. More important, the different processes affecting the hydrochemical conditions could be identified. Important hydrochemical information was also established based on data from the 1700 m deep corehole KLX02.

Episodic events have to a great extent governed the hydrochemical evolution since the last glaciation ended, some 13 000 years ago. At that time glacial melt water was flushed down into the fracture system to a depth of several hundred metres. The next episodic event took place when the Baltic fresh water lake turned to the brackish Litorina Sea some 7 000 years ago. Äspö was covered by the sea and the more dense sea water partly replaces the glacial water down to a depth where the salinity (or rather the density) was as high as in the overturning sea water. 3 000 - 4 000 years ago Äspö started to rise above the sea level, and meteoric water began to infiltrate the rock.

The present day conditions are: A thin lens of meteoric fresh water to a depth of 50 - 200 m. A saline water consisting of proportions of present and ancient Baltic Sea water and glacial melt water to a depth of 400 - 600 metres. Below this level the saline water still contains proportions of the glacial water which might represent even older glaciations and a saline water which has not been in contact with the atmosphere for a very long time, millions of year.

During the construction phase there were changes in the composition of the water flowing into the tunnel at different locations, see *Figure 2-10*. The variation in e.g. salinity was however relatively small, while the variations in the proportions of the different reference waters varied considerably. A view of the situation before and after tunnel construction is presented in *Figures 2-11--2-13*. The proportions of the most important reference waters are shown before and after the tunnel construction phase.

In *Figure 2-14* the dominating water types are illustrated, both for the situation before and after tunnel construction.

Microbial activity

Bacterial processes have influenced the hydrochemical conditions in different ways.

- Biological sulphate reduction has caused a large increase in the bicarbonate concentrations and a decrease in sulphate concentrations compared to

the Baltic Sea water. These reactions to a large extent take place in the sea bottom sediments, but also in the rock mass below the sea and elsewhere in the rock mass under Äspö.

- Microbially catalysed reduction of ferric iron minerals to ferrous iron is a process similar to the sulphate reduction. The iron reduction increases the concentrations of dissolved ferrous iron. Both these processes take place in anoxic conditions.

- Degradation of organic material in the uppermost part of the rock consumes the dissolved oxygen of the infiltrating surface water. The population of bacteria adjusts rapidly to any change in the flow conditions and within three weeks the inflow to a tunnel section at 70 m depth had turned from slightly oxic to anoxic, as a result of bacterial activity.

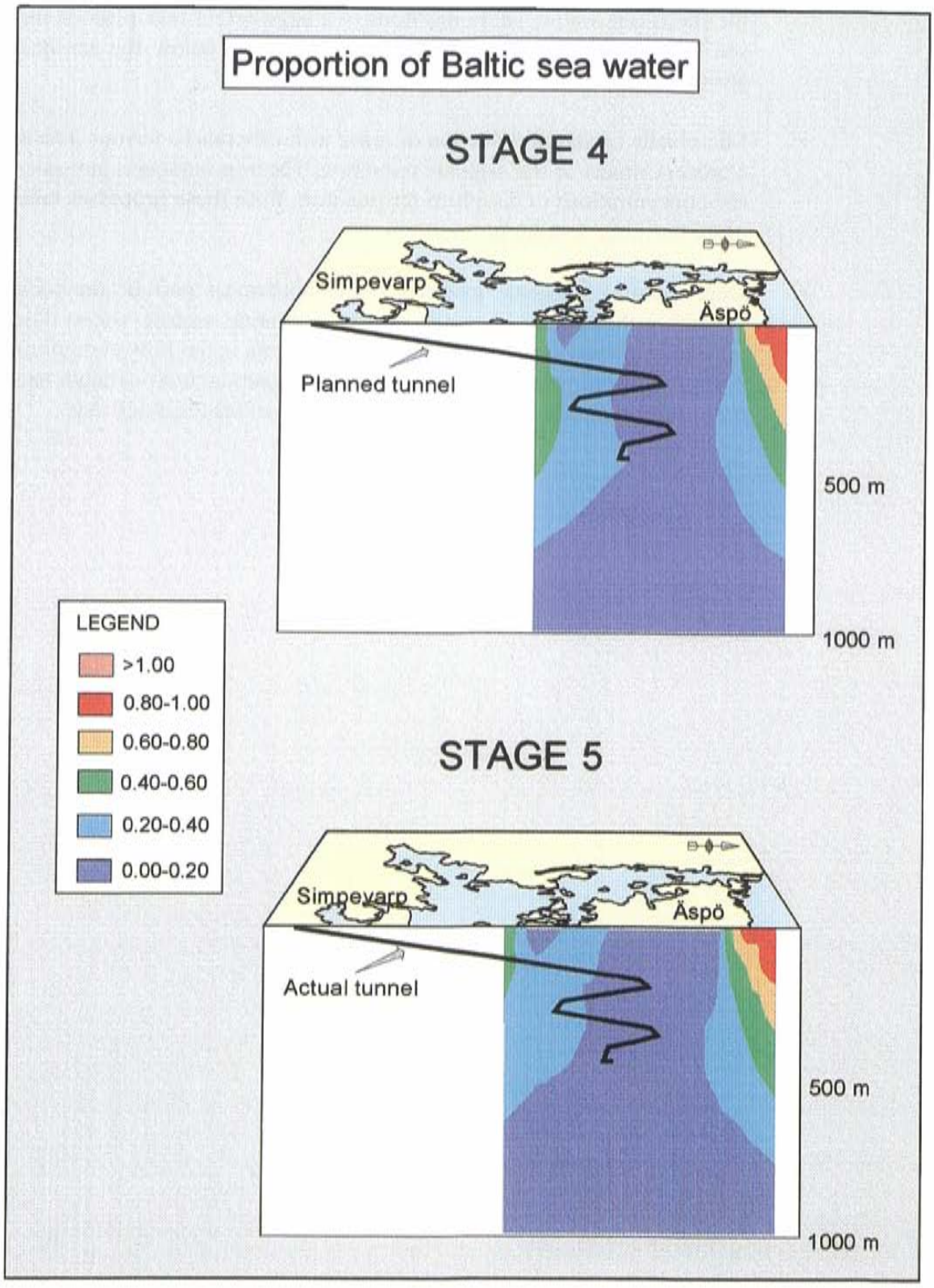

Figure 2-11. *Proportions of Baltic Sea water in the Äspö rock mass prior to and after tunnel excavation.*

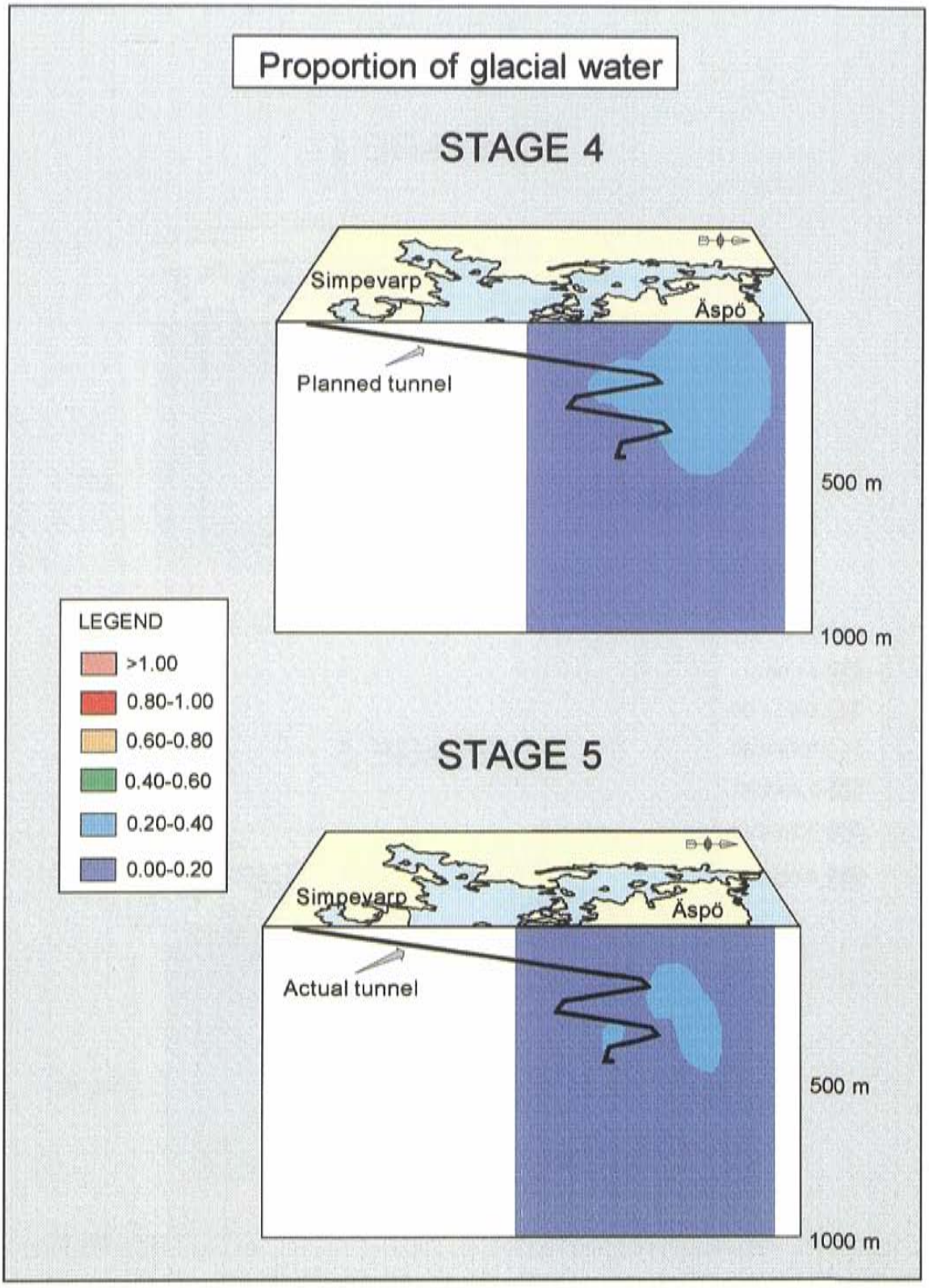

Figure 2-12. *Proportion of Glacial water in the Äspö rock mass prior to and after tunnel excavation.*

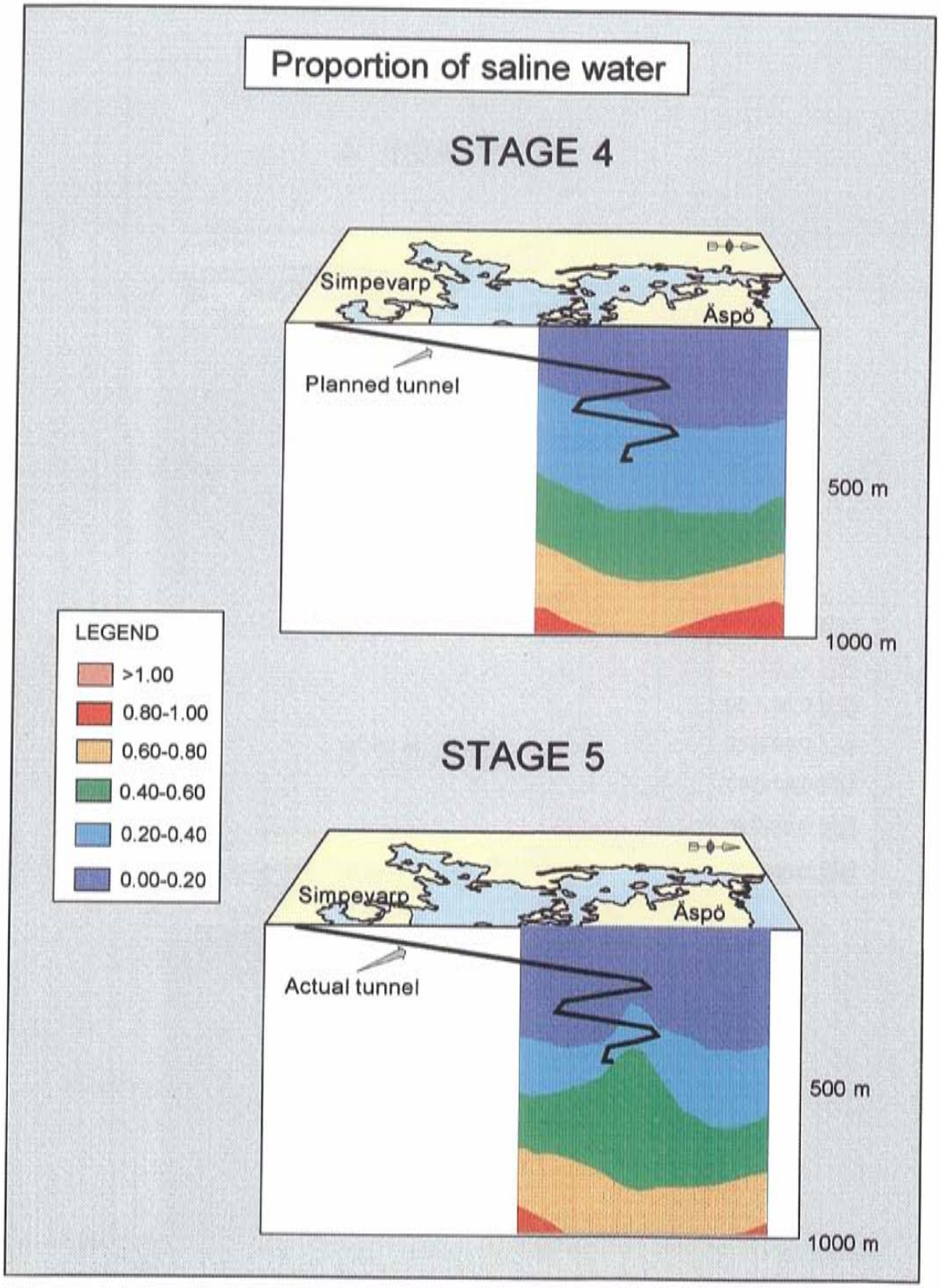

Figure 2-13. *Proportions of saline water in the Äspö rock mass prior to and after tunnel excavation.*

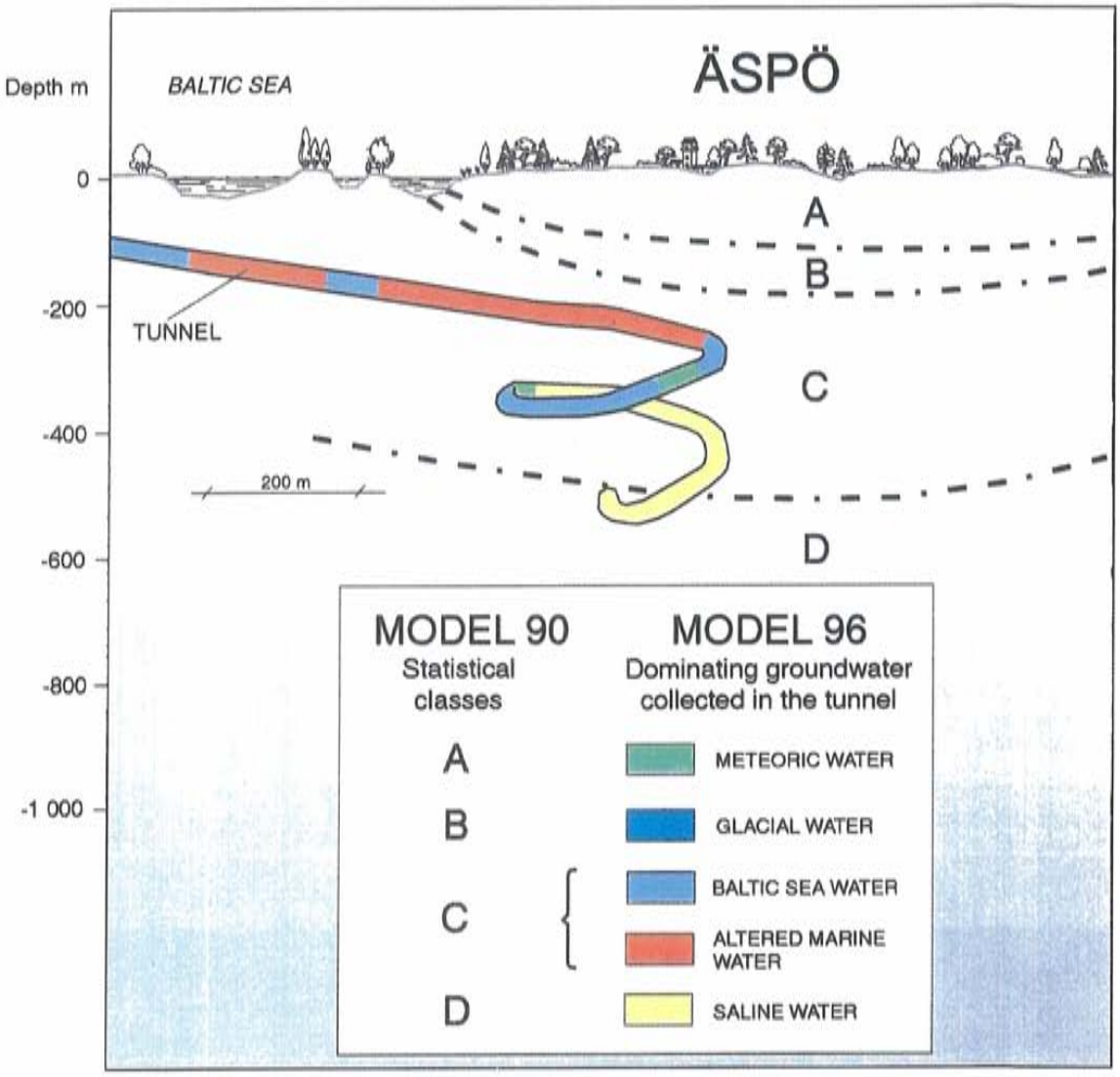

Figure 2-14. *Dominating reference waters in the Äspö rock mass prior to and after tunnel excavation.*

Table 2-1. Conceptual models in regional and site scale modelling for the Äspö Hard Rock Laboratory

Model stage	SKB TR 88-16 Regional flow modelling *Gustafson et al /1988/*	SKB TR 89-16 Regional flow modelling *Gustafson et al /1989/*	SKB TR 91-22 & 23 site scale modelling *Wikberg et al, Gustafson et al /1991/*
Scope	Natural flow Flow to underground laboratory	Natural flow Flow to underground laboratory Cross-hole tests (calibration)	Natural flow Flow to underground laboratory Cross-hole tests (calibration)
Processes	Darcian 2D flow	Darcian 3D flow Salinity	Darcian 3D flow Salinity
Structural units	Homogeneous sub-volumes (lithology, depth)	Planar conductive fracture zones Homogeneous sub-volumes (lithology, depth)	Planar conductive fracture zones Stochastic continuum in sub-units (lithology, depth)
Boundaries	Constant head on top No flow for the rest	Constant head on top No flow for the rest	Top: Fixed recharge (land), constant head (water) Sides: Prescribed pressures Bottom: No flow Tunnel: Given pressures (with or without skin)
Parameters	Hydraulic conductivity Head on boundaries Space coordinates	Hydraulic conductivity Zone transmissivities Head on boundaries Space coordinates	Stochastic distributions for hydraulic conductivity Transmissivity (deterministic for each zone) Salinity linearly increasing with depth Heads and recharge rates on boundaries Space coordinates
Parameter assignment method	Inference from other areas Analysis or regional data Inference from generic modelling Boundary heads = topography	Inference from TR 88-16 modelling Analysis or regional data Site specific conductivity data Boundary heads = topography	Inference from TR 89-16 modelling Analysis of regional data Site specific conductivity data Site specific transmissivity data Water chemistry data Recharge from sensitivity studies Calibrations

3 CONCEPTS USED FOR THE DESCRIPTION OF THE ÄSPÖ ROCK VOLUME AND ITS BOUNDARIES

3.1 INTRODUCTION

This chapter presents the concepts behind the Äspö models in different geometrical scales for the key issues :

- Geological-structural model,
- Mechanical stability,
- Groundwater flow,
- Hydrochemistry and
- Transport of solutes.

The issues chosen are the main issues considered relevant at the beginning of the Äspö HRL project to design, performance assessment and safety assessment of a final repository for spent fuel, see *Figure 3-1.*

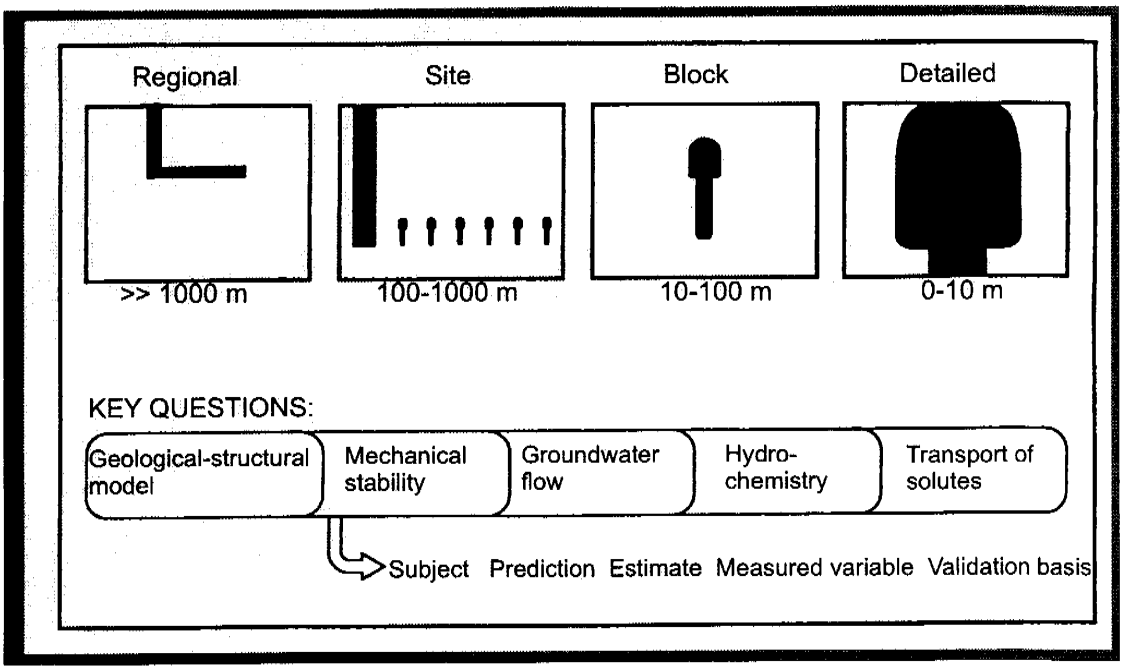

Figure 3-1. *Overview of geometrical scales and key issues. /Bäckblom et al, 1990/.*

3.1.1 Rationale behind key issues

The **geological-structural model** describes structures on different scales and represents a simplification of the real physical medium. The geological model forms the geometrical basis of all models of the geosphere, regardless of the processes described. The geological model not only forms the geometrical basis of the models, but is also of vital importance as decisions on the design of the repository will be influenced by it. A repository volume will in the future be selected to avoid major fracture zones. Deposition tunnels and spent fuel canisters will be positioned to avoid the major flow paths.

Mechanical stability of the rock mass is of interest both in a short and a long-term perspective. Mechanical stability is a necessary condition during construction. The long-term issue is to identify potential zones of movement, so that these can be avoided for emplacement of the spent fuel canisters.

Groundwater flow is an important factor that may influence the service life of the spent fuel canisters and the dissolution of the spent fuel. The description of the groundwater flow provides a necessary, but not sufficient, basis for calculating the transport of nuclides from the repository to the biosphere if the waste package should fail.

Hydrochemistry is an issue as the chemical situation influences the corrosion of the spent fuel canisters and the dissolution of the waste. Hydro chemistry provides a necessary, but not sufficient, basis for calculating the transport of nuclides from the repository if the spent fuel canisters should fail.

Transport of solutes provides a necessary, but not sufficient, basis for calculating radiation doses from a sealed final repository.

3.1.2 Rationale behind the geometrical scales

Characterization on a **regional scale** >1000 m provides a basis for selecting a suitable rock volume for the repository and defining boundary conditions for the site scale. Areas of groundwater recharge and discharge can be defined. The regional assessment will provide a basis for long-term predictions of the future location of discharge areas as well as where potential zones of movement can be found.

The **site scale** characterization, 100 - 1000 m, will be used to locate major fracture zones and/or major flow paths. These investigations are essential as they will provide guidance in determining the repository depth as well as the main layout of the repository. Characterization on this scale also provides data to assess the far-field groundwater flow through the repository and flow paths to the biosphere.

Block scale characterization and data, 10 - 100 m, will be used for detailed layout of the repository. Safety assessments include the transport of solutes from a leaking waste package to major flow paths.

The **Detailed scale**, 0 - 10 m, may be the most important scale, as properties on this scale define the geohydrological, chemical and mechanical near-field of the waste package. By proper selection of waste package positions it will be possible to provide the suitable environment for long-term isolation of the waste.

This definition of geometrical scales is, however, more or less subjective. It may also be pointed out that a real site is likely to be larger than a square kilometre and is of course not limited by the so-called site scale.

3.1.3 Conceptual models

The structure of conceptual models

In order to clarify the assumptions behind models used, a proposal of how to structure these assumptions was made in *Olsson et al /1994/.* The structure is presented in *Table 3-1.* An essential objective has been to condense the model description to one page and still present the essential aspects of each model. It is hoped that in this way it will be easier to obtain an overview of the assumptions underlying each model and facilitate comparison between different models.

Rationale for the structure of the conceptual models

The base for the model description is to specify the *intended use of the model.* Based on the intended use the next step is to decide what *physical processes* should be included in the model. In some cases these processes can be represented by constitutive equations. The next step is to define the *concepts* needed to solve the problem. The concepts may be separated into four groups. Firstly, the type of *geometrical framework* and framework-related parameters have to be defined. Secondly, the type of *material properties* to be assigned to the domains defined by the geometrical framework must be decided. Thirdly, the *spatial assignment method* of the material properties within a domain has to be described. Finally, the model normally has a limited extent and the *boundary conditions* have to be defined to compute or judge the effects within the model. For a real case, the *data* can now be defined for the four groups of concepts by analysing measurements representing the actual case. If needed a *numerical or mathematical tool* that handles the processes and concepts should then be chosen. *Output parameters* of interest for model purposes must then be defined.

Table 3-1. Format for a condensed description of models in the Äspö HRL project. /After *Olsson et al, 1994/*.

MODEL NAME	
Model scope or purpose Specification of the intended use of the model	
Process description Specification of the process accounted for in the model, definition of constitutive equations	
CONCEPTS	**DATA**
Geometrical framework and parameters	
Dimensionality and/or symmetry of model. Specification of what the geometrical (structural) units of the model are and the associated geometrical parameters (the ones fixed implicitly in the model and the variable parameters).	Specification of the size of the modelled volume. Specification of the source of data for geometrical parameters (or geometrical structure). Specification of the size of the geometrical units and resolution.
Material properties	
Specification of the material parameters contained in the model (it should be possible to derive them from the process and geometrical units).	Specification of the source of data for material parameters (could often be the output from some other model). Specification of the value of material parameters.
Spatial assignment method	
Specification of the principles for the way in which material (and if applicable geometrical) parameters are assigned throughout the modelled volume.	Specification of the source of data for model, material and geometrical parameters as well as stochastic parameters. Specification of the result of the spatial assignment.
Boundary conditions	
Specifications of (type of) boundary conditions for the modelled volume.	Specification of the source of data on boundary and initial conditions. Specification of the boundary and initial conditions.
Numerical or mathematical tool Computer code used.	
Output parameters Specification of the computed parameters and possibly derived parameters of interest.	

3.2 GEOLOGICAL CONCEPTS

3.2.1 Scope

In this section the concepts behind the Geological-structural models on different scales are presented, see *Table 3-2* and *Figure 3-2*.

Table 3-2. Condensed description of the geological model of the Äspö site used within the Äspö HRL Project.

GEOLOGICAL MODEL OF THE ÄSPÖ SITE
Scope Description of lithology and tectonic structure to provide a framework for other models of the site.
Process description Geological development of southeastern Sweden in terms of tectonization, post- and anorogenic intrusives, faulting, and fracturing.
CONCEPTS
Geometrical framework and parameters 3D box with Lithological domains: Granitic rocks with lenses and xenoliths of minor rock types (summarized location of domains) Discontinuities: Essentially subvertical fracture zones, possibly also some low-dipping (location, extension, orientation, width)
Material properties Lithological domains: fracture density, composition (descriptive) Discontinuities: character (tensional/shear, classification; major/minor, fracture density)
Spatial assignment method Lithological domains: averaging, probabilistic with trends Discontinuities: deterministic (probability classification)
Boundary conditions Stationary

3.2.2 Process description

The processes are outlined in *Chapter 4*.

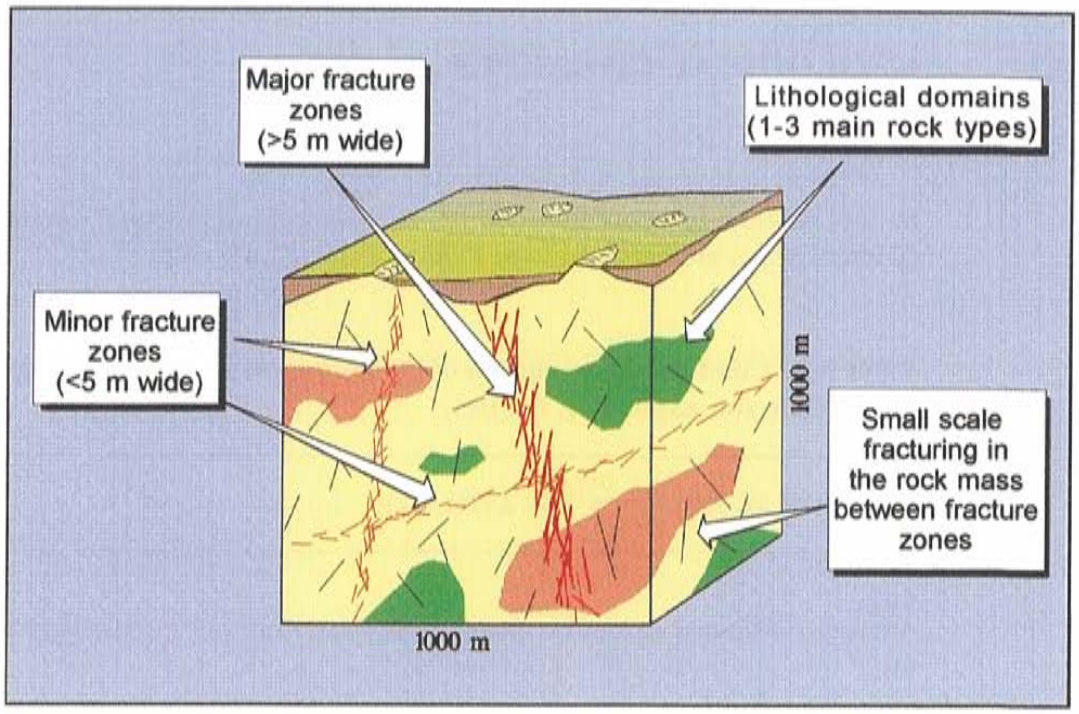

Figure 3-2. *Schematic description of two main components of the geological description. One is for the description of lithology and one for the description of discontinuities (fracture zones and fractures).*

3.2.3 Geometric framework and parameters

The model comprises of the following geometrical concepts:

- lithological domains
- discontinuity domains

Lithological domains are three-dimensional volumes in the rock mass defined by the rock mass classification or rock mass units (see below under material properties).

Discontinuity domains are two-dimensional features, which are mechanical discontinuities (or discontinuities grouped together) in the rock mass having little or no tensile strength.

Lithological domains - Classification : RMU - Rock Mass Units

Based on the pre-investigations the site area was divided into a number of rock mass units (RMU). A RMU is defined as part of the rock mass, bordered by major fracture zones, which is approximately statistically homogeneous with respect to geological and geohydrological characteristics.

Discontinuity domains

In order to define the existence of different discontinuity domains it was necessary to clarify the nomenclature for fracture zones and related topics. This was done during the first phase of the pre-investigations for the ÄHRL, */Bäckblom, 1989/*. The nomenclature and classification system used are presented in more detail in *Appendix A1*.

Nomenclature: Discontinuity domains. Fracture zone - fracture swarms - increased fracturing

This guideline treats aspects for use of nomenclature for site investigations and addresses the way in which geological, geophysical, geohydrological results should be named. A special section is devoted to the uniqueness and completeness of investigations.

According to this guideline, a fracture zone is a fracture zone - only and only - if geological field evidence supports zones **with the characteristic that the intensity of natural fractures is at least twice that of the surrounding rock**. Completely disintegrated and/or chemically altered rock is included in the definition of a fracture zone.

The definition of a fracture zone can be expanded by additional characteristics. A fracture zone can thus be 'a hydraulically conductive fracture zone' or a 'non-conductive fracture zone'.

During mapping in the tunnel it was found that this definition would, however, designate most fine-grained granites as fracture zones. Thus, it was necessary to add a tectonic/kinematic constraint to the definition of 'fracture zone' such as shearing, faulting and clay alteration. Sections in the tunnel with more than 5 fractures/metre, with no obvious tectonic/kinematic influence were mapped as zones with 'increased fracturing'.

The term fracture swarm has also been used and is defined as a zone with relatively high fracture frequency, but not so high as a proper fracture zone */Bäckblom, 1989/* with fractures essentially parallel to the orientation of the swarm boundary */Hermanson, 1995/*.

The term 'major fracture zone' was used for a feature more than about 5 m wide and extending several hundred metres. Features less than about 5 m and more than 0.1 m wide and of less extent were called 'minor fracture zones'.

Persistent, several-metre-long fractures, mostly steep and estimated to be significant hydraulic conductors were called 'single open fractures'.

3.2.4 Material properties

Classification: Rock type

The petrographical classification of the rocks, was done using modal analyses according to the system worked out by *Streckeisen/1967, 1976/* and *IUGS /1973, 1980/.*

The rocks are divided into 4 rock groups, see *Figure 3-3*. The physical properties density and magnetic susceptibility were used to classify the main lithological units.

The density of crystalline rock is very closely related to its mineral composition. The influence of porosity on density, in crystalline rocks is less than one per cent.

The density of the rock is controlled by the amount of mafic minerals and the SiO_2-content. Rocks containing a large amount of mafic minerals and with a low SiO_2-content generally have a high density (> 3 000 kg/m^3) while rocks with a lesser amount of mafic minerals and high SiO_2-content generally have a lower density (2 600 - 2 700 kg/m^3).

The magnetic susceptibility in crystalline rocks is proportional to the content by volume of magnetite (below 10%) and, to some degree, to the content of paramagnetic minerals (iron in silicates).

Magnetite is the most frequent magnetic mineral in crystalline rocks and by using a special classification diagram the effect of magnetite on the density is easily removed. **Silicate density** is the density when the effect of the magnetite has been removed.

A classification limit between one more acid variety of the Småland (Ävrö) granite intrusion and a more basic variety called Äspö diorite was fixed at a silicate density of 2.65 - 2.70 g/cm^3.

The most basic rock variants observed in some boreholes on Äspö, with a silicate density above 2.75 g/cm^3, were assigned to the Greenstone group (including diorites - gabbros).

3.2.5 Spatial assignment method

Discontinuity domains are defined deterministically by the location, extent, orientation and width of the domain. As regards extent the discontinuities are normally estimated to be connected in a network. The discontinuity domain, or parts of it are classified according to judged level of reliability (see *Geometrical framework and parameters in Appendix A1*).

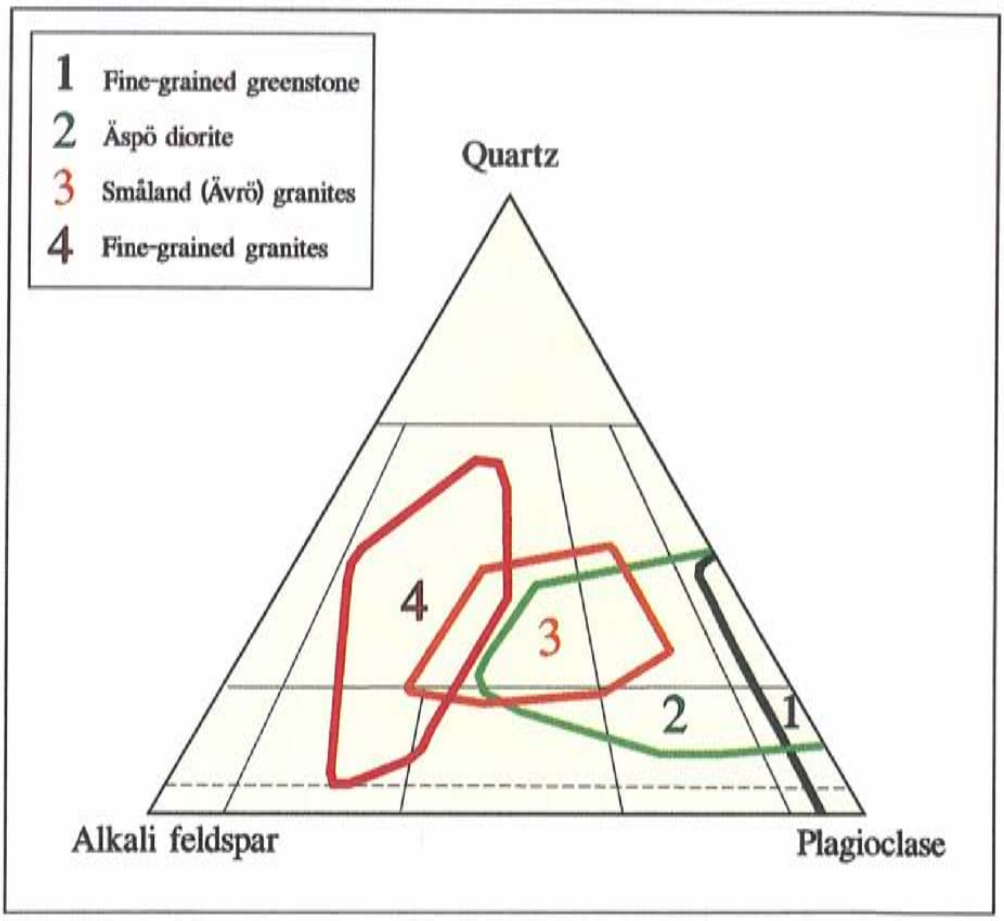

Figure 3-3. *Modal classification /according to IUGS 1973, 1980/ of 4 rock groups from the Äspö area.*

Lithological domains are volumes judged to have approximately the same properties within the volume (statistical homogeneity). Material properties are generally given as a mean value, but may also be given as a probability of existence at a given coordinate within a domain.

3.2.6 Concepts used in different scales

Regional scale

The description on a regional scale consists of following parts:

- Lithological domains
- Major discontinuities (major fracture zones)

Site scale

The description on site scale consists of following parts:

- Lithological domains (four main rock types - Småland (Ävrö) granite, Äspö diorite, greenstone and fine-grained granite)

- Discontinuities (major fracture zones, minor fracture zones, fracture swarms and small scale fracturing in the rock mass).

The site scale is illustrated in *Figure 3-4.*

Block scale

The description on block scale consists of following parts:

- Lithological domains (four main rock types - Småland (Ävrö) granite, Äspö diorite, greenstone and fine-grained granite)

- Discontinuities (minor fracture zones , fracture swarms and small scale fracturing in the rock mass)

The purpose is to make a generic description of typical blocks (approximately 50x50x50 m), considering the rock type composition and discontinuities likely to be found within the rock volume, or part of it, described under site scale. The block scale is illustrated in *Figure 3-5.*

Detailed scale

The description on detailed scale consists of following parts:

- Lithological domains (four main rock types - Småland (Ävrö) granite, Äspö diorite, greenstone and fine-grained granite)

- Discontinuities (small scale fracturing in the rock mass).

The purpose is to make a generic description of each rock type (approximately 5x5x5 m) likely to be found within the rock volume. The detailed scale is illustrated in *Figure 3-6.*

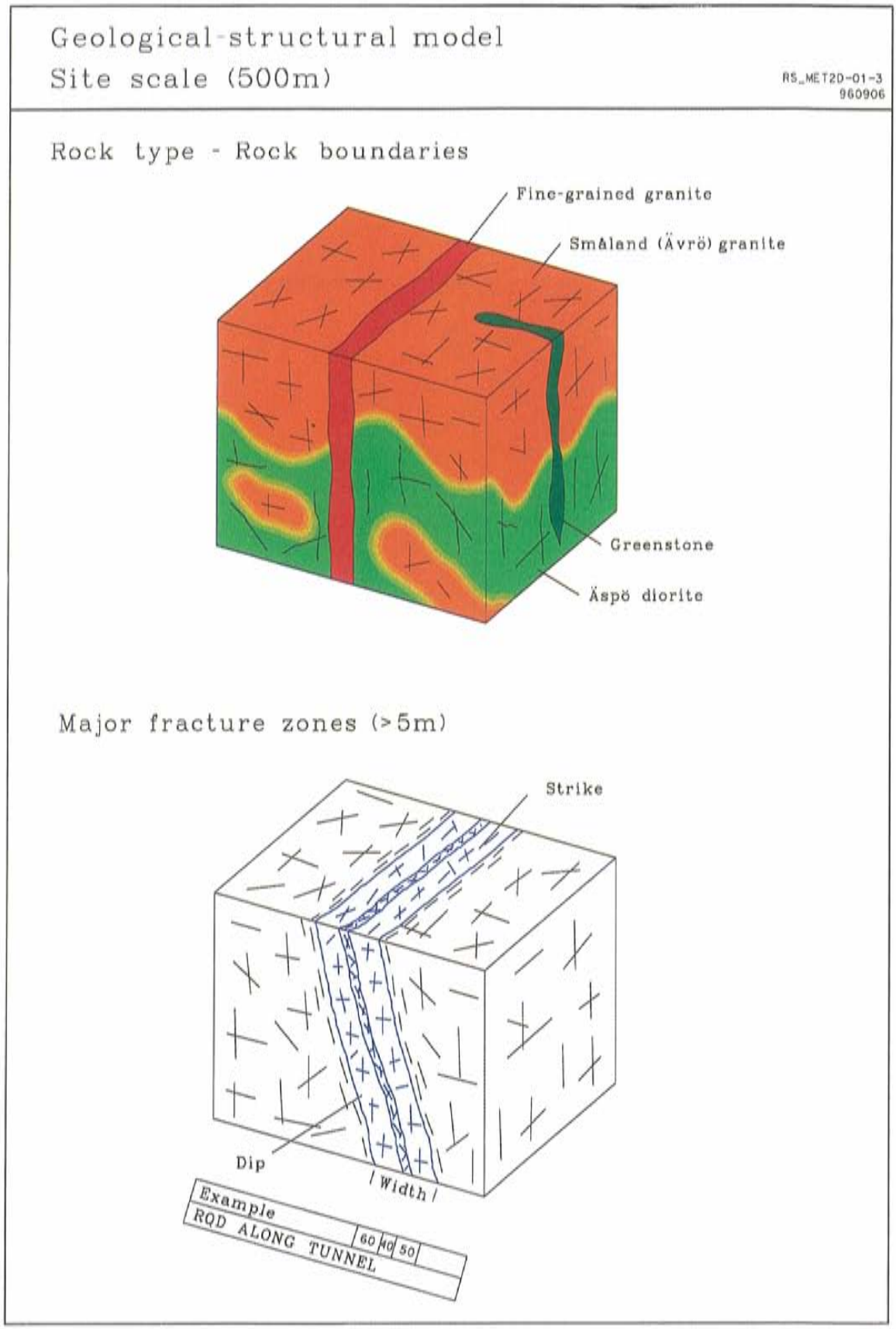

Figure 3-4. *Rock types, rock boundaries and major fracture zones of the geological-structural model, addressed on the site scale.*

Geological-structural model
Block scale (50m)

RS_MET2D-02-2
940322

Single open fractures
Mylonite
Minor fracture zones (< 5m)

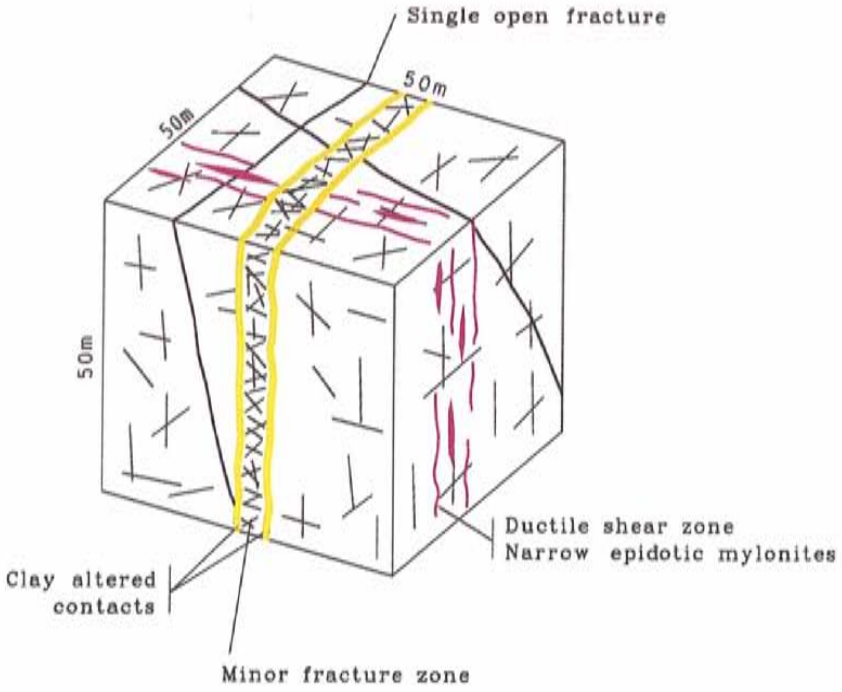

Rock composition

Occurence and extension of greenstone and
fine-grained granite in host rock

Rock boundaries

Number of rock boundaries

Fracture system

Main fracture set orientation

Figure 3-5. *Single open fractures, mylonite, minor fracture zones, rock composition, rock boundaries and fracture systems of the geological-structural model, addressed on the block scale.*

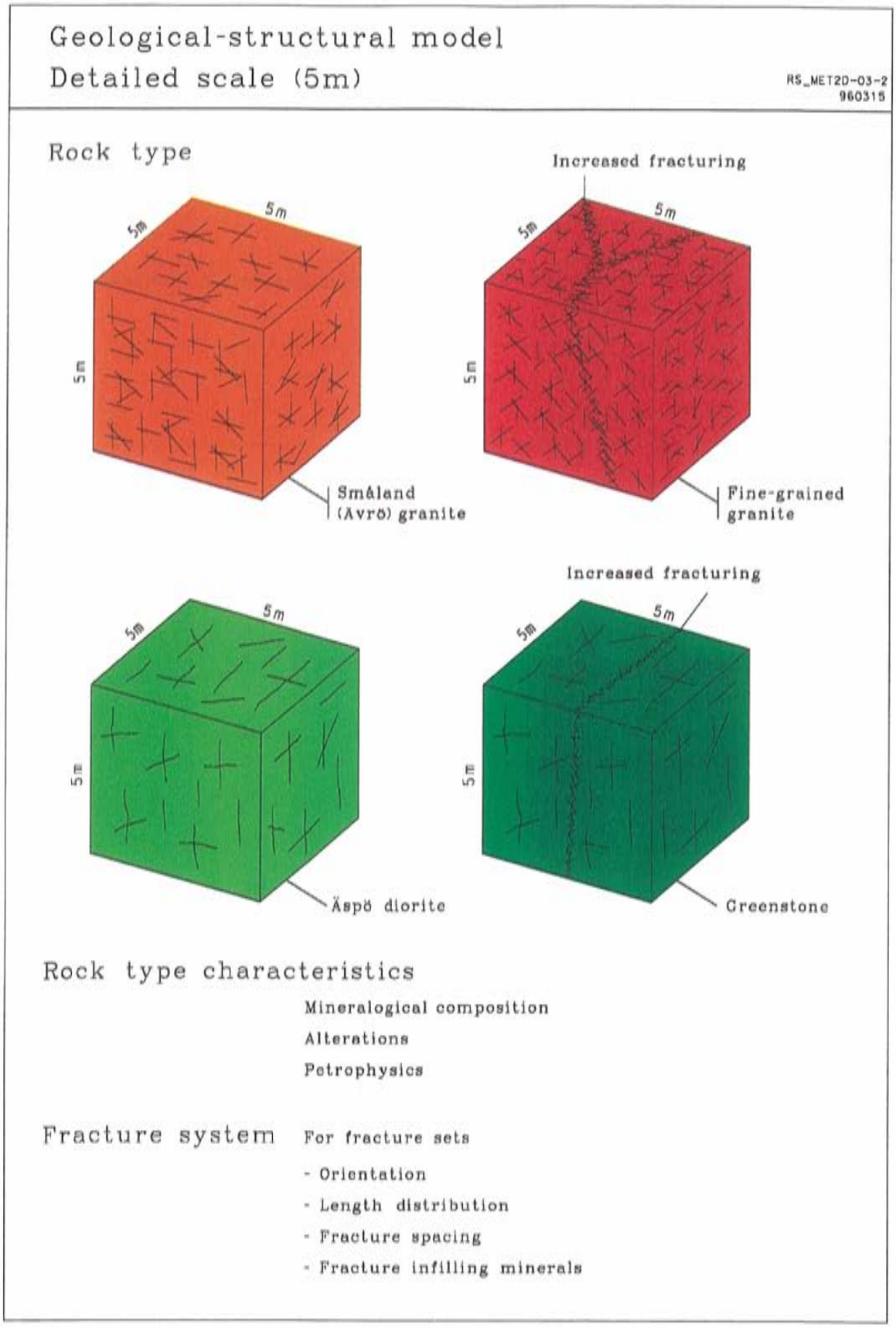

Figure 3-6. *Rock type characteristics and fracture system of the geological-structural model (for the four main rock types), addressed on the detailed scale.*

3.3 MECHANICAL STABILITY CONCEPTS

3.3.1 Scope

In this section the concepts behind the Mechanical Stability models on different scales are presented, see *Table 3-3--3-5*.

Table 3-3. Condensed description of the concepts for rock stress at the Äspö site within the Äspö HRL Project.

MODEL NAME
Rock stress

Model scope or purpose
State of stress.

Process description
State of stress: Calculation of rock stress field assumes continuum, homogeneous, isotropic, linear elastic material based on measured strains (overcoring) or evaluation of measured pressure responses and tensile strength of the rock (hydraulic fracturing).

CONCEPTS

Geometrical framework and parameters
Rock stress: Three-dimensional box for primary stresses at boundaries. Shape of opening for rock stresses close to excavation.

Material properties
Rock stress: Young's modulus, Poisson's ratio and tensile strength of the rock (hydraulic fracturing).

Spatial assignment method
Homogeneous.

Boundary conditions
Primary stresses at measurement points and linear regression of stresses with depth.
Vertical stress calculated from weight of overburden.

Numerical or mathematical tool
-

Output parameters
Rock stress.

Table 3-4. Condensed description of the concepts for excavation stability at the Äspö site within the Äspö HRL Project.

MODEL NAME
Excavation stability

Model scope or purpose
Assessment of potential non-elastic behaviour of rock, assessment of potential engineering problems.

Process description
Empirical-based expert system, like Rock Mass Rating.

CONCEPTS

Geometrical framework and parameters
Based on geological model (lithology, discontinuities) and empirical relations.

Material properties
RMR: (strength of intact rock material, drill core quality (RQD), spacing of discontinuities, condition of discontinuity, groundwater and strike and dip of discontinuities). Joint surface parameters for characteristic joint sets: (JRC, JCS, spacing, RQD).

Spatial assignment method
Grouping of RMR in five classes and deterministic determination of mean and range of RMR for the tunnel. Application of the Bayesian Markov geostatistical model to spatial assignment of RQDs was also tested.

Boundary conditions
-

Numerical or mathematical tool
-

Output parameters
Potential for excavation instability, assessment of rock quality for engineering purposes.

Table 3-5. Condensed description of the concepts for rock burst at the Äspö site within the Äspö HRL Project.

MODEL NAME
Rock burst

Model scope or purpose
Assessment of potential non-elastic behaviour of rock, assessment of potential engineering problems.

Process description
Empirical-based expert system, measurement of brittleness on cores.

CONCEPTS

Geometrical framework and parameters
Geological model, stresses and empirical relations.

Material properties
Empirical assessment based on values of rock stress and unconfined compressive strength. Brittleness based on comparison of energy used prior to failure and energy after failure as measured on intact specimen.

Spatial assignment method
-

Boundary conditions
Local stress field.

Numerical or mathematical tool
-

Output parameters
Assessment of potential for rock burst in each rock type, potential for excavation instability, assessment of rock quality for engineering purposes.

3.3.2 Process description

The process description discusses the virgin stress situation in relation to regional tectonic events such as stress field resulting from plate drift and stress release during and after the latest deglaciation.

Based on the geometrical conditions of the underground facility, e.g. layout and size of tunnel, an elastoplastic analysis was made to indicate the present mechanical stability conditions.

3.3.3 Geometric framework and parameters

Rock quality is estimated for the different lithological domains *(Section 3.2)*.

The rock quality comprises a number of parameters all of which are related to the general stability conditions.

3.3.4 Material properties

Mechanical characteristics

Rock strength (unconfined compressive strength)

Elastic moduli

Poisson's ratio

Brittleness

Fracture properties

Joint Roughness Coefficient
(JRC)

Joint Wall Compression
Strength (JCS)

Fracture frequency

Fracture density
(RQD)

Rock mass stability

The purpose of the classification was to divide the rock mass into representative groups in which the rock mechanics characteristics are different. For this classification the Geomechanics Rock Mass Rating (RMR) */Hoek, 1980/* system proposed by Bieniawski was used. This system employs five parameters describing the rock mass and is simple to use when the classification is based on pre-investigation data. If any parameter is missing, it is possible to estimate the value of the missing character.

In the Geomechanics Classification System the parameters describing the rock mass are allocated points according to a proposed scale. The rock mass is described by parameters for strength of the rock material, RQD (Rock Quality Designation) value, spacing of discontinuities, conditions of discontinuities and the flow of water into the underground development.

The sum of all points allocated to the different parameters describes the rock mass in the form of a value called the RMR value (Rock Mass Rating). Finally the RMR value is adjusted for the joint orientation.

The RMR value varies between 0 and 100 and in general terms the different RMR values are often described as follows:

RMR	**Classification**
100-81	Very good rock
80-61	Good rock
60-41	Fair rock
40-21	Poor rock
20-0	Very poor rock

Stability classification : Rock blocks

The purpose of the classification was to estimate what failure mechanisms that would be present at different ranges of RMR value. The mechanism of failure will decide the demand, type and intensity, of rock support.

Class A	Refers to	RMR >72
Class B	"-	RMR 60-72
Class C	"-	RMR 40-60
Class D, E	"-	RMR <40

For the classification of the rock mass in the Äspö tunnel the RMR-system was applied. This system employs five parameters describing the rock mass and is more simple to use when the classification is based on pre-investigation data. If any parameter is missing, it is possible to estimate the value of the missing parameter. The Q-system is more complex and employs more parameters. The

RMR-system is usually divided into five different groups which correspond to 'very good rock' to 'very poor rock'. To get a more accurate prediction for the Äspö tunnel the rock mass was divided into five groups which were estimated to better apply to the different stability conditions expected to be significant */Stille and Olsson, 1996/.*

The following stability conditions were in the prediction estimated to apply to the different rock mass classes:

Class A Instability of single blocks.

Class B Instability of single key blocks which may progress to failure of the roof arch. Orientation of joints will determine the amount of rock support necessary.

Class C Instability in the roof. Difficult to locate all unstable areas. Both small and large blocks have to be supported. Large blocks are supported by bolts and smaller blocks by shotcretes. Bolts and Shotcretes are applied systematically.

Class D General instability in walls and roof. A rock arch has to be established to make the tunnel stable. This necessitates systematic installation of bolts and shotcretes.

Class E As class D.

3.3.5 Spatial assignment methods

The rock mechanics properties and rock stress measurement data within a special domain are normally given as a mean value for the entire domain.

Estimates of potential movements or displacements in existing discontinuities are mainly based on expert judgement.

Estimates of rock burst are based on measured mean values for elastic material properties and rock stress conditions. Finally, a great portion of expert judgement is applied.

3.3.6 Concepts used in different scales

Regional scale

The model comprises of the following concept:

- Rock stress

The purpose is mainly to make an analysis of the possible risk of spalling in the investigation areas. The analysis is based on rock stress measurement data and laboratory tests on rock samples.

Site scale

The model comprises of the following concepts:

- Rock quality
- Rock stress
- Long-term stability

The purpose is to make a description of the rock quality in different rock units based on the RMR system, make an evaluation of the rock stress situation based on rock stress measurements (horizontal and vertical) and estimate the long-term stability with special respect to zones of potential movement.

Block scale

The model comprises of the following concepts:

- Rock quality
- Rock stress
- Stability

The purpose is to make a description of the rock quality (RMR) in the typical blocks (approximately 50 x 50 x 50 m) described in *Section 3.2.4*. Analysis of in-situ stresses and estimates of mechanism of failure are also made for the same rock blocks.

Detailed scale

The model comprises of the following concepts:

- Rock stress
- Stability
- Rock burst

The purpose is to estimate the rock stress situation in a number of special rock blocks (approximately 5 x 5 x 5 m) described in *Section 3.2.5*. Mechanisms of failure and the rock burst (spalling) risk are also estimated for these rock blocks.

3.4 GROUNDWATER FLOW

3.4.1 Scope

This section deals with the concepts behind the geohydrological models on different scales. The concepts described in *Table 3-6* and *Figure 3-7* have been the base for the numerical groundwater flow modelling with the finite-volume code PHOENICS */Spalding, 1981/*. A few of the concepts below have not been used for the numerical groundwater flow modelling with the code PHOENICS up to summer 1997 but are outlined in the model description, *Chapter 6*, as suggestions for future simulations. Some concepts for evaluation of the material parameters are also presented in *Section 3.4*.

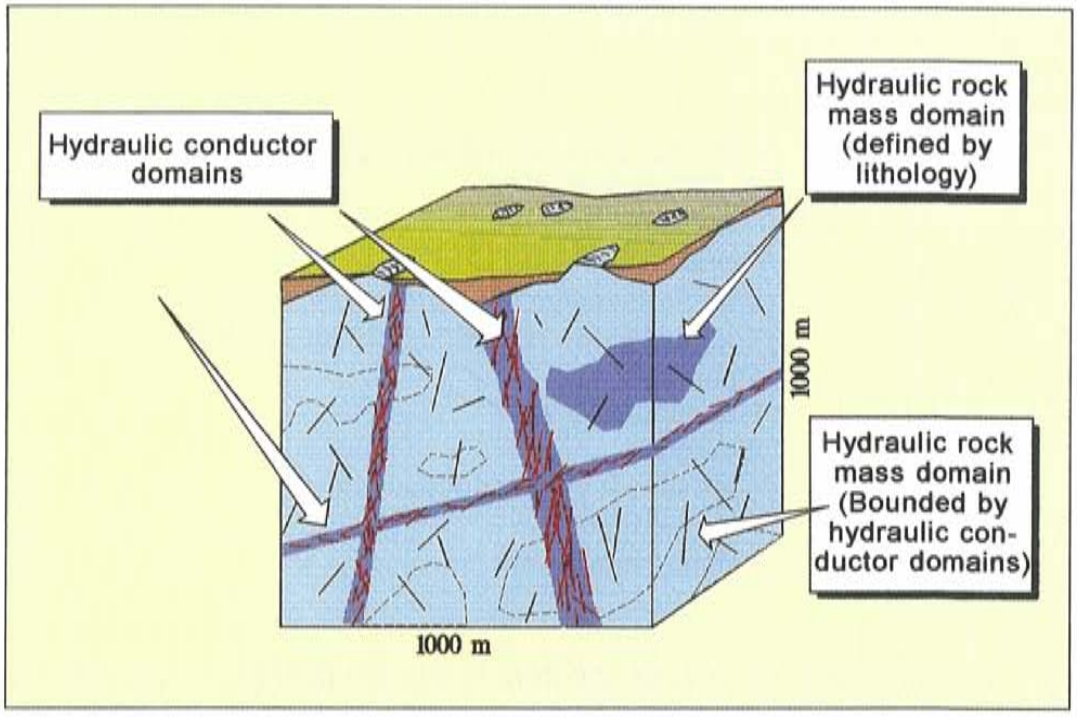

Figure 3-7. *Schematic description of two main hydrogeological concepts. Hydraulic conductor domains: 2-D features (location, extent, orientation) and hydraulic rock mass domains: 3-D features.*

3.4.2 Process description

The process description describes the continuity, state and motion equations in the groundwater flow model:

The continuity equation (Mass balance equation):

$$-\nabla \rho \mathbf{q} = \frac{\delta(n\rho)}{\delta t} + \rho Q \qquad (3\text{-}1)$$

The equation of motion:

$$\mathbf{q} = - \frac{\mathbf{k}}{\mu} (\nabla p + \rho \cdot g \cdot \nabla z) \qquad (3\text{-}2)$$

The equation of state:

$$\rho = \rho(p, C, T) \qquad (3\text{-}3)$$

$$\mu = \mu(p, C, T) \qquad (3\text{-}4)$$

$$\nabla = \left(\frac{\delta}{\delta x}, \frac{\delta}{\delta y}, \frac{\delta}{\delta z} \right) \qquad (3\text{-}5)$$

C	=	Concentration of different components	(kg/m^3)
g	=	Acceleration of gravity	(m/s^2)
k	=	Permeability (tensor)	(m^2)
p	=	Pressure	(Pa)
q	=	Specific discharge or filtration velocity (vector)	(m/s)
Q	=	Volumetric flow rate of fluid withdrawn/unit volume	(m^3/s)
t	=	Time	(s)
T	=	Temperature	(°C)
z	=	Elevation	(m)
μ	=	The dynamic viscosity of the fluid	(Pa s)
ρ	=	Fluid density	(kg/m^3)
n	=	Volumetric porosity	(-)

Equation 3-1 assumes that there is only one fluid phase to consider, but the equations can be changed to incorporate multi-phase flow. If some of the variables mentioned above can be considered constant or almost constant the equations can be simplified:

- The influence of p and T on the density are neglected in the numerical simulations. It is assumed that the concentration of salts (salinity) controls the density (see *Equation 3-10*). The salinity (s) is dependent on the advection and the dispersivity, see *section 3.6* for details.

- It is also assumed that the matrix behaves as an elastic medium, dependent on a coefficient of bulk compressibility and a slightly compressible fluid. The fluid is assumed to have a constant coefficient of compressibility and that ρ can be considered approximately constant which lead to *Equation 3-8* This permits reformulation of *Equation 3-1* to *Equation 3-6*. However, up to summer 1997 only steady state simulations have been performed with the code PHOENICS.

Table 5-1. Condensed description of the groundwater flow model of the Äspö site used within the Äspö HRL Project up to 1995.

GROUNDWATER FLOW MODEL OF THE ÄSPÖ SITE
Stochastic continuum model

Scope
Natural groundwater flow, flow to laboratory tunnel

Process description
Continuity equation (mass balance equation).
Equation of motion (Darcy's law, including density-driven flow).
Equation of state (Salinity-density relationships).

CONCEPTS

Geometrical framework and parameters
Three-dimensional box divided into:
- Hydraulic conductor domains. 2-D features (location, extent, orientation).
- Hydraulic rock mass domains. 3-D features (location of boundaries).

Material properties
Hydraulic conductor domains: Transmissivity (T).
Hydraulic rock mass domains: Hydraulic conductivity (K).

Spatial assignment method
T: Deterministic assignment.
K : log-normal distributions for hydraulic conductivity (K_g, $s(Log_{10}(K))$.
K and s are dependent on the cell size within a domain in the numerical model.

Boundary conditions
Upper: Infiltration rate dependent on the drawdown (*Model 96*) or fixed infiltration rate on Äspö, constant head at sea and peat areas (-1995).
Lower: no flow.
Side: prescribed pressure (hydrostatic).
Salinity: prescribed initial conditions, linear increase with depth at vertical boundaries (see concepts for the transport of solutes).
Tunnel: hydraulic resistance (skin factor) around the tunnel and prescribed pressure (atmospheric) **or** flow rate into the tunnel.

Numerical tools
Finite-volume code PHOENICS.

Output parameters
Groundwater pressure
Groundwater flux

- It is also assumed that μ and ρ can be considered approximately constant which lead to reformulation of *Equation 3-2* to *Equation 3-7* based on *Equation 3-9.*

$$-\nabla \rho \mathbf{q} = \frac{1}{g} S_s \cdot \frac{\delta(p)}{\delta t} + \rho Q \qquad (3\text{-}6)$$

$$\mathbf{q} = \frac{\mathbf{K}}{\rho \cdot g} \cdot (\nabla p + \rho \cdot g \cdot \nabla z) \qquad (3\text{-}7)$$

$$S_s = \rho_0 \cdot g \, (\alpha_b + n \cdot \beta_l) \qquad (3\text{-}8)$$

$$\mathbf{K} = \frac{\rho_0 \cdot g \cdot \mathbf{k}}{\mu} \qquad (3\text{-}9)$$

$$\rho = \rho_0 \cdot (1 + \alpha \cdot s) \qquad (3\text{-}10)$$

g	=	Acceleration of gravity	(m/s^2)
$\mathbf{k}$	=	Permeability (tensor)	(m^2)
$\mathbf{K}$	=	Hydraulic conductivity (tensor)	(m/s)
p	=	Pressure	(Pa)
$\mathbf{q}$	=	Specific discharge or filtration velocity (vector)	(m/s)
s	=	Salinity	(kg/kg)
S_s	=	Specific storage	(1/m)
z	=	Elevation	(m)
α	=	Expansion coefficient	(-)
α_b	=	Compressibility of porous medium (bulk)	(m^2/N)
β_l	=	Coefficient of compressibility of a fluid	(m^2/N)
μ	=	The dynamic viscosity of the fluid	(Pa s)
ρ	=	Fluid density	(kg/m^3)
ρ_0	=	Reference fluid density	(kg/m^3)
n	=	Volumetric porosity	(-)

In the PHOENICS simulations ρ_0 was set to 1000 kg/m^3 and α to 0.8. In the site model of *Model 96* α was set to 0.78.

If the hydraulic head gradient within a feature is constant over the entire thickness b of the feature, the flow field can be described as a two-dimensional feature with material properties :

$$\mathbf{T} = \int_0^b \mathbf{K}\, d\xi \tag{3-11}$$

$$S = \int_0^b S_s\, d\xi \tag{3-12}$$

b	=	Thickness of the feature	(m)
K	=	Hydraulic conductivity (tensor)	(m/s)
S_s	=	Specific storage	(1/m)
S	=	Storage coefficient	(-)
T	=	Transmissivity (tensor)	(m^2/s)
ξ	=	Coordinate axis parallel to line with constant hydraulic head gradient	(m)

3.4.3 Geometric framework and parameters

The model comprises of the following geometrical concepts:

- Hydraulic conductor domains
- Hydraulic rock mass domains.

Hydraulic conductor domains are large two-dimensional features with hydraulic properties different from the surrounding rock. Generally they are defined geologically as major discontinuities but in some cases they may mainly be defined by interpretation of results from hydraulic interference testing.

Hydraulic rock mass domains are geometrically defined volumes in space with properties different from surrounding domains (rock mass domains and hydraulic conductor domains). They may either be defined by lithological domains or purely by interpretation of results from hydraulic tests.

3.4.4 Material properties

The material properties chosen for the domains are

- Hydraulic conductor domains — Transmissivity (**T**); Storage coefficient (S)
- Hydraulic rock mass domain: — Hydraulic conductivity (**K**(xyz)); Specific storage (S_s(xyz)).

T and **K** are assumed to be isotropic and each tensor can therefore be described by a single parameter value (T, K). ((xyz) are coordinates.)

Up to summer 1997 only steady state simulations have been performed with the code PHOENICS.

3.4.5 Spatial assignment method

The properties within a domain may be given as an mean effective value for the entire domain, a trend within the domain, a statistical distribution within the domain with or without spatial correlation or any other function describing the distribution within the domain. The description of the properties assumes that the domains can be described as a continuum considering the processes. For the groundwater flow model at Äspö HRL the following spatial assignment methods were used for T and K and suggestions for S and S_s are given below.

The properties for a hydraulic conductor domain are given as constant values for the domain. The storage coefficient (S) is given as a function of T if no evaluated S is available (see *Chapter 6*).

The properties of a hydraulic rock mass domain are given as a stochastic distribution for the domain. The distribution of K is assumed to be lognormal with characteristic values K_g (geometric mean) and s_{LOG10K} (standard deviation of $Log_{10}(K)$). K_g and s_{LOG10K} are scaled according to the cell size in the numerical model (see *Chapter 6* for scale function). No spatial correlation is assumed in most cases. The stochastic distribution of K is in this report assumed to have a lower limit representing an approximate value for the more or less unfractured rock mass (see *Chapter 6*).

The specific storage (S_s) is given as a function of K with a lower limit for S_s (see *Chapter 6* for the function).

3.4.6 Boundary conditions

The boundary conditions used in the numerical models on site and regional scales are:

Upper boundary:

Up to 1995: Fixed infiltration rate on Äspö, constant pressure head at sea and peat areas.

Model 96, Regional model: Net precipitation (P-E) = 200 mm per year and net groundwater recharge depending on level of topography and water level. Constant pressure head at sea.

Model 96, Site scale model: Net precipitation (P-E) = 100 mm and net groundwater recharge depending on level of topography and water level. Constant pressure head at sea.

In *Model 96*, as implemented in the numerical model, the groundwater recharge is dependent on the level of the water table. Drawdown increases the local groundwater recharge. The upper boundary in *Model 96* is modelled in the following way: P-E, Precipitation minus Evaporation, is set to specified value (mm/year) in the model. Capillary forces are not considered, which means that pressure in the unsaturated zone will be equal to the atmospheric pressure, here set to zero. It then follows that the vertical conductivity, K_z, is equal to P-E close to the ground surface. This can be understood from the balance of forces:

$$0 = -\frac{\delta p}{\delta z} - \frac{\rho g}{K_z} w\varphi - \varrho g,$$

where w is the vertical Darcy velocity, ϱ density and g the gravitational constant. φ is estimated by iteration in order to achieve p = 0 in the unsaturated zone */Svensson, 1997a, 1995b/.* The resistance factor φ also reduces the horizontal hydraulic conductivities. For the unsaturated zone close to the ground p = 0 and w = -(P - E) and hence K_z = P - E.

Side boundary:

Up to 1995: Prescribed pressure (hydrostatic with an assumed salinity distribution). Salinity: linear increase with depth at vertical boundaries and water flowing into the model is given the salinity value corresponding to the depth for the inflow (see *Section 3.6* - transport of solutes - for details).

Model 96, Regional model: Boundaries facing the Baltic (eastern and part of the southern boundary) are assigned hydrostatic pressure and two linear functions for the increase of salinity by depth, based on measurements of natural conditions at Laxemar and Äspö. No flow for other boundaries.

Model 96, Site model: Boundary conditions from regional model except for the uppermost 100 m in the model where zero flux conditions were used due to the resolution of the computational net.

Lower boundary:

Up to 1995: No flow.

Model 96, Regional model: No flow.

Model 96, Site model: boundary conditions from regional model.

Internal boundaries:

Tunnel: skin (local hydraulic resistance) for rock around the tunnel and prescribed pressure (atmospheric) **or** no skin for rock around the tunnel and flow rate into the tunnel.

3.4.7 Method for evaluation of hydraulic properties

Transmissivity (T): T for a section in a borehole is generally evaluated from transient tests using the method developed by *Cooper and Jacob /1946/*, and is valid for the test section or hydraulic conductor interpreted to control the measured pressure change. If it has only been possible to evaluate the specific capacity (Q/s), the transmissivity is estimated as T= f(Q/s), where the function f(Q/s) is the linear least-square-fit of $Log_{10}(T)$ versus $Log_{10}(Q/s)$ for tests with evaluated T and similar test length and test time. The rationale for this is that Q/s is roughly proportional to T */Carlsson and Gustafson, 1984, Domenico and Schwartz, 1990/*. If T is evaluated for the entire borehole (T_{tot}) and flow logging has been done, the approximate T distribution along the borehole is estimated according to *Earlougher /1977/* as $T_i = T_{tot} \cdot dQ_i / Q_{tot}$, where Q_{tot} is the total flow rate and dQ_i is the flow rate change per length i. The dynamic viscosity of the fluid and fluid density was assumed to be approximately constant within the rock volume tested.

The evaluated T for two-dimensional feature is normally based on a transient test where the feature has been straddled by packers. If there were no tests where the feature was straddled by packers, T_i (defined as above) was used for the feature. If no test at all had been performed in a geologically defined fracture zone, the geological character, properties for other hydraulic conductor domains and expert judgement were used to estimate possible properties.

Hydraulic conductivity (K): It is assumed that the medium is stochastic continuum and a local K, in the text called *effective hydraulic conductivity*, is generally evaluated as T/L, where L is the test section length, also here in the text called *test scale*. Evaluated K is always linked to the test scale in the approach used. It is discussed further in *Chapter 6*.

The rationale for using a 2D approach for the evaluation is that in most cases the flow-dimension can be interpreted to be radial flow.

Storage coefficient or storativity (S): This is evaluated from interference tests for a two-dimensional feature if the concepts for two-dimensional flow are interpreted to be valid. If no evaluated value is available S is estimated at S=f(T) (see *Chapter 6*).

Specific storage (S_s) can in principle be evaluated from interference tests but this is mostly impossible for conceptual reasons as the flow field in the fractured rock in many cases cannot be expected to be as assumed in the evaluation

methods generally used. If no evaluated value is available S_s is estimated at S_s=f(K) (see *Chapter 6*).

3.4.8 Concepts used in different scales

Regional scale

The model comprises of the following geometrical concepts:

- Hydraulic conductor domains
- Hydraulic rock mass domains.

Transmissivities for the hydraulic conductor domains are assigned deterministically and are in almost all cases based on geological classification combined with the evaluated transmissivities for the hydraulic conductor domains at Äspö, as no hydraulic tests has been performed in the structures.

Two concepts are used for assigning hydraulic properties to the hydraulic rock mass domains. The first concept is to divide the rock mass vertically by zonation, not taking lithological domains in consideration. In the second concept the lithological domains define the hydraulic rock mass domains. The hydraulic conductivity is assumed to have a stochastic distribution with no spatial correlation.

Boundary conditions are assigned in the way described in *Section 3.4.1.*

Site scale

The model comprises of the following geometrical concepts:

- Hydraulic conductor domains.
- Hydraulic rock mass domains.

Transmissivities (T) for the hydraulic conductor domains are assigned deterministically. T is based on transient hydraulic tests in most cases but is sometimes based on geological classification combined with the evaluated transmissivities for the hydraulic conductor domains at Äspö, when no hydraulic tests have been performed in the structures.

The concept is to divide the rock mass vertically by zonation, not taking lithological domains in consideration except for a large body of fine-grained granite within the tunnel spiral. The hydraulic conductivity is assumed to have a stochastic distribution with no spatial correlation.

Boundary conditions are assigned described in *Section 3.4.1.*

Block scale

The model comprises of the following geometrical concept:

- Hydraulic conductor domains.

The block scale comprises a description of the expected distance between hydraulic conductors with transmissivities (T) greater than a given value of T. The purpose is not to use the estimates directly in the numerical simulations, but to provide a generic description of hydraulic characteristics of blocks within the site scale.

Detailed scale

The model comprises of the following geometrical concept:

- Hydraulic rock mass domains.

The detailed scale prediction comprises a description of the expected hydraulic conductivity (K) for each lithological unit. The purpose is not to use the estimates directly in the numerical simulations, but to provide a generic description of hydraulic characteristics of lithological units within the site scale.

3.4.9 Numerical tool

PHOENICS

The code mainly used within the Äspö HRL project is PHOENICS, a finite-volume code */Spalding, 1981/*. Depending of the purpose of the modelling different concepts have been used. A brief overview of the modelling performed within the Äspö HRL with PHOENICS up to summer 1997, including modelling concerning the transport of solutes, is given in this section. Site scale models normally included density driven flow caused by differences in salinity concentrations.

Hemström and Svensson /1988/ examine how dispersion, diffusion and changes in the hydraulic conductivity field and infiltration rates affect the fresh water/saltwater interface. *Svensson /1988/* studied the way in which stochastic hydraulic conductivity fields and dispersion affect the fresh water/saltwater interface. The salt-dome and Henry's problem were also tested. Before the performance of the LPT1 pumping tests simulation of the pumping test was performed */Svensson, 1990b/*. Before the performance of the LPT2 pumping tests simulation of the pumping test was also performed. Flow paths were calculated using the particle-tracking technique assuming an effective porosity */Svensson, 1991b/*. In *Svensson /1990a/* the Äspö site was modelled and the principle of how the hydraulic conductor domains were included in the model

were presented. In *Svensson /1990c/* the Äspö site was modelled and test case 2 HYDROCOIN, Level 1 was also modelled. The drawdown caused by the Äspö HRL was predicted before the start of excavation */Svensson /1991a/.* The drawdown caused by the Äspö HRL was remodelled a number of times, but with the actual flow rates into the tunnel. The model from 1990 was used but modified structural models were also used */Svensson /1994a,c, 1995c/.* Several subprograms for PHOENICS have been developed and tests of different modelling techniques were made during the project. *Svensson /1992a/* tested the way in which micro dispersion and sorption could be incorporated into a particle-tracking routine. *Svensson /1992b/* dealt with effective conductivity versus standard deviation of hydraulic conductivity, modelling of the groundwater recharge, high resolution around boreholes and dispersion in fractured rock. *Svensson /1994b/* tested routines for stochastically generated transmissivities for hydraulic conductor domains, particle tracking with sorption and desorption and visualization. In *Kuylenstierna and Svensson /1994/* an effective algorithm for generating fracture aperture distributions was presented. Visualization possibilities were tested further in *Svensson /1995a/* and in *Svensson /1995b/* an algorithm for the unsaturated zone was developed. The composition of the flow into the tunnel was studied by reversing the velocity field and releasing particles at the observation point to see where the particles ended up (back tracking) */Ittner and Gustafsson, 1995/.* New regional and site scale models were made late 1996 to summer 1997 */Svensson 1977a,b/.* Some of the results are presented in *Chapter 8.*

Other numerical codes used within the Äspö HRL project

A few other codes have been used but the concepts behind these are not outlined here. The reader is referred to the reports mentioned below.

Generic modelling of the drawdown due to different designs of the planned Äspö HRL was presented in */Axelsson, 1987/.* Before the performance of the LPT1 pumping test simulations of the pumping test were performed using a finite element model */Grundfelt et al, 1990/.* In order to see if it was possible to estimate effective values of the hydraulic conductivity of a rock block measuring 50 m simulations using a Discrete Fracture Network (DFN) model were made */Axelsson et al, 1990, La Point et al, 1995/.*

3.5 HYDROCHEMISTRY CONCEPTS

3.5.1 Scope

The hydrochemistry concepts are presented in *Table 3-7.*

Table 3-7. Condensed description of the components of the hydrochemical models of the Äspö site.

HYDROCHEMICAL MODELS OF THE ÄSPÖ SITE
Scope: Present and past groundwater composition in fracture zones and hydraulically interconnected single fractures. (Does not include water isolated in the rock matrix, e.g. fluid inclusions.)
Process description: Mixing of water with different origin and composition. Groundwater/rock interaction: Calcite saturation, redox defining processes, biological activity, ion exchange.
CONCEPTS
Geometrical framework: Mixing in deterministic fracture zones defined as planes in the rock volume. Distribution of groundwater types in the rock mass.
Groundwater properties: Concentrations of Na, Ca, K, Mg, Cl, SO_4, HCO_3, Fe, HS. The master variables pH, Eh, and contents of TOC (Total Organic Carbon), dissolved gasses, microbes, isotopes.
Spatial assignment method: The following alternative methods have been used: • Traditional hydro-geochemical evaluation methods, • Multivariate (Principal component) analyses, • Linear regression, • Kriging, • Neural Networks.
Boundary conditions: Conditions affecting the groundwater chemistry presently and in the past, i.e. End-members and reference waters for mixing calculations.
Output parameters: Mixing proportions of reference waters and end-members, Saturation index, equilibrium concentrations, Data on groundwater properties and residence time.

The hydro-geochemical properties of the rock mass at Äspö were characterized by sampling at different points of the rock mass and fracture zones. The identified major fracture zones are commonly also the major hydraulic

conductor domains[1]. The hydraulic properties of these can vary by several orders of magnitude. Because of this the groundwater flow and the chemistry in the different zones can also vary.

The groundwater composition was first correlated with depth and then to the specific fracture zones. The function for the dependence was evaluated from the data collected during pre-investigations. The predictions of the conditions to be found in the tunnel were then based on the spatial distribution of the data. The concentration of a constituent [i] was seen as a function at the geometrical position, = $f_i(x,y,z)$, for all the major constituents: Na, Ca , Mg, Cl, HCO_3, SO_4, (see *Figure 3-8*). As the groundwater chemistry is changing, especially during the tunnel construction phase, time need to be included as well, f_i (x,y,z,t).

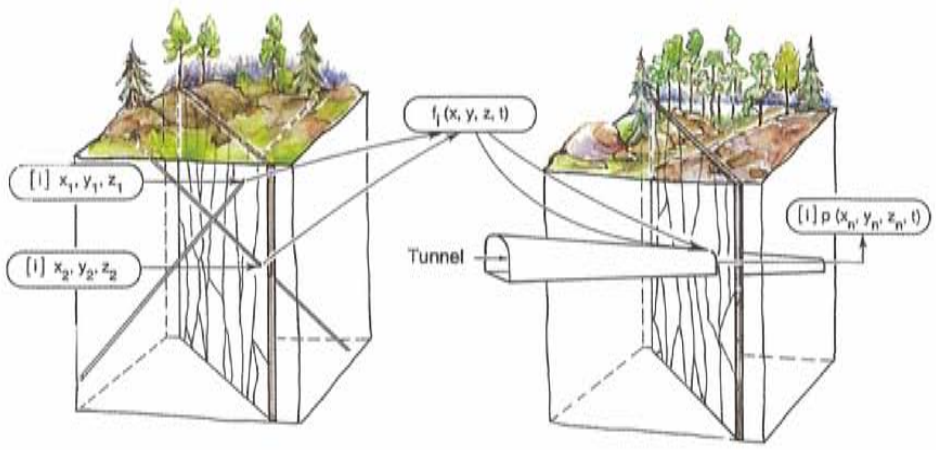

Figure 3-8. *A schematic illustration of the way the hydrochemical predictions were made on the basis of borehole data collected during the course of the pre-investigations.*

In the past, different chemical processes and hydrological conditions have affected the hydrochemistry. These processes are far back in the past and can be defined to e.g. t=-13000 years, when the last glaciation retreated from the Äspö area. The hydrochemistry is affected also by the different stages of the

---

1 Depending on the rock stress situation and the genesis of the fracture zones single open fractures can be more water conducting than large fracture zones. In such cases the groundwater sampling and the predictions are also made for the conducting single fractures.

Baltic Sea up to present day. The anticipated most important episodes are defined under boundary conditions, *Section 3.5.6.*

The inflow to the tunnel causes changes on a much shorter time scale. The data collected from the tunnel are therefore evaluated at fixed time steps from start of the tunnel construction, e.g. at 150, 350, 550 days. The transient effects caused by the water inflow to the tunnel and its relation to hydrochemical conditions is presented in the *Part 3* (Transport of solutes) in the report on assessing the pre-investigation methodology */Rhén et al 1997/.*

3.5.2 Process description

Mixing of water with different origin and composition

The observed hydrochemistry is a result of mixing and reactions. Mixing calculations were made to establish feasible mixing ratios of different groundwater types that describe the observed groundwater composition. The mass balance calculations are then made to describe the extent of reactions, chemical and biological, needed to explain the measured groundwater composition which cannot be accounted for by mixing. For the mixing calculations end-members and reference waters are selected.

A standard multi-variate technique called Principal Component Analysis (PCA) was used for the calculations. */Chatfield and Collins, 1989/.* This technique was used to classify and compare groundwater data */Laaksoharju and Nilsson, 1989, Laaksoharju, 1990, Smellie and Laaksoharju, 1992/.* The major components Cl, Ca, Na, Mg, K, SO_4, HCO_3 and the isotopes ^2H, ^{18}O and ^3H were used in the PCA calculations */Laaksoharju and Skårman, 1995/.*

Groundwater/rock interaction

The interaction between the groundwater and the rock minerals will approach an equilibrium between the dissolved and the solid phases. However, some reactions are fast while some are extremely slow. Equilibrium modelling is therefore done routinely only for those reactions which are considered to have reached equilibrium, i.e. the calcite - carbonate - pH system and the ferric oxide - ferrous iron system and a few others involving the solid phases FeS, FeS_2, CaF_2, $CaSO_4$, $BaSO_4$, $Mg(OH)_2$, etc.

The groundwater/rock interaction is not expected to have a major influence on the present day conditions since the reactions are so slow. However, for the genesis of the deep saline water (the brine) the water-rock interaction has played an important role.

Calcite saturation

Calcite saturation is commonly reached in all deep groundwater systems. Through the concentrations of calcium and bicarbonate and the pH value it is possible to calculate the calcite saturation index. For the quality control of the groundwater samples it is necessary to check the saturation index. A large deviation from saturation could indicate errors in the analyses or sample treatment. However, mixing of water with different composition can also cause supersaturation. A change in the groundwater flow conditions in the future could influence the hydraulic properties of the calcite filled fractures, through dissolution and opening of sealed fractures, while others could be sealed by precipitation.

Redox properties

The investigated groundwaters are generally reducing at a depth of a few tens of metres, even though in some cases oxidizing waters are found at depths of 100 m. An oxidizing groundwater exhibits an absence of ferrous iron, sulphide and manganese and has high uranium concentration (ppm levels). Dissolved oxygen in a measurable quantity solely defines oxidizing conditions. Reducing conditions are defined by the presence of ferrous iron, sulphide and manganese together with low uranium concentrations (ppb levels).

The empirical pH-Eh relation is established on a firm understanding of the iron redox couple. The reactions determining electrode potentials are transitions between dissolved ferrous iron and ferric iron oxyhydroxide */Grenthe et al. 1992/*.

Biological activity

A number of microbially related processes in subterranean environments can be identified. Most of them influence geo-chemical processes and some would not occur at all unless bacteria catalysed the reactions */Pedersen and Karlsson, 1995/*:

- **The cycling of carbon.** Most deep rock environments have relatively low content of organic carbon but measurable amounts of carbon dioxide. The participation of bacteria in the carbon cycle implies their interaction with fracture mineral formation and degeneration. Bacterial production and consumption of carbon dioxide may have an effect on the pH and alkalinity of groundwaters.

- **The cycling of nitrogen.** Deep groundwater is usually depleted in nitrate, nitrite, ammonia and other nitrogen compounds except for dinitrogen gas. Nitrification processes are usually aerobic and will be limited by the anaerobic character of the deep rock environments and the limited availability of ammonium.

- **The cycling of iron and manganese.** The activity of iron-reducing bacteria may help to bring down the redox of infiltrating water by reducing ferric iron to ferrous iron during the oxidation of organic material. When groundwater, rich in ferrous iron, reaches an oxygenated atmosphere in the tunnel, gradients suitable for iron and manganese oxidizing bacteria develop. They precipitate iron or manganese in various forms together with other metals.

- **The cycling of sulphur.** Sulphate reducing bacteria cause anaerobic sulphide production.

- **Hydrogen-related bacteria.** Low concentrations of hydrogen in many environments may be due to the fact that it is consumed by different bacteria and transformed into methane, for instance.

- **Methane-related bacteria.** Many deep groundwater samples contain methane of biological origin, indicating on-going methanogenic activity. Still, much of the evidence for deep biological methanogenic activity depends on stable carbon isotope values for methane. It remains to be determined whether this bacterial gas is produced by on-going processes of methanogenesis or whether it originates in geologically old reservoirs stored in the crystalline rock.

- **Acetogenic bacteria.** Acetogenic bacteria are able to gain energy from the reduction of carbon dioxide by molecular hydrogen. In addition, many acetogenic bacteria produce acetate and hydrogen from sugars. They are thereby a vital link between hydrolysis/acidogenesis and methanogenesis in anaerobic ecosystems.

3.5.3 Geometric framework

The geometrical framework, in which the processes are active, are the major water conducting fracture zones and single fractures. The hydrochemistry of the low-conductivity rock was investigated in a pilot study.

Most features are within the boundaries of Äspö island. However, for the evolution of the hydrochemistry, the descriptions also cover the Laxemar area, west of Äspö.

3.5.4 Groundwater properties

Definitions

For hydrochemical sampling purposes it is practical to classify the borehole sections in relation to their permeability:

- *Highly conductive (transmissive)* relates to a borehole section (zone) with a hydraulic conductivity (transmissivity) *above 10^{-6} m/s (m^2/s)*,

- *Conductive* relates to borehole sections from which it is possible to sample groundwater, with a transmissivity of 10^{-6} - 10^{-8} m^2/s,

- *Low conductive* when the transmissivity is *below 10^{-8} m^2/s*.

The following definition of non-saline water, brackish water and saline water which rembles the one reported by *Davies /1964/* has been used.

- *Non-saline* with a chloride concentration below 1000 mg/l
- *Brackish water* with 1000-5000 mg/l of chloride
- *Saline water* with more than 5000 mg/l of chloride.
- *Brine* when the salinity is above 100 000 mg/l.

Properties

The nature of the groundwater is basically described by the concentrations of major constituents and the master variables pH and Eh.

The major constituents mostly also reflect the origin and evolution of the water. The main constituents, Na, K, Ca, Mg, Cl, HCO_3 and SO_4 indicate the groundwater residence time in the rock by showing the extent of the rock/water interaction. The anions of this group are potential complexing agents for some radionuclides.

F, Br, PO_4 and SiO_2 are useful for identifying the origin of the water and the state of equilibrium. Fe(II), $Fe_{(tot)}$ and S(-II) are primarily analysed in order to describe the redox conditions and thus to support the Eh measurements. They also provide information on the buffer capacity of the water.

The usefulness of the different isotopes are described briefly below.

Oxygen-18 and *Deuterium* are useful for describing the temperature of the recharged meteoric water. Because the temperature has changed dramatically since the most recent glaciation, the oxygen-18 values can be used to indirectly define the residence time of the water. This method is useful for providing a residence time, based on present historic knowledge of the salinity and the climate changes in the Baltic Basin. Oxygen-18 and Deuterium are expressed as $\delta^{18}O$ and $\delta^{2}H$ in per mil deviation from Standard Mean Ocean Water (SMOW).

Carbon-14 is a classical groundwater age-determination method. For deep groundwater the analyses are performed on the bicarbonate dissolved in the water, or on the organic carbon (fulvic and humic acids) dissolved in the water. In order to give correct results these substances should be conservative, i.e. have the same history as the water. This is, however, never the case so the carbon-14 date cannot be directly interpreted as the age or residence time of the

water. Typically the analyses performed on the bicarbonate give too high an age, whereas the analyses performed on the organic carbon are perhaps more correct. At Äspö all carbon-14 data were obtained from the bicarbonate, since the content of organic substances was too low for analyses. Carbon-14 dating cover the range up to 35 000 years, and is frequently expressed as PMC (Percent Modern Carbon).

Carbon-13 is another stable isotope which is useful in tracing different ongoing processes in the groundwater. The carbon cycle, especially in the shallower groundwaters, can be examined qualitatively and quantitatively using carbon isotopes. The $\delta^{13}C$ values tell us if there is an atmospheric CO_2 input, biogenic degradation of organic matter as well as carbonate dissolution processes. It is important to trace the carbon source in order to understand redox-processes and changes in the pH of the groundwater, e.g. biological activity. The Carbon-13 values are expressed as $\delta^{13}C$ per mil deviation from a standard */Clark and Fritz, 1997/.*

Tritium is a good tracer for determining the proportion of modern water. Tritium levels above a background of about 0.3 TU (tritium units) clearly indicate the presence of water that has infiltrated the ground since fusion bomb tests in the atmosphere were started in the late 1950s. In the period since then the amount of tritium in precipitating rainwater has varied from 2500 TU in 1963 to a present-day value of less than 20TU.

Strontium-87 is a useful isotope for tracing the origin of the water. The strontium entering a groundwater is usually derived by chemical weathering and diagenesis from the host rock mass. Therefore, the isotopic composition of strontium in the groundwater reflect a specific source. The strontium isotope fingerprint is hence useful in studies of groundwater mixing. The apparent isotopic homogeneity of the strontium isotope ratios in the different end-members observed at Äspö enable us to use the $\delta^{87}Sr$ values as a criterion for e.g. distinguishing between non-marine and marine waters. In addition, $\delta^{87}Sr$ values of the groundwater, can be used an indicator of ion exchange reactions between the water and rock. Strontium-87 is expressed as $\delta^{87}Sr$ deviation in per mil from a standard */Clark and Fritz, 1997/.*

Sulphur-34 is a useful isotope for tracing the sulphate source. The isotopic ratio of $\delta^{34}S$ may, however, easily be affected by bacterial sulphate reduction processes as well as oxidation of sulphides. Hence, observed changes in the $\delta^{34}S$ value of the dissolved sulphate by time in the groundwater is used to trace certain ongoing processes. Sulphur-34 is expressed as $\delta^{34}S$ deviation in per mil from a standard */Clark and Fritz, 1997/.*

3.5.5 Spatial assignment method

Traditional geo-chemical evaluation incorporates the integration of all the collected data into a description which is mostly qualitative. The traditional evaluation is tightly linked to the people doing the work and is thus unreproduc-

ible. It is nevertheless the only way of starting the evaluation work. As working tools for the data interpretation cross correlations (uni-variate analyses) is commonly used. Variations as a function of depth, hydraulic properties, etc. are investigated.

The multiple *Linear regression* model is based on the least-square method. The linear regression analysis minimizes the squared difference between the observations and a straight line as a function of the position (x,y,z). The basic requirements of the model is that the observations are independent, normally distributed and have the same variance. In order to give a good correlation all observations need to be linearly dependent on the position (x,y,z). The computer program used was *STATISTICA for Windows /1994/* and *STATGRAPHICS PLUS for Windows /1994/.* Separate calculations were made for each of the major components separately.

Multivariate (principal component) analysis is a mathematical way of treating the different parameters all together. The values to be predicted could be considered as missing data in a matrix. The principal components are computed directly from the known data values as a linear function of all the underlying parameters. The principal components are independent and extrapolated to the position (x,y,z). A predicted value for each constituent is recalculated from the linear correlation of the principal component as a function of position. The method used was *Fillas* in the computer program PARVUS */Forina et al, 1988/.*

Kriging is an interpolation method based on a non-linear correlation function. The basic assumption is that the modelled properties are continuous and that positions physically close to each other also have properties numerically close to each other. Thus, an observation physically close to a position to be predicted has a larger weight than an observation which is physically further away from the position to be predicted. The correlation function is obtained from the calibration data and the predictions are more uncertain the further they are from an observation. All values have an uncertainty, a variance, associated with them. There are different ways of estimating the unknown values and their corresponding variances. The computer program used was *SURFER for Windows /1994/.* Separate calculations are made for each element to be predicted.

Neural networks contain artificial neurones organized in layers and connected to each other in a way simulating the human brain. Each neurone in a layer is connected to all neurones in the previous and the following layers. The connections between the neurones have different strengths. The neurone computes its output signal as a weighted sum of its input signals. Neural networks learn by associations, from examples, by comparison, and by repetition. The neural network is non-linear, highly interconnected and is therefore able of capturing complex relationships between input and output. Thus, neural networks possess an ability to treat complicated non-linear problems, generalize, analyse large amounts of data, interpolate and optimize data. The software *BRAINMAKER PROFESSIONAL for Windows /1993/* was used to create, train and run neural networks */Hecht-Nielsen, 1991, Hertz et al,*

1991 and *Lawrence, 1992/* on the chemical data in both the pre-investigation and construction phases.

3.5.6 Boundary conditions

For the mixing calculations reference waters are identified and end members are defined. These are mostly resulting from episodes which have influenced the groundwater system dramatically during distinct time spans.

Composition of groundwater end-members and reference waters

Groundwaters which are well sampled and well analysed but have an extreme composition are selected as reference waters. The reference waters are used as components in the mixing calculations.

An end-member is a modelled water which is believed to be the original composition of the reference water. A common feature for the end-members in the Äspö groundwaters is that the composition is uncertain due to:

- natural variations i.e. seasonal variations in the precipitation
- assumed compositions i.e. glacial meltwater composition
- uncertain analyses i.e. extracted pore water from sediments.

The selected *reference waters* and **end-members** are:

- *Glacial reference water* and **glacial melt water**, with an extremely low oxygen-18 and a low salinity.

- *Baltic Sea reference water* and **Litorina Sea water** with an extremely high oxygen-18 content.

- *The Altered marine reference water,* and **sediment pore water.**

- *The Meteoric reference water* and **1960 precipitation** with a high tritium content.

- *The brine reference water* with an unknown end-member with an extremely high salinity.

3.6 TRANSPORT OF SOLUTES CONCEPTS

3.6.1 Scope

The transport of solutes concepts are presented in *Table 3-8*. Concepts for the flow field are not presented here but in *Section 3.4*. The concepts described in

Table 3-8. Condensed description of the transport-of-solutes model of the Äspö site used within the Äspö HRL Project.

TRANSPORT OF SOLUTES MODEL OF THE ÄSPÖ SITE

Scope
Flow paths during natural flow, interference tests and flow to the laboratory tunnel.
Solute transport of non-sorptive elements.
Solute transport of elements affected by retardation.

Process description
Flow processes - see process description for groundwater flow.
Advection.
Hydrodynamic dispersion (Mechanical dispersion + Molecular diffusion).
Retardation (Chemical reactions , Molecular diffusion in rock matrix).

CONCEPTS

Geometrical framework and parameters
Three-dimensional box divided into:
- Hydraulic conductor domains. 2D features (location, extent, orientation).
- Hydraulic rock mass domains. 3D features (location of boundaries).

Material properties
Kinematic porosity, (n_e).
Dispersivity (α_L ,α_T). (Mechanical dispersion).
Molecular diffusion coefficient.
Retardation coefficients.

Spatial assignment method

Effective porosity :	Deterministic assignment within a domain, - constant
Mechanical dispersion:	Deterministic assignment within a domain, or by a probable density function for particle movement (pdf(p)).
Molecular diffusion:	Deterministic assignment within a domain
Retardation:	Deterministic assignment within a domain or by pdf(p)

Boundary conditions

Flow field:	See concepts for groundwater flow.
Mass or concentration:	Mass flux or prescribed concentration of the solute.

Numerical tools
PHOENICS finite-volume code.

Output parameters
Salinity distribution
Flow paths

Table 3-8 has been the base for the numerical groundwater flow modelling with the finite difference code PHOENICS. However, kinematic porosity as a function of hydraulic conductivity (K) or transmissivity (T) has not been used in simulations up to summer 1997 but is suggested in *Chapter 8.*

3.6.2 Process description

Advection

Flow paths within the model are studied by tracking particles in the direction of flow in the flow field, or in the opposite direction of the flow. The advective transport is defined by the linear velocity **v** :

$$\mathbf{v} = \frac{\mathbf{q}}{n_e} \qquad (3\text{-}13)$$

$\mathbf{q}$	=	Specific discharge (vector)	(m/s)
$\mathbf{v}$	=	Linear velocity (vector)	(m/s)
n_e	=	Kinematic porosity	(-)

The linear velocity in a 2D feature can be calculated by dividing the flow rate in the feature with the effective fracture width, here called the transport aperture (e_T). If the feature is given a width the kinematic porosity for the feature can be calculated from the transport aperture.

Advection and hydrodynamic dispersion

The transport equation including hydrodynamic dispersion is formulated as below */Marsily, 1986/*:

$$\nabla (\mathbf{D} \cdot \nabla C - C \cdot \mathbf{q}) =$$

$$= n_e \frac{\delta C}{\delta t} + (n_e - n) \frac{\delta C'}{\delta t} + Q_S \qquad (3\text{-}14)$$

$$\nabla = \left(\frac{\delta}{\delta x}, \frac{\delta}{\delta y}, \frac{\delta}{\delta z} \right) \qquad (3\text{-}5)$$

$$\mathbf{D} = \begin{vmatrix} D_L & 0 & 0 \\ 0 & D_T & 0 \\ 0 & 0 & D_T \end{vmatrix} \qquad (3\text{-}15)$$

$$D_L = \alpha_L \cdot |\mathbf{q}| + D^* \qquad (3\text{-}16)$$

$$D_T = \alpha_T \cdot |\mathbf{q}| + D^* \qquad (3\text{-}17)$$

C	=	Concentration of the solute	(kg/m^3)
C´	=	Concentration of the solute in the immobile fraction	(kg/m^3)
D	=	Dispersion tensor in its principal directions of anisotropy	(m^2/s)
D^*	=	Effective diffusion coefficient (m^2/s)	
D_L	=	Hydrodynamic dispersion coefficient parallel to the principal direction of flow	(m^2/s)
D_T	=	Hydrodynamic dispersion coefficient perpendicular to the principal direction of flow	(m^2/s)
n	=	Volumetric (total)porosity	(-)
t	=	Time	(s)
Q_S	=	Mass change of substance /(unit volume and unit time)	($kg/(m^3s)$)
α_L	=	Longitudinal dynamic dispersivity	(m)
α_T	=	Transverse dynamic dispersivity	(m)
ρ	=	Fluid density	(kg/m^3)

Diffusion

The effective diffusion coefficient (D^*) is a function of the diffusion coefficient in a pure fluid (D_0), the total porosity (n), the kinematic porosity (n_e) and the shape of the flow path (tortuosity). The effective diffusion coefficient (D^*) is estimated according to *Equation 3-18:*

$$D^* = \frac{n}{n_e} \cdot \frac{D_0}{\tau} \qquad (3\text{-}18)$$

D_0	=	Molecular diffusion in the fluid phase	(m^2/s)
D^*	=	Effective diffusion coefficient	(m^2/s)
τ	=	Tortuosity	(-)

The dispersion varies with the absolute value of the specific discharge and a dimensionless Peclet number (P_e) is sometimes defined as *Equation 3-19* to *3-21*:

$$P_e = \frac{|\mathbf{v}| \cdot \sqrt{k}}{D_0} \qquad (3\text{-}19)$$

$$P_e = \frac{|\mathbf{v}| \cdot L_c}{D_0} \qquad (3\text{-}20)$$

$$P_e = \frac{|\mathbf{v}| \cdot L_c}{D_L} \qquad (3\text{-}21)$$

P_e	=	Peclet number	(-)
k	=	Permeability	(m^2)
L_c	=	Characteristic length of the medium open for flow	(m)
$\mathbf{v}$	=	Linear velocity (vector)	(m/s)

If it is assumed that the system is a double porosity system with fracture porosity and matrix porosity, the flow is generally assumed to be controlled by the hydraulic conductivity of the fractures, assuming that the matrix hydraulic conductivity is much lower than the hydraulic conductivity of the fractures. In such a case there is diffusion in the fracture planes and there is diffusion into the rock matrix. The diffusion into stagnant pools in the fracture planes and into the matrix blocks will retard the solute transport.

Dispersion

The groundwater velocity at a certain point in the medium can be greater or less than the linear velocity (**v**). As a result the velocity will vary along a flow path and there will be a mixing along the flow path, called mechanical dispersion (**D**). The reasons for mechanical dispersion in a fracture plane are:

- Friction in the flow channel causing a parabolic velocity distribution perpendicular to the fracture plane.

- Velocity differences caused by a difference of aperture and channel width.

- Difference in channel length.

In a larger scale the interconnected fractures also introduce heterogeneity into the velocity field (variability in fracture transmissivity, connections between fractures and fracture density). The dispersivity that occurs at field scale flow lengths is sometimes called macro-dispersion. Dispersivity is thus just a factor that takes into account the heterogeneity of the velocity field within a volume where the hydraulic conductivity and kinematic porosity are assumed to be constant. Compilations of field-measured values of longitudinal dispersivity (α_L) have shown that α_L increases as test scale increases. The probable reason is that larger heterogeneities are affecting the velocity field as test scale increases but these heterogeneities are not described in detail for the site. It has also been shown that if the hydraulic conductivity has definable statistical distribution the apparent macro-dispersion is increasing but approaches an asymptotic limit at long travel distances, which are much longer (in the order of 10 times) than the correlation length for the hydraulic conductivity */Marsily,1986/*. This implies that if the heterogeneity of the hydraulic conductivity and effective porosity are given as a stochastic distribution, with a correlation length = L, the size of the domain to be assigned parameter values should be greater than L*10 and dispersivities should be based on the size of the element discretization of the domain. However, as these element dispersivities should be smaller – or much smaller – than apparent dispersivities for the domain for a domain with stochastically distributed properties, the hydrodynamic dispersion can probably be approximated with only the effective diffusion (D^*). It is then assumed that heterogeneity and correlation within the domain is reasonably well described.

The transverse dispersivities (α_T) are generally assumed to be less than the longitudinal dispersivities (α_L). Field tests have indicated a relation of approximately 1/5 to 1/100 for α_T/α_L */Marsily,1986/*.

In the numerical modelling, with the code PHOENICS, at Äspö HRL up to summer 1997 the dispersion was assumed to be constant or dependent of the Darcy velocity within the model. The hydrodynamic dispersion has so far with the code PHOENICS been modelled as $\alpha \cdot L \cdot q$ where α is a dispersivity coefficient, L is the dimensionless length that can be associated with the cell size and q is the darcy velocity or specific discharge. In all site scale models the hydrodynamic dispersion was assumed to be a constant within the model and not dependent on the direction of the flow ($D_L = D_T$) when the salinity distribution within the model was calculated. The dispersion was set proportional to the Darcy velocity ($\alpha \cdot L$ = constant = 2 m. The sensitivity of $\alpha \cdot L$ was evaluated in *Svensson /1997a/*). However, a technique was also tried with probability density function controlling the particle movements (pdf(p)) in each

cell in the model in order to simulate the effect of the heterogenous medium (see *Section 3.4.9*).

Mass change of substance /(unit volume and unit time), (Q_S)

There are a number of mechanisms that may change the mass concentration in the fluid:

- Filtration through the pores
- Geo-chemical reactions
- Radiological decay
- Biological activity

These mechanisms can be incorporated into *Equation 3-14* in different ways */Marsily,1986/*. Up to 1995 only some tests with sorption/desorption of particles on their flow path had been performed with the code PHOENICS (see *Section 3.4.9*).

3.6.3 Geometric framework and parameters

The model comprises of the same geometrical concepts as for groundwater flow:

- Hydraulic conductor domains
- Hydraulic rock mass domains

Hydraulic conductor domains are large two-dimensional features with hydraulic properties different from the surrounding rock. Generally they are defined geologically as major discontinuities but in some cases they may mainly be defined by interpretation of results from interference testing.

Hydraulic rock mass domains are geometrically defined volumes in space with properties different from surrounding domains (rock mass and discontinuities). They may either be defined by lithological domains or purely by interpretation of results from hydraulic tests.

3.6.4 Material properties

The material properties chosen for the domains are:

- Advection : Kinematic porosity (n_e), transport aperture (e_T).
- Mechanical dispersion: Dispersivity (α_L, α_T).
- Molecular diffusion: Effective diffusion coefficient (D^*).

(Retardation parameters are not described here as there has only been generic modelling of techniques of how to incorporate retardation in the model.)

Kinematic porosity (n_e) is either approximated with a constant value for a domain or expressed as a function of hydraulic conductivity (K). A feature with a given transmissivity (T) is either approximated with a constant value of the transport aperture (e_T) or expressed as a function of the transmissivity if no deterministic value based on evaluated field tests is available. The suggested relations are shown in *Chapter 8* of the report. The rationale for expressing n_e as a function of K and e_T as a function of T is the relation between fracture aperture and the equivalent hydraulic conductivity for a system of parallel and continuous fractures, where the hydraulic conductivity of the matrix (K_m) is neglected. See *Chapter 8* for a detailed discussion.

If the transmissivity or hydraulic conductivity is given as a stochastic distribution, the dispersivities for the domain are neglected or estimated based on the cell size in the model and diffusion is included if it is considered relevant for the problem studied.

If the transmissivity or hydraulic conductivity is constant within the domain and no evaluated dispersivities are available for a domain, the dispersivity is approximated based on compiled results of longitudinal dispersivity as function of scale of measurements and the size of element within a domain, the size of the domain or expected flow distance in a domain for a particular case.

In the site scale numerical groundwater flow modelling at Äspö HRL with the code PHOENICS (up to summer 1997) the effective porosity was assumed to be constant within the model volume. The concept with e_T has not been used so far with the code PHOENICS. Hydrodynamic dispersion has either been approximated to a constant value (not dependent of the linear velocity) or dependent on the Darcy velocity and neglecting the diffusion.

3.6.5 Spatial assignment method

The properties within a domain may be given as an mean value for the entire domain, a trend within the domain, a statistical distribution within the domain etc. The description of the properties assumes that the domains can be described as a continuum considering the processes.

Kinematic porosity (n_e) is either assigned as a constant value for the domain or as a function of the hydraulic conductivity (K) assigned to the elements within the domain. Transport aperture (e_T) is either assigned as a constant value for the domain or as a function of the transmissivity (T) assigned to the elements within the domain In the numerical simulations performed up to summer 1997 n_e has been assumed to be a constant value within the modelled volume.

Effective diffusion coefficient (D^*) is assigned as a constant value for the domain stated, or neglected if mechanical dispersion is assumed to dominate.

Dispersivities (α_L, α_T) are either assigned as a constant value for the domain or neglected (see *Material properties* above). In the numerical simulations performed up to 1995 with the code PHOENICS hydrodynamic dispersion was assumed to be a constant value within the modelled volume or the dispersivity was assumed to be a constant value within the modelled volume.

3.6.6 Boundary conditions

The following conditions were assumed in the numerical simulations:

Upper boundary

Up to 1995: Salinity of the Baltic Sea is assumed to be 0.7 %. Precipitation is assumed to have a salinity of 0 %

Model 96, Regional and Site scale models: Salinity of the Baltic Sea is assumed to be 0.6 %. Precipitation is assumed to have a salinity of 0 %

Side boundaries

Up to 1995: Salinity is 0.7 % at sea-surface and increases linearly 1.8% at a level of 1300 m below the sea surface.

Model 96, Regional model: Boundaries facing the Baltic (eastern and part of southern boundary) are assigned two linear functions for the increase of salinity by depth, based on measurements of natural conditions at Laxemar and Äspö. No prescribed conditions of salinity and zero flux conditions for other boundaries.

Model 96, Site model: Boundary conditions from regional model, except for the uppermost 100 m of the model where zero flux conditions were used du to the resolution of the computational net.

Lower boundary

Up to 1995: Zero flux conditions.

Model 96, Regional model: Zero flux conditions.

Model 96, Site model: boundary conditions from regional model.

3.6.7 Concepts used in different scales

Regional scale and site scale

Numerical groundwater flow modelling was only performed for regional scale and site scale and, depending on the purpose of the modelling, different concepts of effective porosity (n_e), dispersivity (α_L, α_T) and effective diffusion coefficient (D*) were included.

The main purpose of including transport of solutes in the numerical modelling was to estimate the salinity distribution within the modelled volume in order to describe the fluid density distribution within the modelled volume, which affects the fluid flow (see *Section 3.4* - Groundwater flow). Salinity is also used as a tracer to study the salinity within the flow field during natural (undisturbed) conditions and during construction of the Äspö HRL.

Another important use of the numerical model was to study flow paths during natural (undisturbed) conditions and during construction of the Äspö HRL in order to trace the origin of sampled groundwater (see below).

Mixing and transport in the major water conducting fracture system

The composition of the flow into the tunnel results from the mixing. One way of describing this process is to reverse the velocity vectors and release particles at the observation point and see where the particles end up (back tracking). So far this is a qualitative procedure which will be tested further during the evaluation stage.

In transport calculations conductors were given a specific water composition. Inflow to the tunnel was distributed according to the measured inflow and the transport time and rate were calculated.

In monitoring points in observation boreholes the water composition is a result of mixing with a certain proportion of water coming from different parts of the conductive fracture zones. A change in time is predicted on the basis of the changing proportions with time of different groundwater origins. Also the water flux in the monitored borehole section is predicted and observed.

3.6.8 Numerical tool

The code mainly used within the Äspö HRL project is PHOENICS, a finite-volume code */Spalding 1981/*. Depending of the purpose of the modelling different concepts were used. A brief overview of the modelling performed within the Äspö HRL using PHOENICS up to 1995 is given in *Section 3.4.9*. Site scale models normally included density-driven flow caused by differences in salinity concentrations.

Two tracer tests were performed with non-sorbing tracers and the larger of the two tests were modelled using the site-scale numerical model. The site-scale numerical model was also used to predict flow times for some flow paths to the tunnel.

Some generic modelling was also performed to study techniques of how to model sorption and desorption of particles, see *Section 3.4.9*.

4 GEOLOGY

4.1 MODELS ON A REGIONAL SCALE

The model on a regional scale covers some 100 km^2 around Äspö. The regional scale model was developed mainly during the siting stage and consequently based mostly on data gathered during that stage of the project. Further minor adjustments of the regional scale model were made at later stages of the pre-investigation and after excavation of the tunnel.

For the geological-structural model, airborne geophysical (magnetic, electromagnetic and radiometric) measurements were interpreted and lineament interpretation of terrain models was used to identify the major fracture zones and their extent. Some of the indicated fracture zones were also characterized by means of surface mapping, petrophysical measurement of rock samples and ground geophysics (gravity, refraction seismics, etc.). The regional geological model comprises the following concepts:

- lithological domains
- major discontinuities (major fracture zones)

4.1.1 Geological process description and geological history of the Äspö region

The dominant rocks on Äspö belong to the 1700-1800 million year-old Småland granite suite, with mafic enclaves and dikes probably formed in a continuous magma-mingling and magma-mixing process */Kornfält and Wikman, 1988/*. The result of this mingling (mixing) process is a very inhomogeneous rock mass, ranging in mineralogical composition from true granites to dioritic or gabbroid rocks */Wikström, 1989/*. Older folded basic sheets and xenoliths older than Småland granite, often hybridized in a belt trending NE-ENE across central Äspö. All the rock mass at Äspö is intruded by fine-grained granites of at least two or three generations, related to the Småland granite. About 1350-1400 million years old anorogenic granites formed diapir-like massifs in the older bedrock. An intrusion of this kind is the Götemar granite, only about 2 km to the north of Äspö. Late, about 1000 million-year-old, dolerite dikes striking approximately N-S are the youngest rocks actually on Äspö but still younger are the decimetre wide clastic dikes of Cambrian age (500-600 Ma), near Äspö (e.g. at Figeholm and Götemar).

The ductile foliation imposed while the rock mass was deep and relatively hot, was homogeneous and penetrative on a regional scale. A mostly steep, penetrating foliation trending NE-ENE is the most dominant structural element in the Äspö granitoids and seems to be the oldest sign of the ductile deformation related to the subhorizontal NNW-SSE compression. This deformation is also marked by the orientation of mafic sheets often back veined by two or

three generations of fine-grained granites */Talbot, 1990, Figure 4-1/*. Intensified strain formed in the amphibolite-facies is marked by gneissic zones trending NE-ENE, dipping to the NNW. Elevated to a higher structural level between 1700 and 1400 million years ago, these old gneissic zones were reactivated as mylonitic shear-zones trending NE, especially in central Äspö in a ductile/semi-ductile deformation phase.

The brittle strain of the region can be regarded as the combined effect of two mechanisms; fragmentation, the generation of new fractures, and jostling, the reactivation of old fractures. The ratio of fragmentation to jostling generally decreased with each episode of strain as inferred from the Äspö region. Fewer new fractures formed in successive episodes of strain as the orientation spectra of pre-existing fractures widened */Munier, 1995/*.

Most fracture zones on Äspö are reactivated older structures. The style of each fracture zone tends to depend on the nature of any older structure being reactivated, such as E-W gneissic zones, mylonites trending NE or E-W and gently dipping alteration zones. Fracture zones trending N, NE or E-W on Äspö normally had ductile precursors whereas those trending NW apparently did not.

The first brittle faults probably developed in the region in response to the emplacement of younger granites. These faults and older ductile zones were reactivated several times. The rock mass became increasingly brittle as it was uplifted and unroofed about 1000 million years ago. Epidotic vein systems became chlorite, zeolite and carbonate filled fractures with time.

Net slip ranges between approximately 30 cm for large faults and approximately 1 cm for smaller faults. In the absence of post-Cambrian markers on Äspö it is not possible to determine which fracture sets in Äspö formed or reactivated later than approximately 500 million years.

Munier /1993c/ investigated faults in the Cambro-Ordovician platform sequence on the island of Öland SE of Äspö. In contrast to the basement rocks exposed in and around Äspö, fault surfaces there are well exposed and kinematic indicators common.

Though the bedrock of Öland is essentially undeformed, in all practical aspects, geometrical configurations of fractures indicate that faults in the lower Palaeozoic cover reactivated fractures at least once.

This result is confirmed by a more thorough study performed by *Milnes and Gee /1992/*, who concluded that bedrock deformation on Öland is negligible. The rocks exposed there only show signs of minimal instability over the last 500 million years.

Some attempts have been made to undertake direct fault dating investigations in order to constrain the minimum age of the most recent movements on some brittle structures at the Äspö site */Maddock et al, 1993/*. Approximately seventy rock samples were collected and examined to provide information on the history

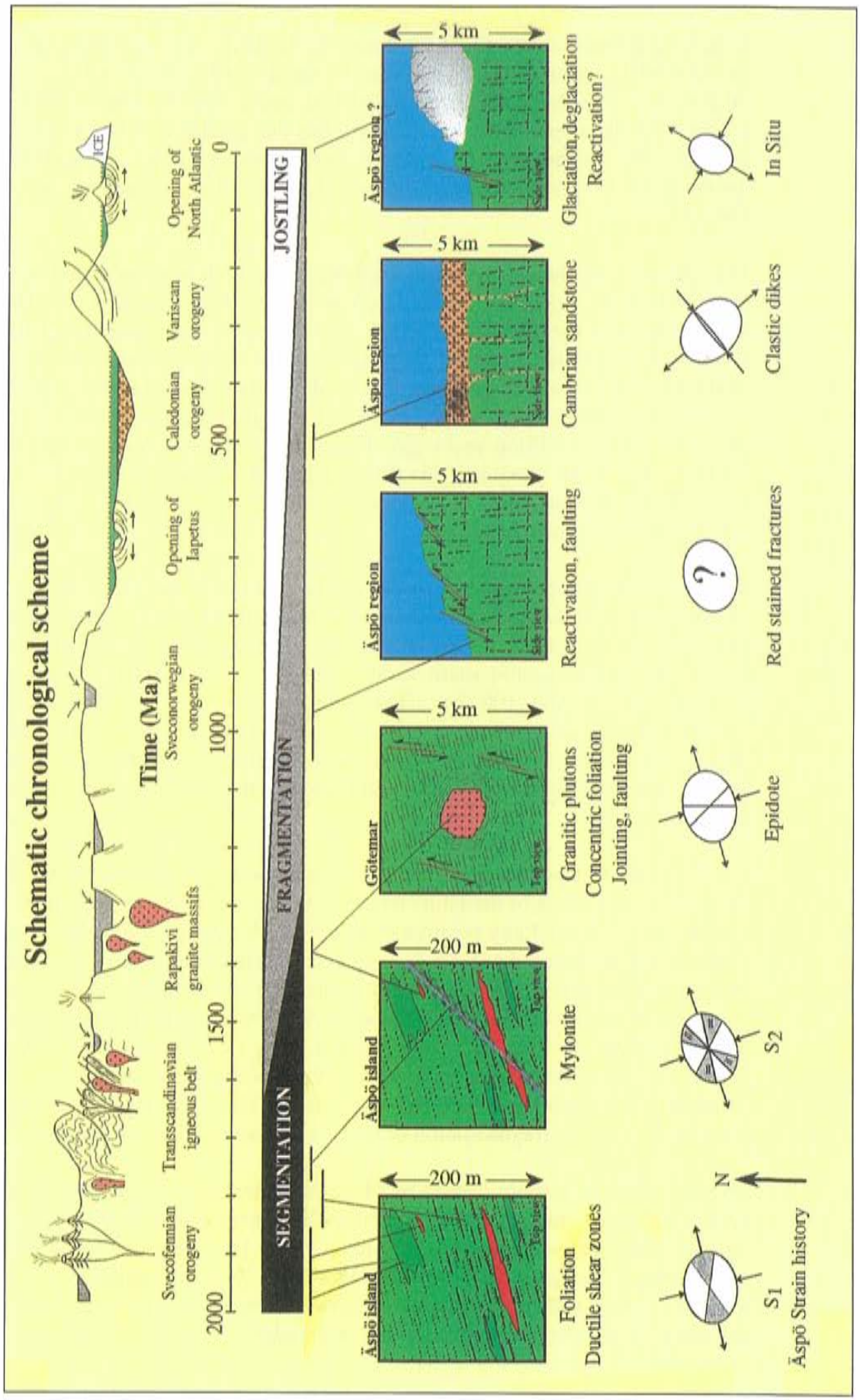

Figure 4-1. *Tentative chronological scheme summarizing the main lithological units and tectonic events affecting the rock mass studied (after Munier, /1993c/).*

of fault movements and to assess the suitability for dating. The characterization included XRD, electron microprobe analysis together with optical and electron microscopy. The analysis demonstrated that many fracture zones contain sequentially-developed fault rocks and verifies that reactivation has occurred through time. Palaeomagnetic, electron spin resonance (ESR) and isotopic dating (K-Ar, Rb-Sr) techniques were then employed for dating the fault gouge material.

The ages given by the various dating methods reflect both inherent differences in the techniques and differences in the phase or phenomenon being dated. The interpretation of the ESR dating which was limited by the resolution of the method, gave minimum ages of movements in the order of several hundred thousand years to one million years. The results of the palaeomagnetic and K-Ar analyses strongly suggest that growth of fracture infilling minerals took place at least 250 million years ago. The most recent fault movements are interpreted to have preceded this mineral growth. *Maddock et al /1993/* conclude that any quaternary and holocene activity (jostling) had little effect on the fracture zones they examined.

The sub-Cambrian peneplain, exposed on the east coast, has been used as a fault marker to demonstrate post-Cambrian brittle tectonics. E.g. *Tirén et al /1987/* demonstrated the relative kinematics on regional blocks bounded by fracture zones in the south-eastern Sweden. The blocks studied range in the size between 25 km^2 and 100 km^2. The interpretation says that differential movements have occurred along existing faults both during periods of uplift and subsidence. The relative and maximum accumulated vertical offsets along any regional faults in the Äspö surrounding are less than ±25 m during the last 600 million years.

Mörner /1989/ mapped a great number of supposed 'post-glacial faults' on Äspö. However, none of the faults reported, which were later investigated in greater detail, showed any positive evidence of kinematics */Bäckblom (ed), 1989/*. Some of the reported 'faults' had Precambrian markers that were not offset, other had their bases exposed by excavation and ice plucking could be positively demonstrated. *Talbot and Munier /1989/* discuss post-glacial faults having studied 'post-glacial scarps', abrupt steps in the glacially polished surface of Äspö. According to *Munier /1995/* post-glacial reactivation of individual fractures is most likely to have occurred. However, despite searches, no evidence of such fragmentation or jostling has been found on outcrops.

Ongoing tectonic activity caused by plate movements and land upheaval is manifested in seismic events and aseismic slip, *Larsson-Tullborg /1993/*. In Sweden earthquakes have been registered from 1891 */Wahlström, 1990/*. According to *Slunga et al /1984/* the Protogine Zone of southern central Sweden has been shown to be the border between a more seismic west Sweden and the more aseismic part of southeastern Sweden.

4.1.2 Lithological model

The main rocks in the Äspö area belong to the vast region of Småland-Värmland intrusions (or Trans-Scandinavian Granite-Porphyry Belt */Gaal and Gorbatschev, 1987/* (*Figure 4-2*).

A number of massifs of basic rocks elongated E-W have been indicated by positive magnetic and gravity anomalies. Besides the more coarse-grained types, such as gabbro and diorite, fine-grained irregular bodies and xenoliths of greenstone (old volcanites) were found as remnants within the granite mass. They occupy only a minor part of the Äspö area.

Some circular/semi-circular structures in the area investigated are interpreted as granite diapirs. They are all represented by a more or less round, non-magnetic pattern and negative Bouger gravity anomalies. The Götemar and Uthammar anorogenic granites are two of these structures which have been indicated as true diapirs. Very low-dipping pegmatites and, to lesser degree, aplite granite are characteristic of the area around the Götemar granite.

Fine-grained greyish-red granite is common in the whole area. In the inner area, which has been mapped in detail, the fine-grained granite occurs both in smaller massifs and in dikes in the older rocks. Often the direction of the dikes follows the foliation in roughly the direction E-W to NE-SW.

The dikes are usually about 0.5-5 metres thick but some measuring 30 metres across have also been found.

4.1.3 Structural model

Major discontinuities (major fracture zones)

Information from all geological and geophysical investigations support a tectonic picture dominated by one almost orthogonal system of major structures trending N-S and E-W and one trending NW and NE, all extending >10 km. They often coincide with some hundred-metre-wide low-magnetic zones with a central more intense fracture zone up to some tens of metres wide. The N-S structures most probably have vertical to subvertical dips and seem to be of a tensional, more open character (magnetic and VLF indications).

The structures trending E-W are mostly vertical or moderately low dipping. They seem to be more complicated, with an early dip-slip ductile phase and a late stage of reverse faulting, with local development of thrust sets with a mainly low to moderate dip to the SSE. A major structure trending NE-SW across the island of Äspö, is indicated by mylonites in outcrops and boreholes. According to a general interpretation most of the structures trending NE-SW are older than the systems trending N-S and E-W. Most of the structures trending N-S are probably younger than the E-W trending ones */Nisca, 1987* and *Tirén et al, 1987, Tirén and Beckholmen, 1987 and 1988/*. The N-S fracture zones were estimated to be the most probable water-bearing structures

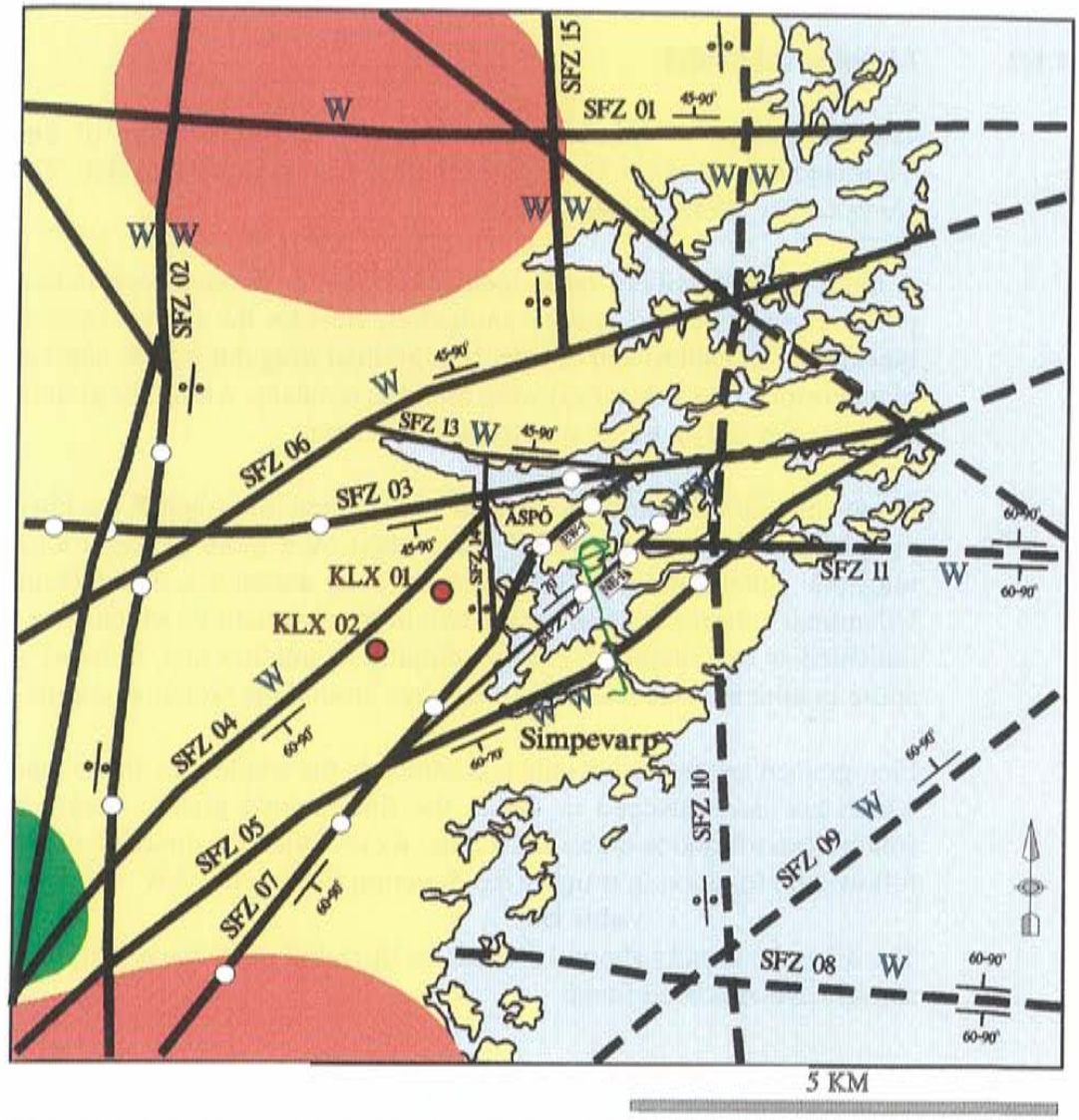

Figure 4-2. *Regional geological model of the Äspö area. (W and WW: possible waterbearing properties based on expert judgement). Götemar and Uthammar granites are situated in the northern and southern part of the area respectively.*

according to combined magnetic and VLF fracture interpretation. E-W fracture zones are less likely water-bearing structures.

A depth of at least 1500 m to several kilometres (supported by indications in the 1705 m deep borehole KLX02) is estimated for most of the major structures. */Andersson, 1994/.*

Table 4-1 presents a summary of geological and geophysical structure indications and *Table 4-2* shows interpretation data for all major structures included in the model. Data in the table contribute to judgement of structure reliability regarding extension, orientation and character. A classification of the main structures into three groups (possible, probable and certain) with the aspect to reliability is also presented in *Table 4-2*.

It is important to point out that most of the parameter values should be regarded as 'best estimates' based on geophysical data which have only been confirmed in a few cases by borehole or geological observations.

Small scale fracturing in the rock mass

The fracture sets mainly coincide with the most conspicuous lineament directions (valleys) in the region. The general pattern based on 10400 outcrop fractures shows evident strike directions around N-S and N50°W (*Figure 4-3*). A predominant fracture set also strikes in an E-W direction. In the sector between N40°W and N80°E there appears a fracture set with a somewhat less predominant peak in the direction N65°E. This sector coincides with the most common foliation strikes in the region. The different rosette diagrams of the road cut mapping verify the main fracture sets that have been described for the outcrops. The main directions E-W, N50°W, N-S, N40°E, with some spread in the foliation peak varying around N70°E. Even if gentle fracture dips have been underestimated during the road-cut mapping an interpretation also shows that the predominant dips are vertical or almost vertical.

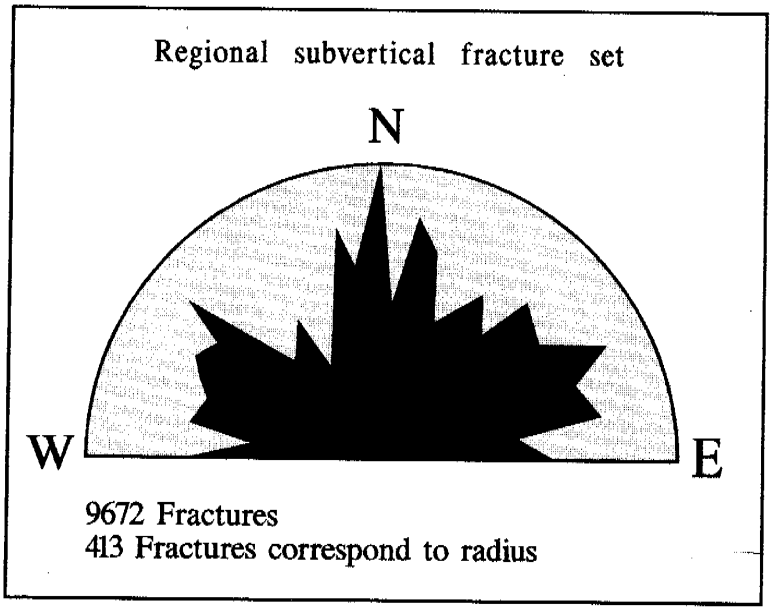

Figure 4-3. *Rosette diagram for all outcrop fractures in the region with dips of 70 to 90 °/Ericsson, 1987/.*

Table 4-1. Summary of geological and geophysical structure indications.

Structure	Lineament Topographical	Aerogeophysics Magnetic	VLF	Verification Ground geophysics	Surface geology	Borehole	Tunnel Äspö HRL
SFZ 01	+	+					
SFZ 02	+	+	+	+			
SFZ 03	+	+	+	+	+		
SFZ 04	+	+				KLX 01-02**	
SFZ 05	+	+	(+)	+	+	Ä-1*** (AR 84-14)	+
SFZ06		+					
SFZ 07 (EW-1*)	(+)	+		+	+	KAS04 KA1755A**	+
SFZ 08		+					
SFZ 09		+					
SFZ 10		+	(+)				
SFZ 11	(+)	+					
SFZ 12 (NE-1)*	(+)	+		+		KAS 09, 14, 16, KBH 02*	+
SFZ 13		+	+				
SFZ 14	+	+	+	+			
SFZ 15	+	+	+				

\+ *Means clear indication and* (+) *uncertain indication.*

* *Designation of the structure in the primary structural model of Äspö HRL (Figure 4-2)*
** *Cored borehole in Äspö HRL /Stanfors et al, 1991/*
*** *Cored borehole on Ävrö island /Gentzschein et al, 1987/*

Table 4-2. Summary of structure interpretation data.

Structure	Uncertainty of positions** (m)	Width*** (m)	Dip	Water****	Reliability*****
SFZ 01	±100	50-300	45-90° N	W	Possible
SFZ 02	±50	150-250(5-10)	~ vert.	WW	Probable
SFZ 03	±50	30-300 (10-20)	40-90° S	W	Probable
SFZ 04	±100	50-300	60-90° SE	W	Possible
SFZ 05	±20	50-200	60-70° SE	WW	Prob.-certain
SFZ 06	±100	50-300	45-90° N	W	Possible
SFZ 07	±20	70-200 (10-40)	70-90° NW	W	Certain
(EW-1)*			60-90° SE		
SFZ 08	±100	50-300	60-90° N or S	W	Possible
SFZ 09	±100	50-300	60-90° NW	W	Possible
SFZ 10	±100	50-300	~ vert.	WW	Possible
SFZ 11	±100	50-300	60-90° N or S	W	Possible
SFZ 12	±20	50-100 (5-10)	70° NW	WW	Certain
(NE-1)*					
SFZ 13	±100	50-100	45-90° N	W	Possible
SFZ 14	±50	50-100	~ vert.	W	Probable
SFZ 15	±100	50-100	~ vert.	WW	Possible

* *Designation of the structure in the primary structural model of Äspö HRL (Figure 4-2). EW-1 part of SFZ 07 indicated in Äspö HRL.*

** *Estimated uncertainty of position of the zone at surface perpendicular to main strike.*

*** *Estimated total width - aerogeophysically indicated - of increased fracturing and oxidation. Width of intense fracturing and/or alteration indicated by ground geophysics, borehole or tunnel documentation shown in brackets.*

**** *Estimated water-bearing ability based on geological and geophysical indications.*
WW=*water-bearing*
W= *less water-bearing*

***** *Total evaluation of the reliability of all available data concerning the major structures.*

4.2 MODELS ON A SITE SCALE

The site scale model covers some 1 km^2 of Äspö island. The framework for the site scale modelling was the existing regional scale model. Refinement of the site scale model was mainly done during the siting stage and the site description stage when extensive investigation data was gathered. Further detailing of the site scale model was done during the prediction stage based on results from further deep borehole investigations. The final refinement was done based on data from tunnel documentation after excavation.

The site scale model comprises the following concepts:

- lithological domains with four main rock types - Småland (Ävrö) granite, Äspö diorite, greenstone and fine-grained granite
- discontinuities with four major classes - major fracture zones, minor fracture zones, fracture swarms and small scale fracturing in the rock mass

4.2.1 Lithological model

Four main rock types - Äspö diorite, Småland (Ävrö) granite, greenstone and fine-grained granite make up most of the rock mass in the Äspö tunnel area.

During the early investigations of the bedrock the dominant rock type in the Äspö area was mapped as 'Småland granite'. The most frequent variety of 'Småland granite' is medium-grained, porphyritic and ranging in composition between granite-granodiorite - quartz monzonite. A variety called Ävrö granite, being more like a real granite in composition, is found in minor amounts on the southern part of Äspö. Later on there was a need for a classification system based more on core logging data. A limit was fixed at the silicate density 2.65-2.70 g/cm^3 between the acid varieties of what is now called 'Småland (Ävrö) granite' (including Ävrö granite) and the more basic and heavier variety called 'Äspö diorite'. This classification was also followed during mapping in the tunnel.

Äspö diorite

Rocks belonging to this group are by far the most common within the Äspö area, both on the surface and in the tunnel. Usually the rocks are grey to reddish grey, medium-grained, and contain more or less scattered, large crystals of potassium feldspar *(Figure 4-5)*. Granodiorites and quartz monzonites are most common, but there are also some tonalites, quartz diorites and quartz monzonites included in this group. The larger number of rock names suggests a rather heterogeneous group, but a look at the modal classification diagram reveals that the group falls in a rather restricted area *(Figure 4-4)*. The 'Äspö diorite' group is not as heterogeneous as the many rock names may indicate. The diversity in modal composition is to some extent due to the abundance of large potassium-feldspar crystals which can vary quite a lot in frequency. During the first years of investigation it was believed that the rocks within this group were more basic at depth than near the surface. At this time the designation Äspö diorite was created pointing to its affinity to the more basic, true diorites. Later studies showed that such a depth difference not really exists and that the rocks within this group are no true diorites. The rocks in the tunnel are on the whole comparable to those found on the surface of the island. The relatively small number of samples from the surface is mainly due to the difficulties of sampling this type of rock as fresh outcrops are rare */Wikman and Kornfält, 1995/*.

To get better and more precise knowledge of the age of the bedrock within the Äspö area one sample of a typical 'Äspö diorite' has been collected for age determination. The selected rock is a reddish grey, medium-grained granodiorite with scattered megacrysts of potassium feldspar. The analysis gave a well defined age of 1804±3 million years, which corresponds to the crystallization age of the rock. This age can be compared with the result from age determination of Småland granite at Ramnebo in eastern Småland. That granite has yielded an age of 1802±4 million years */Mansfeld, 1991/*, which means that the two granites are almost of the same age.

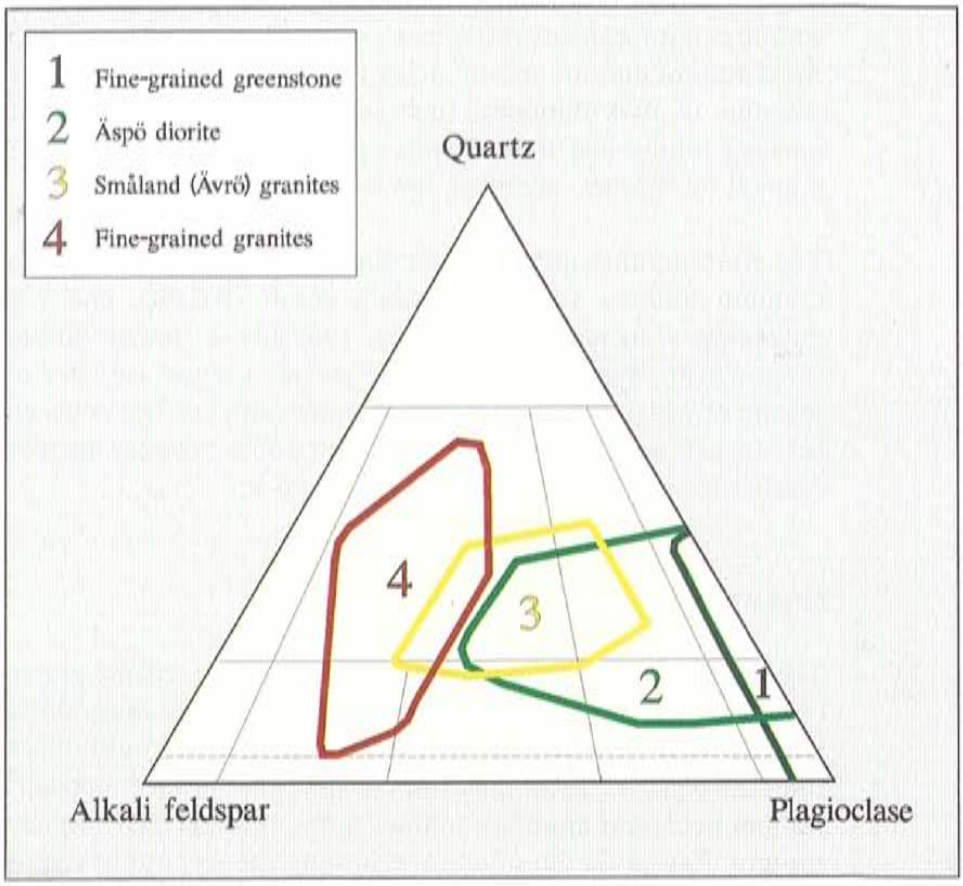

Figure 4-4. *Modal classification of the four main rock groups from the Äspö area /according to IUGS 1973, 1980/.*

Småland (Ävrö) granite

Macroscopically these granitoids differ from the previous group in their brighter, sometimes distinctly more reddish colour. The amount of potassium feldspar phenocrysts is lower and the crystals are much more irregularly distributed. In many places one can see that the Ävrö granite cuts the Äspö diorite, which implies that the former is younger. The age difference between the two groups is probably very small.

The designation 'Ävrö granite' was originally used for rocks which are greyish red in colour */Kornfält and Wikman, 1988/*. Later studies, both from the surface and above all from the tunnel, show that they can also be light reddish grey *(Figure 4-6)*. This colour variation may be caused by weathering or oxidation and does not mean any difference in modal composition. Compared with the Äspö diorites they are mostly richer in quartz and potassium feldspar, and the amounts of dark minerals, such as biotite, are lower. Amphibole is often missing totally and the amounts of sphene, which is a very characteristic mineral for diorites, are much lower *(Table 4-9)*.

The Ävrö granites and the Äspö diorites plot on the same linear trend in the titanium dioxide versus zirconium graph */Wikman and Kornfält, 1995/* indicating a chemical relationship, probably a similar differentiation path *(Figure 4-9)*. These two rocks can be regarded as two varieties of the Småland granite of which the Ävrö granite is more evolved. The Ävrö granite is rather homogeneous and plots in a very restricted area, whereas the plots of the Äspö diorites are much more scattered *(Figure 4-9)*.

Greenstone

The greenstones - fine-grained and medium to coarse-grained greenstone (diorites to gabbros) *Wikman and Kornfält /1995/* are easily distinguished from the granitoid rocks by their very dark, greenish or greyish black colour. As a rule they occur as minor inclusions or irregular, often elongated bodies within the granitoids and dioritoids following the common E-W foliation trend within the area. Except for the smallest inclusions, the greenstones are often intensely penetrated by fine-grained, granitic material *(Figure 4-7)*.

According to reports presented earlier *Kornfält and Wikman /1988/* most of the greenstones are inclusions. They may be of different age and origin but the majority of them are probably connected with the Småland granitoid magma evolution. At least in some cases one can suspect that they are supracrustal rocks formed on the surface of the earth and later incorporated into the rising granite magma. There are also some rare observations of greenstone occurring as dikes and thus younger than the rocks they cut through. In the tunnel we also found examples of so called composite dikes where a central greenstone is bordered on both sides by fine-grained granite *(Figure 4-8)*.

Figure 4-5. *Reddish grey 'Äspö diorite' with large, scattered megacrysts of potassium feldspar. Äspö, access ramp 1770 m, photo Kristian Annertz in Wikman and Kornfält /1995/.*

Figure 4-6. *Light reddish grey Småland (Ävrö) granite. Äspö, access ramp 1775 m, photo Kristian Annertz in Wikman and Kornfält /1995/.*

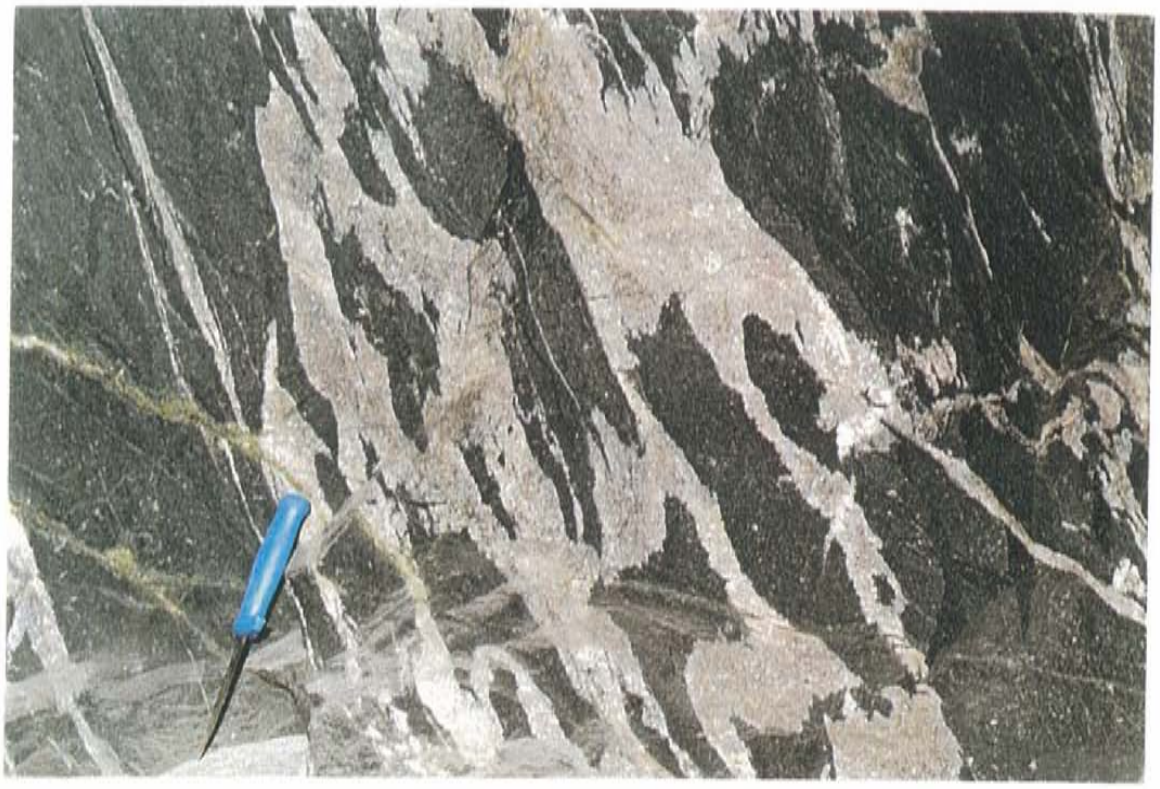

Figure 4-7. *Greyish black, fine-grained greenstone intruded by fine-grained granite. Äspö, access ramp 3040 m, photo Kristian Annertz in Wikman and Kornfält /1995/.*

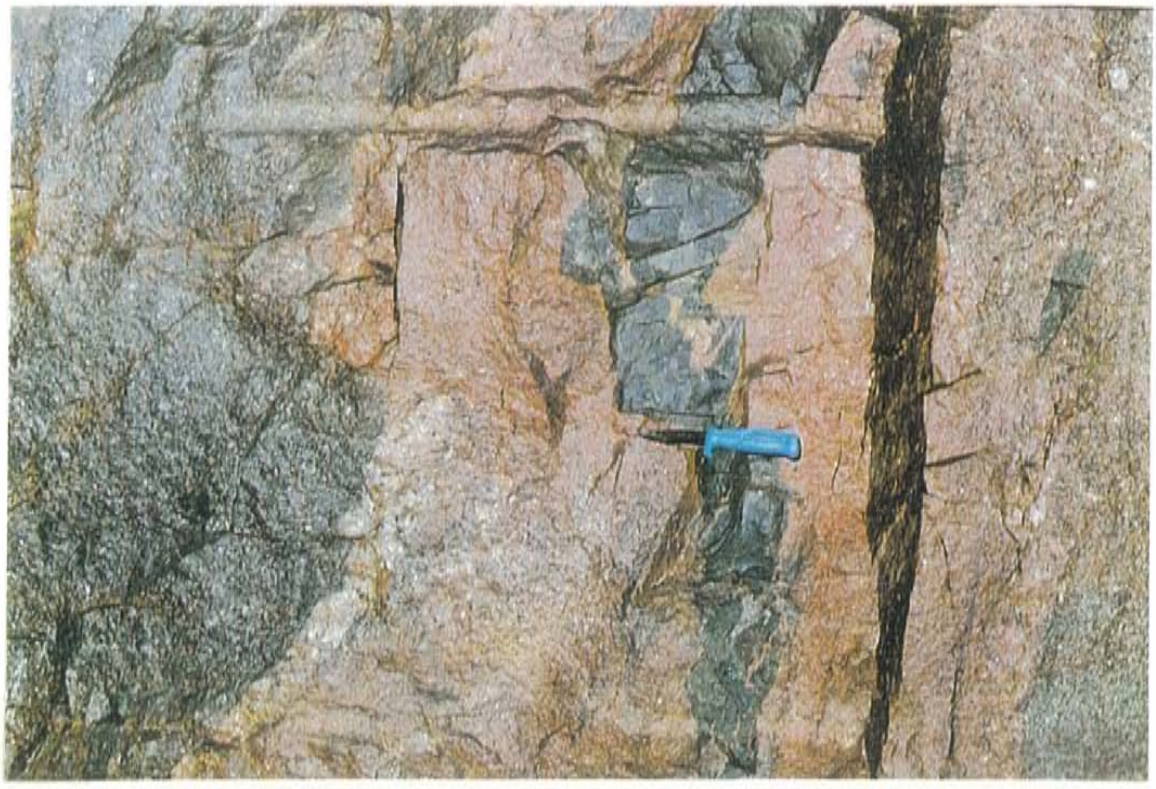

Figure 4-8. *Composite dike with a fine-grained greenstone in the centre boarded by fine-grained granite. Äspö, access ramp 2193 m, photo Kristian Annertz in Wikman and Kornfält /1995/.*

In recent years magma-mixing and mingling processes are believed to play an important role in the formation of magmas. For the different greenstones and granitoids at Äspö such an explanation has been advocated. */Wikström, 1989/.*

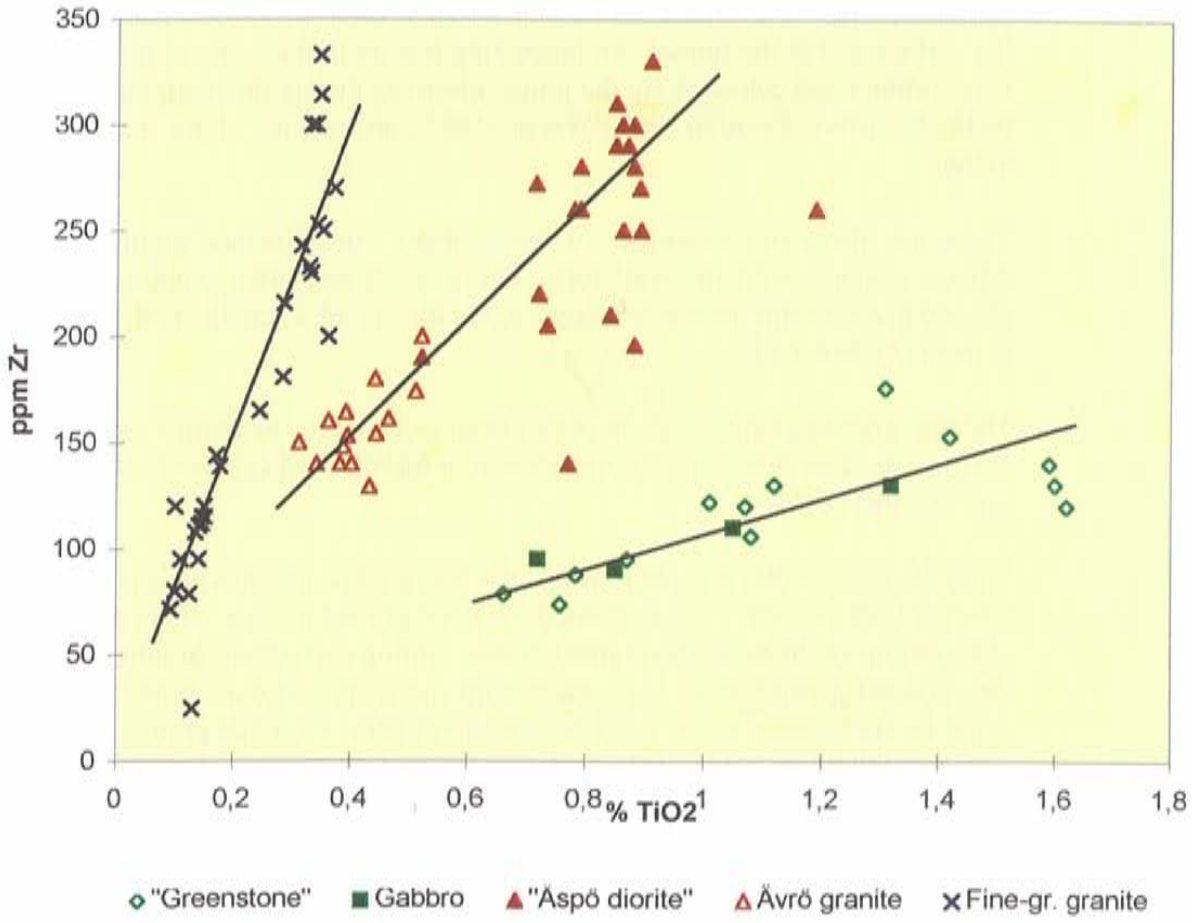

Figure 4-9. *Plots of zirconium (y-axis) versus titanium dioxide (x-axis) for different rock types. Modified after Wikman and Kornfält /1995/.*

The major minerals in the greenstones are plagioclase, amphibole and biotite *(Table 4-3)*. The amounts of epidote and chlorite are high in some samples. There are also samples with unaltered pyroxene. According to IUGS classification most of the greenstones are andesites to basalts *(Figure 4-5)*. The investigations made so far have not shown any significant difference between the greenstones found in the tunnel or in the drillings, and those found on the surface of the island.

Fine-grained granite

Fine-grained granites occur rather frequently, both on the surface of the Äspö island and its surroundings, as well as in the tunnel. From the surface mapping it is clear that many of the granites occur as dikes. The dike character is sometimes not very clear because of strong deformation in the fine-grained granites, which has obscured contacts.

The brittle deformation has caused a joint pattern in the fine-grained granites, often characterized by many short joints lying closely together, which divide the rock into small blocks. This is quite different from the pattern in the medium to coarse-grained granitoids where joints are much more widely spaced. No significant difference has been found between the joint patterns on the surface and in the tunnel. An interesting feature in this context is that the very common red colour along the joints, observed during the mapping of the bedrock surface *Kornfält and Wikman /1987/*, also occurs along the whole tunnel.

There are also many examples of fine-grained, not deformed granite with diffuse contacts with the wall rock. These small and often winding, fine-grained granite veins are easily recognized in the tunnel where the rock surface is fresh *(Figure 4-7)*.

The fine-grained granites vary in colour from reddish grey to distinct red. They are in most cases rich in quartz and potassium feldspar and can be classified as true granites *(Table 4-3)*.

From the field studies it is obvious that the fine-grained granites all seem to be younger than the more coarse-grained Småland granite groups. There are also observations of dikes of fine-grained granite cutting each other. Studies of the fine-grained granites have been made with the suspicion that some of them could be anorogenic, as the neighbouring anorogenic Götemar granite massif is also cut by a generation of fine-grained granites. However, no fine-grained, undoubtedly anorogenic granites were found within the area.

Two samples from the fine-grained granite were collected for U-Pb isotope age determinations. The dating of sample 908 was most reliable and gave and age of 1794+16/-12 million years. The dating of the other sample, 2972, was less reliable yielding an age of 1808+33/-30 million years */Wikman and Kornfält, 1995/*.

As regards their trace elements the different linear trends of the fine-grained granite and the Äspö diorite/Ävrö granite may indicate different way of differentiation.

Alteration features in the Äspö granitic rocks

The fracture network in the Småland (Ävrö) granite and Äspö diorite is characterized by the red-coloured salvages, generally a few centimetres wide, occurring beside the fracture planes *Eliasson /1993/*. The microscopic investigation shows that the red colouration of the granite adjacent to the fractures is mainly caused by the presence of dispersed, very fine-grained, reddish Fe-oxyhydroxides/ hydroxides 1) in saussuritic and clouded plagioclase grains, 2) along grain boundaries and 3) subordinately along microfractures within individual grains. The clouding of plagioclase is also partly a result of the optical effect of the extremely fine-grained nature of the alteration products and the common occurrence of micropores.

According to */Eliasson, 1993/* the reddish colouring of the granite spatially coincides with the hydrothermal metamorphic alteration mineralogy occurring along the fracture planes. This fact, together with the observed oxidized mineral assemblage in the hydrothermally metamorphosed zones, indicates that the formation of the ferric compounds (colouring) is contemporary with, and a function of, the hydrothermal alteration.

The petrophysical properties of porosity, density and magnetic susceptibility exhibit a good correlation with the intensity of alteration. This illustrates the importance of these parameters for identifying fractures/fracture zones in the Äspö area *(Figure 4-10)*.

Distribution of rock

The distribution of the four main rock types at different depths are quite similar except for the first 700 m of the tunnel (level 0-100 m) where the Småland (Ävrö) granite is more frequent than the Äspö diorite and in the bottom level 400-460 m where only Äspö diorite has been mapped */Markström and Erlström, 1996; Markström, 1997/*. The Småland (Ävrö) granite - which is exposed on Ävrö south of Äspö and on Äspö over the southern part *(Figure 4-11)* of the spiral probably extends northwards folded beneath the Äspö diorite. This could explain the concentration of Småland (Ävrö) granite in the northern part of the spiral area at depth *(Figure 4-12)*.

Most of the greenstone has the character of inclusions but dikes are also mapped mostly trending EW to the NE. One rather big massif of greenstone occurs at 1600-1700 m in the tunnel and in the shaft at 230 m.

All the rock mass is veined by fine-grained granite but the number of veins in the Småland (Ävrö) granite in the tunnel is sparse compared to veins and dikes in the Äspö diorite. Most of the dikes of fine-grained granite trending NE confirm the idea that the fine-grained granite is closely related to the Småland (Ävrö) granite which is obviously younger than the Äspö diorite.

Table 4-3. Arithmetic mean values of modal analyses of the four most common rock groups in the Äspö area. Samples from bedrock surface, core boreholes and tunnel. ***/Wikman and Kornfält, 1995/.***

	Fine-grained greenstone (%)	**Äspö diorite** (%)	**Småland (Ävrö) granite** (%)	**Fine-grained granite** (%)
Quartz	2	15	25	30
K-feldspar	+	12	25	39
Plagioclase	27	46	37	20
Biotite	18	15	7	2
Chlorite	2	1	1	2
Muscovite	-	+	+	3
Fluorite	-	+	+	+
Pyroxene	1	-	-	-
Amphibole	36	2	+	-
Allanite	-	-	+	-
Epidote	9	6	2	2
Monazite	-	-	-	+
Prehnite	+	+	+	+
Pumpellyite	+	+	+	+
Sphene	1	2	1	+
Calcite	+	+	+	+
Apatite	1	1	+	+
Zircon	+	+	+	+
Opaques	2	1	1	1

\+ = small quantities (<0.5%)
\- = not detected

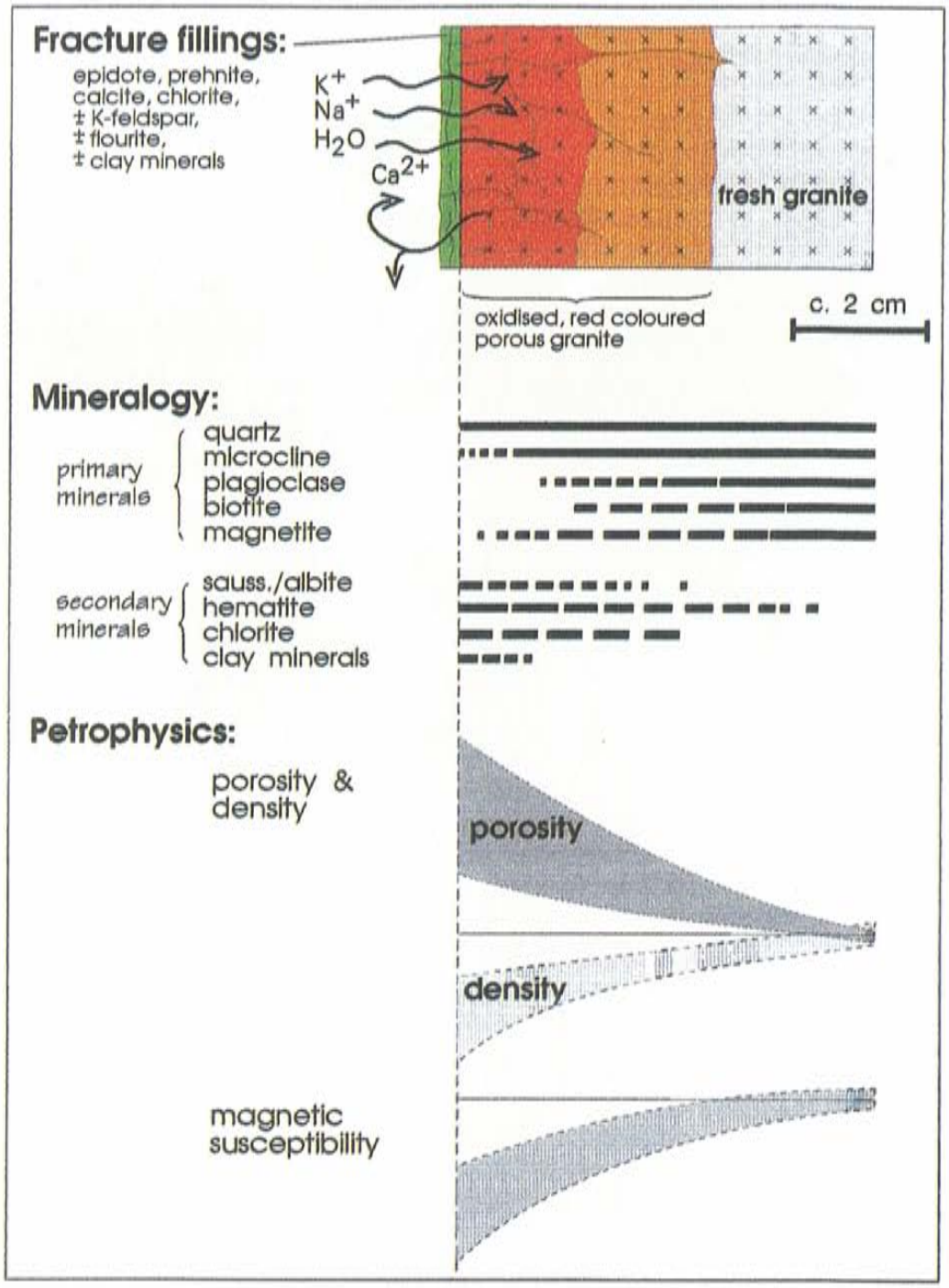

Figure 4-10. *Schematic illustration of the most important fractures in the red-coloured wall rock along fractures in the Äspö granitic rock, /Eliasson, 1993/.*

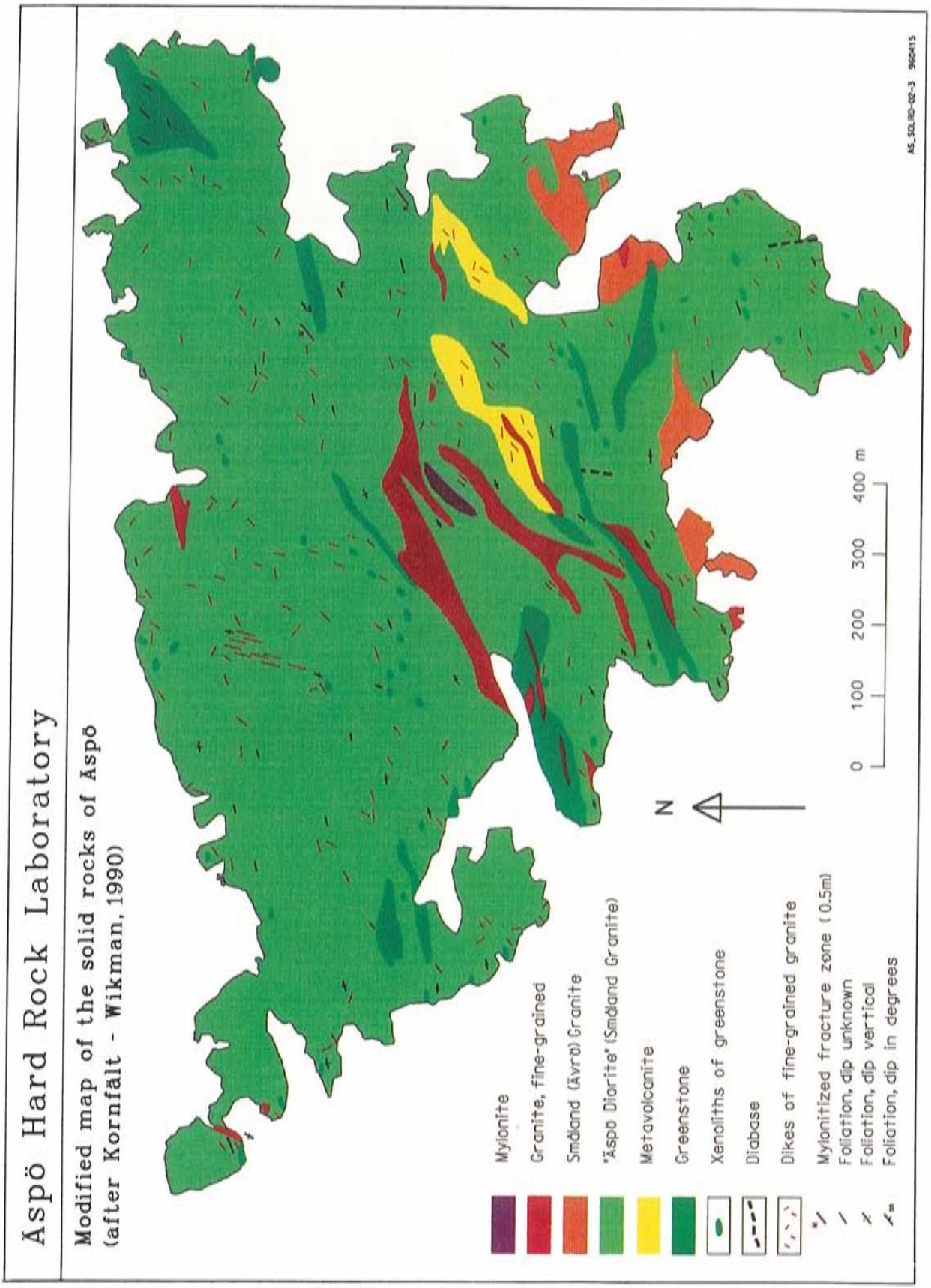

Figure 4-11. *Map of solid rocks on Äspö.*

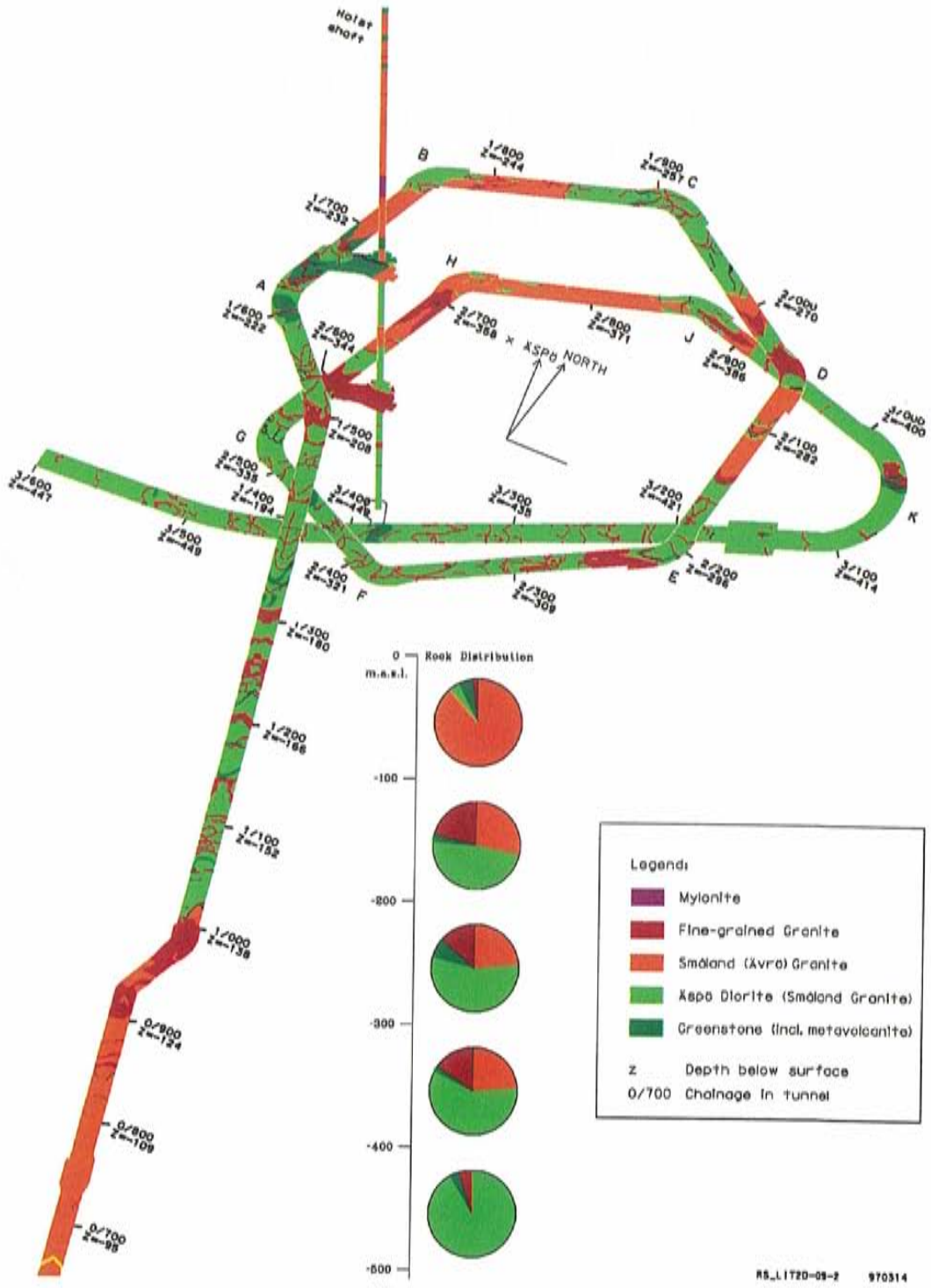

Figure 4-12. *Lithology of the Äspö tunnel. Diagrams illustrate distribution of main rock types at depth.*

In *Rosén and Gustafsons* work of the development and application of a Bayesian Markov Geostatistical Model (Bay Mar) as a decision tool in repository construction, they produced a probability model for the lithology at Äspö from the ground surface to 800 metres below sea level */Rosén and Gustafson /1993, 1995/*. The model was produced using a three-dimensional grid with a cell-size of 20x20x20 metres. The model was based on the surface bedrock map (1991), surface boreholes, access tunnel boreholes, and access and TBM-tunnel mapping data.

The horizontal boundaries of the model were as follows in the Äspö coordinate system *(Figure 4-13)*:

Minimum Easting:	1050 m
Maximum Easting:	2750 m
Minimum Northing:	6750 m
Maximum Northing:	8250 m

Since the objective was to describe the probability distributions for all lithologies of Äspö, the most appropriate differentiation of lithologies with respect to available information was considered to be: Greenstone, Fine-grained granite, Medium-grained granite (Småland (Ävrö) granite), Äspö diorite and Mylonite.

The results from the probability estimations for the lithologies in the Äspö area are shown in one horizontal map with the most likely lithologies at 450 metres below sea level *(Figure 4-14)* and two vertical east-west sections along the 7300 NORTHING Latitude in the Äspö coordinate system */Rosén and Gustafson, 1995/*.

The map in *Figure 4-15* shows high probabilities of a Äspö diorite body between 300 and 600 metres depth in the area of the access and TBM-tunnels. The medium-grained granite dominates in most of the volume. Fine-grained granite and greenstone occur as thin dikes and slabs, and have in general a probability of less than 0.1, except close to borehole observations. At about 300 metres depth, unusually high probabilities for fine-grained granite occur.

The Bayesian convincement maps show (example in *Figure 4-16*) how the certainty of the lithologies decreases away from the borehole observations and at greater depth. It shows where further observations are needed to increase the certainty of the results, if required. Away from observations, Småland (Ävrö) granite rapidly becomes the most likely rock type, since it is very dominating both on the surface map and in the boreholes. Given the resolution of 20 metre cells, fine-grained granite, greenstone, and mylonite can only make up part of cells and occur therefore very seldom as the most likely rock type.

The probability models for the lithology can be compared to the tentative lithological model presented in *(Figure 4-17)*. The model is based on borehole and tunnel mapping data (Section A-A' represent data from a some hundred metres wide vertical rock slab). Among other things a 25-50 metres thick,

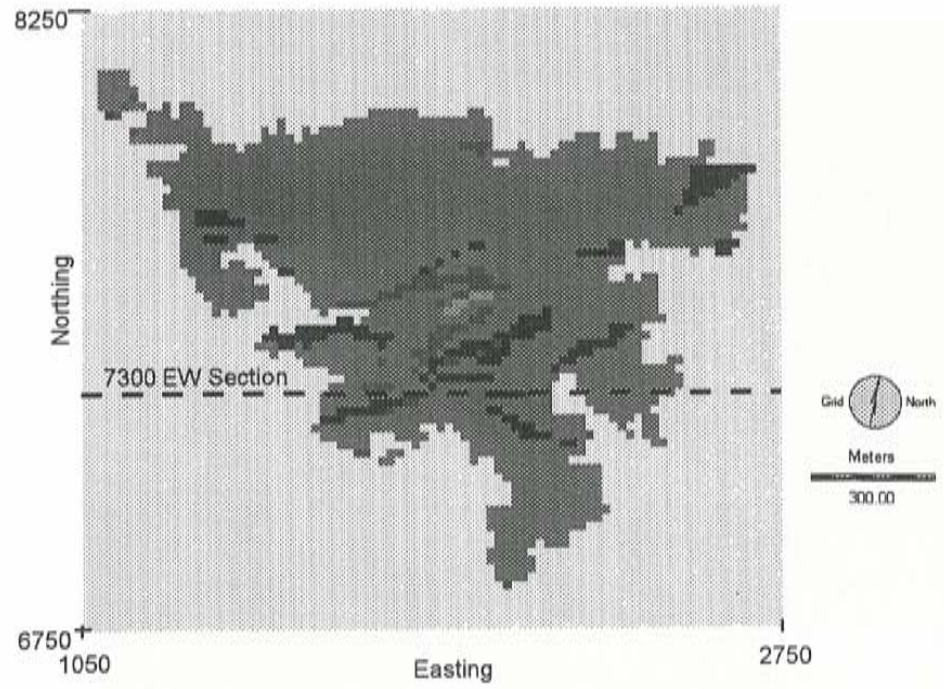

Figure 4-13. *The horizontal boundaries of the model and position of the 7300 EW section. /Rosén and Gustafson, 1995/.*

almost sub-horizontal, irregular body of fine-grained granite probably occur at a depth between 300 and 400 metres in the tunnel volume.

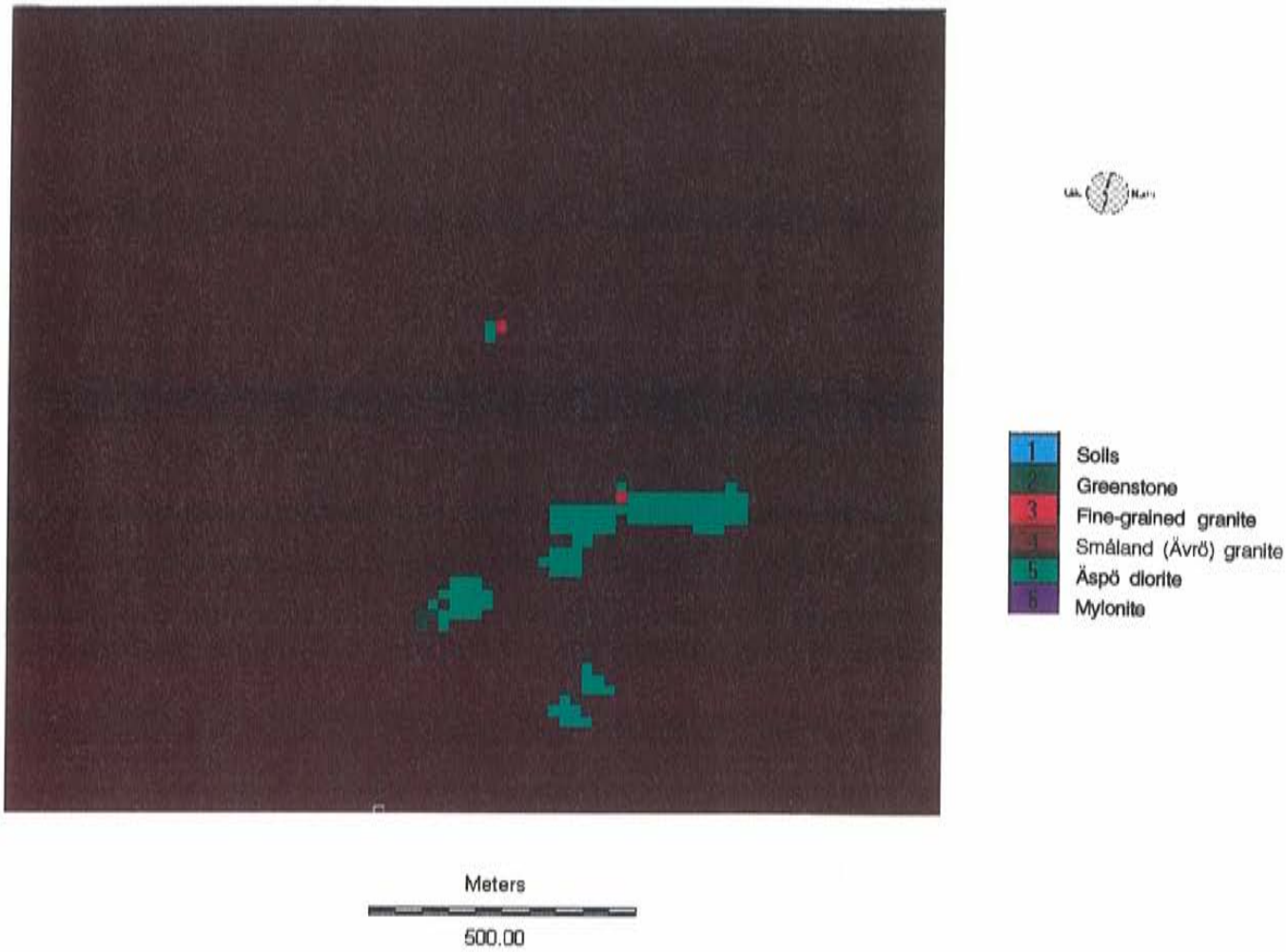

Figure 4-14. *Most likely lithologies, 450 metre level. /Rosén and Gustafson, 1995/.*

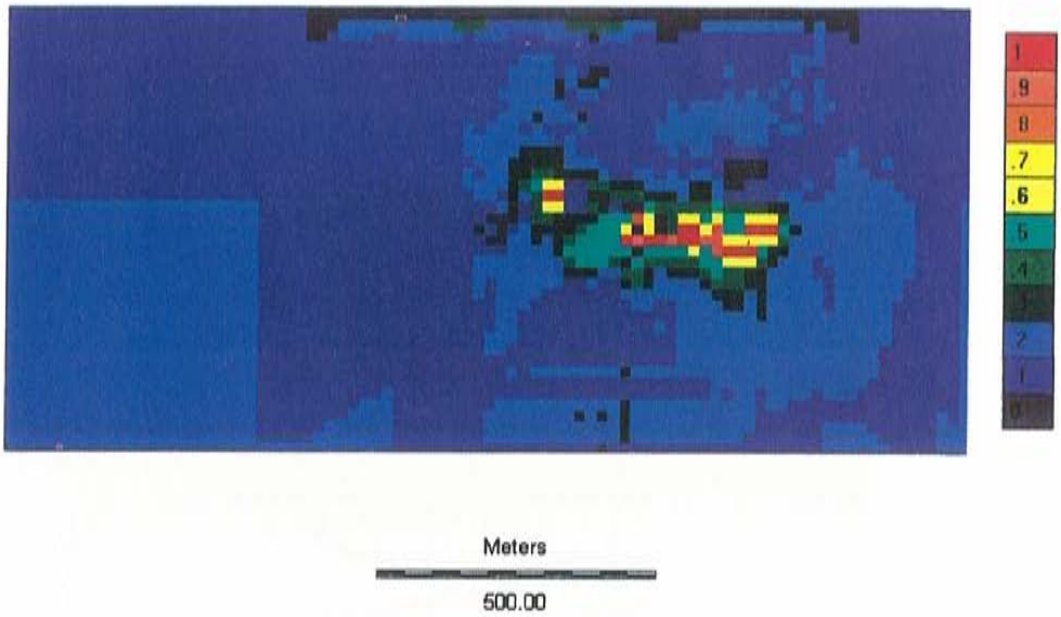

Figure 4-15. *Probability map Äspö diorite, 7300 east-west section. Legend: Probability values. /Rosén and Gustafson, 1995/.*

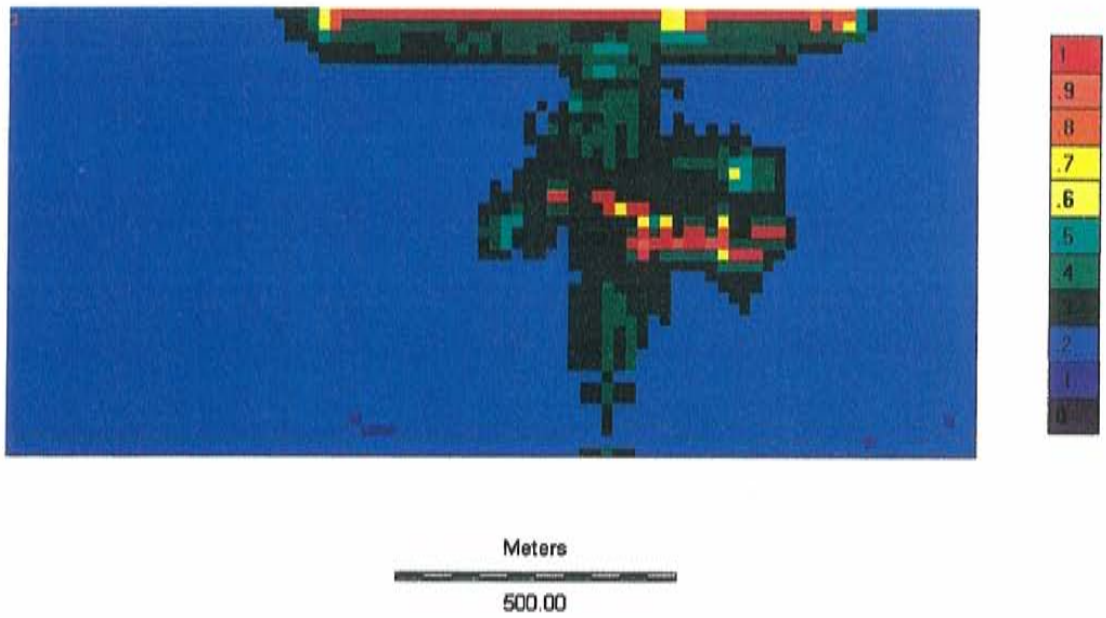

Figure 4-16. *Bayesian Convincement, 7300 east-west section. Legend: Probability values. /Rosén and Gustafson, 1995/.*

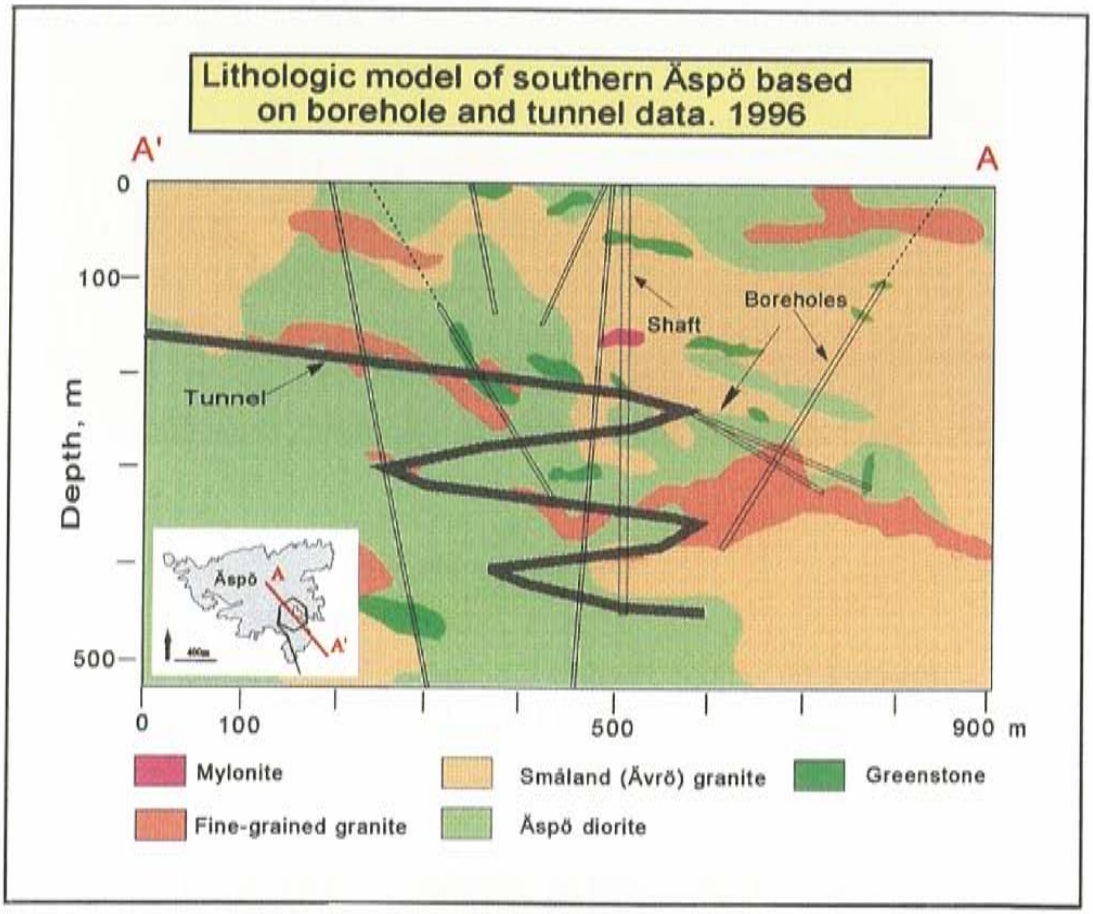

Figure 4-17. *Lithological model of southern Äspö.*

4.2.2 Structural model on a site scale

The geological-structural model describes the geometrical distribution and character of discontinuities in a rock volume. Discontinuity is the general term for any mechanical feature in a rock mass having zero or low tensile strength */Brown, 1981/*. It is the collective term for most fractures, weak schistosity planes, weakness (fracture) zones and faults.

During pre-investigations and tunnel mapping of the Äspö ÄHRL discontinuities were divided into **fracture zones** (major and minor) and small scale **fractures** in the rock mass between fracture zones.

Fracture zones are normally defined as subplanar and continuous volumes of rock. This provides a basis for interpolation of information between boreholes and extrapolation outside them. So even if we know that fracture zones are never exactly planar it seems often to be a useful first approximation geometrically easy to work with */Olsson, 1993/*.

Development of ductile structures and fracture zones

An almost vertical, penetrating foliation trending NE-ENE is the most dominant structural element in the 1700-1800 million year old Äspö granitoids and seems to be the oldest sign of the ductile deformation related to the sub-horizontal NNW-SSE compression. This deformation is also marked by the orientation of mafic sheets often back-veined by two or three generations of fine-grained granites */Talbot, 1990/*.

Intensified strain formed in the amphibolite-facies are marked by gneissic zones trending NE-ENE, dipping to the NNW. Elevated to a higher structural level between 1700 and 1400 million years ago, these old gneissic zones were reactivated as mylonitic shear-zones trending NE especially in central Äspö in a ductile/semi-ductile deformation phase. Strong foliation and mylonites are common in the Äspö shear zone - where more than 10-metre-long bodies of mylonite occur trending E-W and dipping steeply to the north. Regional evidence suggests that the E-W trending mylonites are older than those trending NE */Talbot and Munier, 1989/*. Small scale mylonitic shear planes less than about one centimetre wide and up to a few metres long, with very different orientation, are to be found in many parts of the island.

The first brittle faults probably developed in the region in response to the emplacement of younger granites. These faults and older ductile zones were reactivated several times. The rock mass became increasingly brittle as it was uplifted and unroofed about 1000 million years ago. Parts of the epidotic vein system reactivated and its fractures were later filled by chlorite, zeolite and carbonate.

Fracture zones on Äspö have a wide range of orientations and styles and most of them reactivate older structures *(Figure 4-18)*. The style of each fracture zone tends to depend on the nature of any older structure being reactivated, such as EW gneissic zones, mylonites trending NE or E-W and gently dipping alteration zones. Fracture zones trending N, NE or E-W on Äspö normally had ductile precursors whereas those trending NW apparently did not.

(Figure 4-18) illustrates the Äspö HRL fracture zone pattern in a framework of major regional structures. The main fracture sets, mapped in the tunnel, are presented *(Figure 4-19)* for the major fracture zones and for the rock mass.

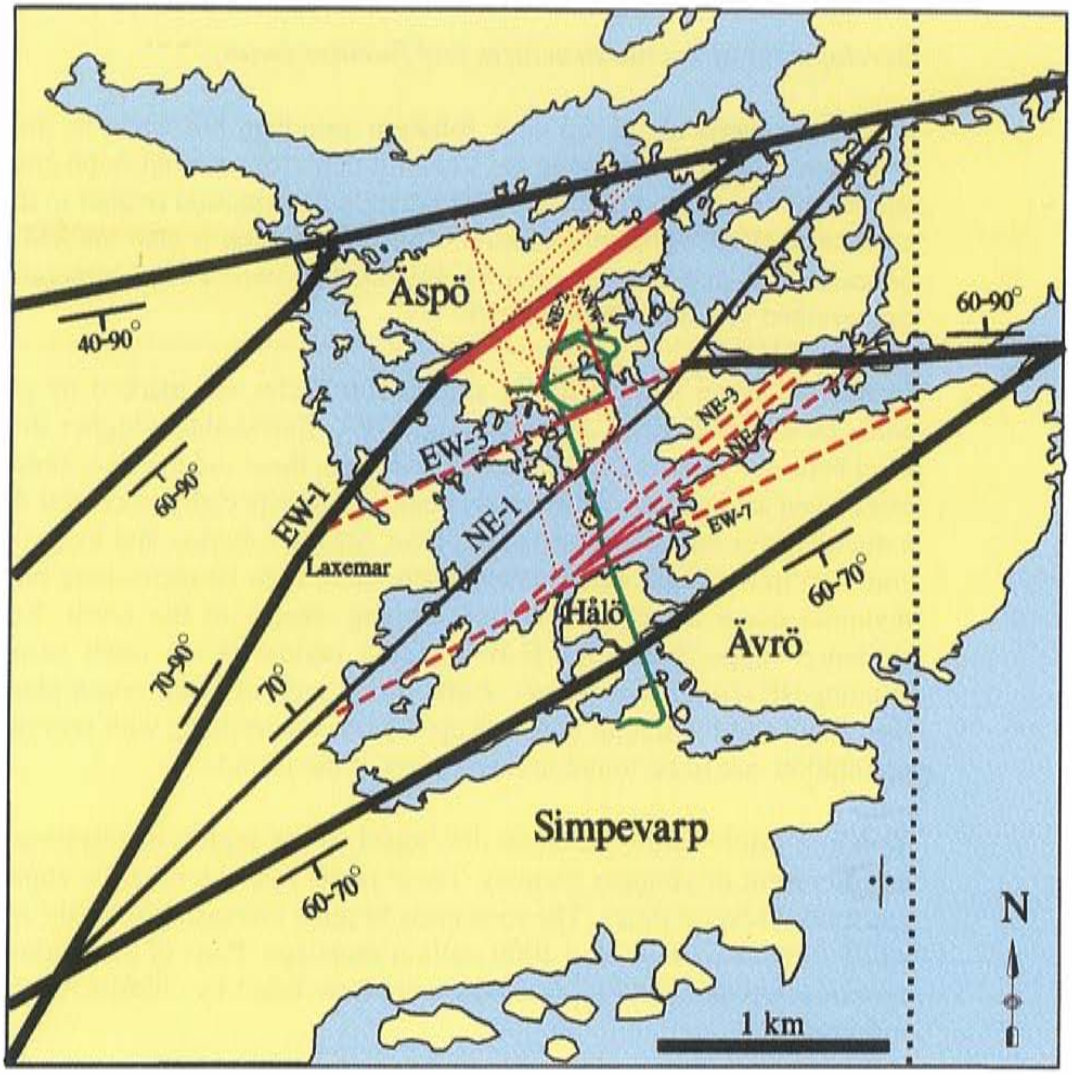

Topographically, geologically and aerogeophysically indicated extensive structure (>approx. 10 km)

Less extensive structure (3-5 km)

Aerogeophysically indicated extensive structure (>approx. 10 km)

60-70° Strike and dip

Certain (in tunnel or borehole)

Probable (geophysically/geologically indicated)

Major fracture zone in the Äspö HRL model

Certain

Possible

Minor fracture zone in the Äspö HRL model

Figure 4-18. *Fracture zones in the Äspö HRL (red) fit in the pattern of regional structures (black).*

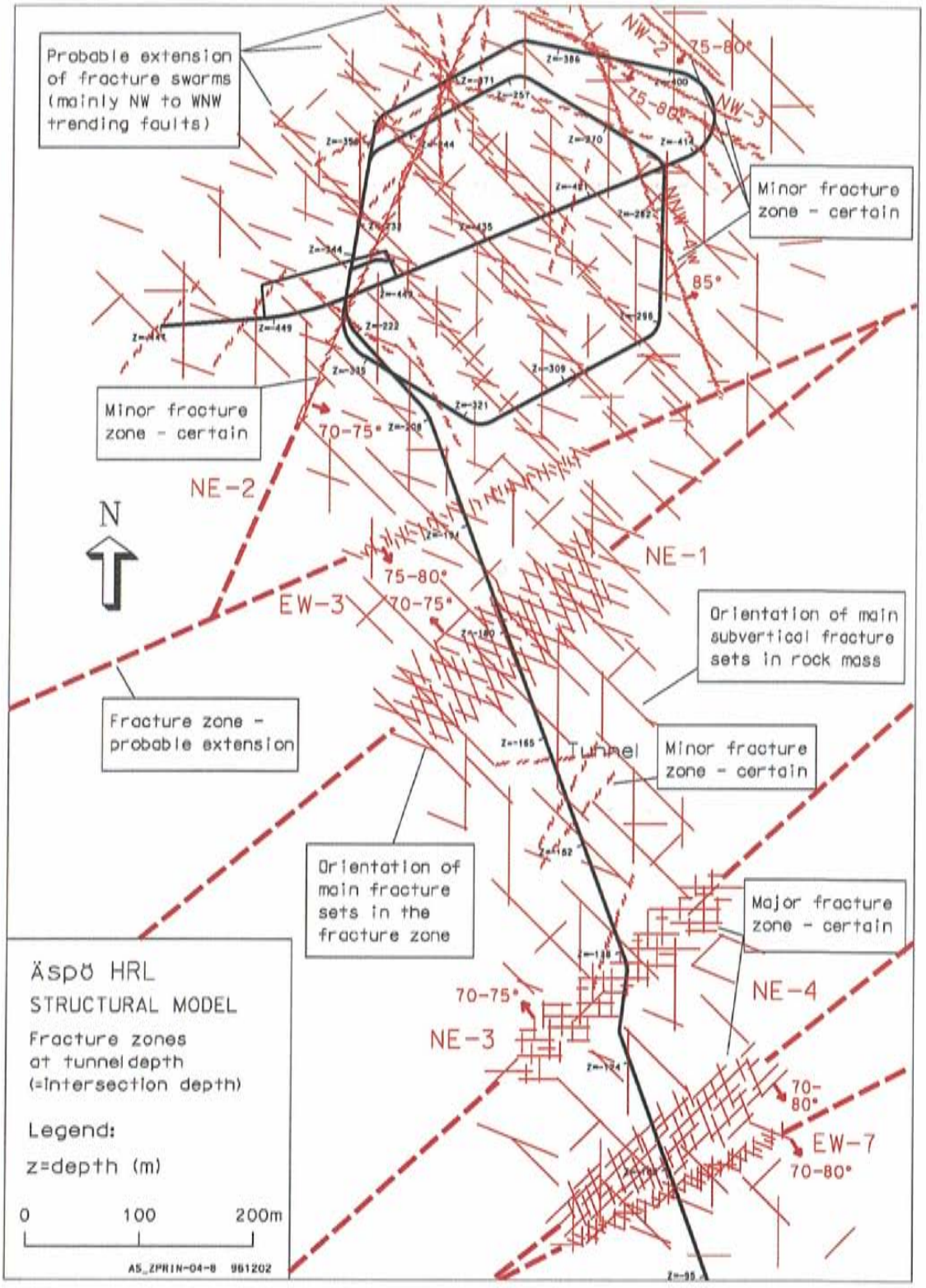

Figure 4-19. *Structural model of the rock mass surrounding the Äspö tunnel. The model represents position and estimated extension of fracture zones (swarms) at tunnel level. Orientation of the main subvertical fracture sets in major fracture zones and the intact rock mass is based on tunnel mapping data. 'Fracture swarms' comprise concentrations of subparallel, often water-bearing faults.*

The discontinuties are mainly discussed from the geological point of view in the section below. The hydraulic character is presented in more detail in *Chapter 6*.

Fracture zones EW-7 and NE-4

Geometry and properties

EW-7 and NE-4 may be regarded as a composite fracture zone with three branches. On the site scale the southernmost bransch, EW-7 is estimated to be approximately 10 m wide, to dip about 75°S and to strike nearly N75°E *(Figure 4-20) /Stanfors et al, 1997/.*

EW-7 consists of one set of fractures trending NNE - which are the most conductive structures - and one fracture set trending WNW. The dominating rock type in the zone is Småland (Ävrö) granite.

On the site scale the approximately 40 m wide NE-4 - which is found to consist of two more or less continuous branches is estimated to dip about 60°S and strike N50°E. The dominating rock type is Småland (Ävrö) granite with inclusions of mylonite and greenstone. The northernmost branch is clearly connected to a mylonite, which is partly crushed. According to *Munier /1995/* the fracture array, typically with coatings of chlorite, calcite and usually enriched in coatings of epidote and Fe-oxides, consists of three main sets; one is steep and strikes NNW, one is moderately dipping (about 45°) towards the SE and the third is subhorizontal. EW-7 and NE-4 are both assumed to surface in the sea north of Hålö.

Coordinates for three planes that approximate EW-7 and NE-4 are presented in *Appendix 2, Table A2-5*.

Observations

EW-7 is estimated to trend almost parallel to the main geophysical lineaments trending ENE-NE in the Hålö-Äspö area. EW-7 is only indicated in one borehole KBH02 (50-75 m) in the pre-investigations. From the tunnel EW-7 was investigated by two cored boreholes (KA0575A and KA664B) which penetrated three water-bearing sections */Rhén et al, 1993/*. In the tunnel between 779-796 m EW-7 is found to be 9.9 m wide. Mapped features in the zone dip 50-90°S and strike N15-75°E.

NE-4 was indicated during pre-investigations by geophysics (ground magnetics and seismic refraction) and borehole data KBH02 (120-150 m). In the tunnel between 796-858 m, NE-4 is observed to be 41.1 m wide to strike N30-50°E and dip 50-70°S. Vertical Radar Profiling (VRP), Vertical Seismic Profiling (VSP) data and orientation of the intensified foliation has been used to deduce the main orientations of the fracture zones.

Judgement of reliability

The reliability of existence (width and properties) of EW-7 and NE-4 is high in the tunnel (tunnel mapping and borehole documentation).

Data on orientation, width and properties are estimated to be valid mainly for the parts of EW-7 and NE-4 close (25-50 m) to the tunnel. The extension of the zones outside the tunnel, based only on geophysical data, is estimated to have a rather low reliability. Reliability of dip and properties is very low outside the tunnel.

Fracture zone NE-3

Geometry and properties

On the site scale NE-3 is estimated to consist of several subparallel branches (splays), with a total width of approximately 50 m, that strike about N50°-70°E. Two of them are estimated to dip approximately 80°NW and 70°NW respectively *(Figure 4-21) /Stanfors et al, 1997/.* No further constraints of the geometry can be deduced on a structural basis because the zone is assumed to surface in the sea south of Äspö. Fine-grained granite is the dominating rock type with some intersections of Småland (Ävrö) granite and greenstone. Fracture spacing is mostly 5-20 cm but crushed parts are found locally. Although the zone itself dips steeply towards NNW, as indicated by geophysics, its constituent fractures are steep and strike EW and NS */Munier, 1995/.* Their coatings are typically chloritic and calcitic. Coatings of fluorite, haematite and Fe-oxides are less abundant.

Coordinates for planes that approximate NE-3 are presented in *Appendix 2, Table A2-5.*

ESR dating studies concentrated on the fault gouge in NE-3 and NE-4 indicate no fault movements for a minimum time period of at least hundreds of thousands of years */Maddock et al, 1993/.*

Observations

NE-3 was indicated by ground magnetics and seismic refraction and confirmed in borehole KBH02 (310-400 m) in the pre-investigation phase */Wikberg et al, 1991/.* After excavation NE-3 was documented by tunnel mapping and found to be 49 m wide between section 958-1009 m */Rhén et al, 1995/.*

Judgement or reliability

The reliability of existence (width and properties) of NE-3 is very high in and close (25-50 m) to the tunnel (tunnel mapping and borehole documentation).

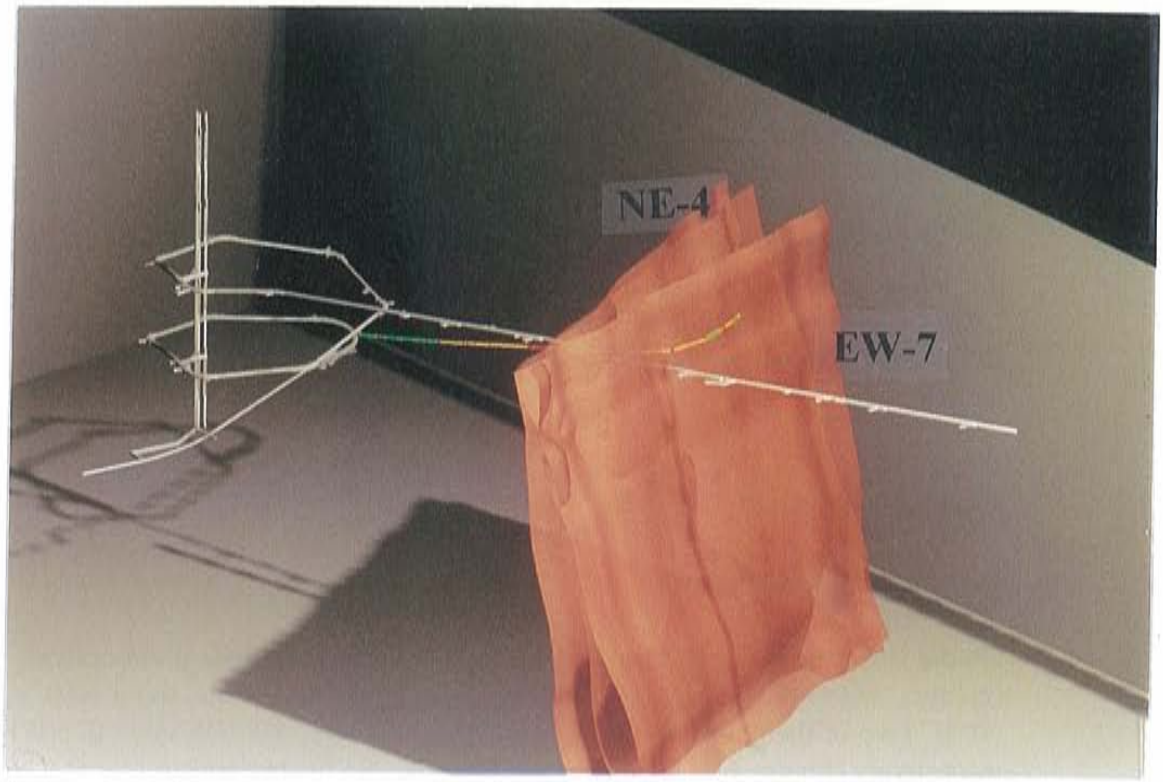

Figure 4-20. *Computer graphics showing the geometry of various zones within the NE-4/EW-7 system. The coloured line represents borehole KBH02 drilled through the structures shown /Munier, 1995/.*

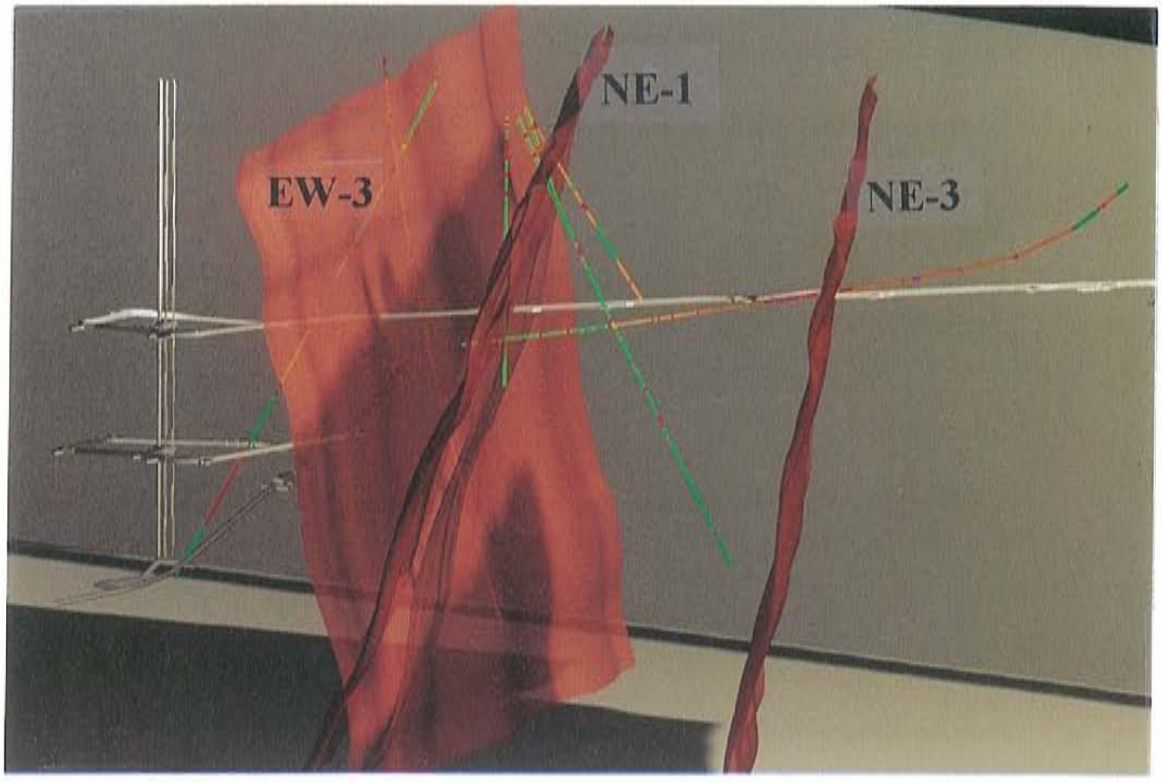

Figure 4-21. *Computer graphics showing the geometries of NE-3, NE-1 and EW-3 /Munier, 1995/.*

The reliability of extension outside the tunnel (based on geophysics) is rather high but less good for dip and properties.

Fracture zone NE-1

Geometry and properties

On the site scale the major fracture zone NE-1 is interpreted to trend N50-60°E and dip 70-75NW *(Figure 4-21) /Stanfors et al, 1997/.* The zone is estimated to be approximately 60 m wide, consisting of three branches. All three branches are connected to a rather complex rock mass with Äspö diorite, fine-grained granite and greenstone. The major part of the zone may be approximated by two planar water-bearing branches. The coordinates for these are presented in *Appendix 2, Table A2-5.*

The two southernmost branches, trending NE and dipping N, can be described as highly fractured and more or less water-bearing. The northern branch, which is approximately 28 m wide in the tunnel, is the most intense part of NE-1 and highly water-bearing. An - approximately 8 m wide - part of this branch, trending N50°E and dipping 75°N, with open, centimetre wide fractures and cavities and partly clay-altered rock, is surrounded by 10-15 m wide sections of more or less fractured rock. The central 1 metre wide section is completely clay altered */Stanfors and Rhén, 1993/.*

The fractures within NE-1 did not in any respect differ from the average rock mass at the HRL except from a slight increase in epidotic/quartzitic coatings and minor (<1 cm wide) mylonitic shear zones. The margins of various strands of NE-1, some of which displayed faults with gouge, are characterized by steep gradients in fracture frequency. The geometry of NE-1 constituent fractures could not be investigated in detail due to safety considerations during construction and extensive reinforcement. However, the results indicate that the fracture array consists of three sets; one is steep and strikes WNW, one is sub-horizontal and a third dips moderately towards NNW. The latter contains long faults with gouge and has been used to determine the local orientation of NE-1.

Observations

The interpretation of NE-1 is based on geophysics and several boreholes in the pre-investigations */Wikberg et al, 1991/.* The surface of the zone in the sea c. 50-100 m south of Äspö is indicated by refraction seismic and magnetic data. No outcropping of NE-1 was found on the island but in the southernmost peninsula of Äspö, immediately north of the zone, outcrops are reddened and display an array dominated by fractures dipping about 50-60° towards NW. NE-1 is well documented in several core boreholes from surface as a series of several metres wide, highly fractured water-bearing and in part mineralogically altered sections.

Borehole identifications are most evident in KBH02 (c. 310-400 m), KAS09 (100-150 m), KAS14 (100-125 m), KAS11 (150-175 m), KAS02 (possibly 805-924 m), KAS08 (570-600 m), KAS07 (520-550 m) and KAS16 (420-430 m).

In the tunnel the zone was mapped between sections c. 1240-1320 m. Two core boreholes, KA1061A (160-208 m) and KA1131B (180-203 m), and 8 percussion boreholes were drilled from the tunnel across the zone.

Judgement of reliability

The reliability of existence (width and properties) of NE-1 is very high in and close to the tunnel (tunnel mapping and borehole documentation).

The reliability of extension dip and properties of NE-1 outside the tunnel, based on geophysics and core borehole (KAS16) and borehole radar is estimated to be rather high for some hundred metres NE of the tunnel intersection */Stanfors et al, 1992/.*

Fracture zone EW-3

Geometry and properties

On the site scale EW-3 is estimated to be approximately 14 m wide, strike approximately N75-80°E and dip 75-80° towards the S *(Figure 4-21)*.

EW-3 is consisting of a 2-3 m wide crushed central section connected to a contact between Äspö diorite and fine-grained granite. The crushed section is surrounded by 5-10 m of highly fractured Äspö diorite. Clay altered rock is common especially in the crushed part of the zone. Coordinates for a plane that approximates EW-3 are presented in *Appendix 2, Table A2-5.*

Compared with other zones investigated EW-3 has a more homogeneous fracture array with one dominating dispersed set that strikes NW and dips approximately 50° towards the SW. EW-3 is also enriched in fractures with oxidized walls when compared with other zones */Stanfors et al, 1997/.*

Observations

The fracture zone EW-3 was very well indicated topographically, and geophysically (magnetic, seismic and electric) and in core boreholes KAS06 (60-70 m) and possibly in KAS07 (c. 420 m) during the pre-investigations and estimated to be approximately 10 m wide */Wikberg et al, 1997/.* In the tunnel between 1407-1421 m, EW-3 was observed to be 12.1 m wide, to strike approximately E-W and to dip 70-80°S.

In the tunnel EW-3 was investigated by mapping and confirmed in two percussion boreholes, HA1405A and 1405B (high penetration rate in 2-3 m wide sections) */Rhén et al, 1995/.*

Judgement of reliability

The reliability of existence (width and properties) of EW-3 is very high in and close to the tunnel (tunnel documentation). The extension of the zone is estimated to be reliable for some hundred metres outside the tunnel intersection (surface geology, geophysics and borehole indications). Reliability of properties and dip is high only for a narrow (approx. 50 m) area outside the tunnel (tunnel and borehole documentation, borehole radar).

Fracture zone NE-2

Geometry and properties

On the site scale fracture zone NE-2 is estimated to trend NNE/NE and expected to follow a somewhat winding course dipping 75-80°SE. *Figure 4-22* shows the interpretation of NE-2

The brittle deformation of this zone is probably greatly influenced by the former ductile shearing and mylonitization */Stanfors et al, 1997/.*

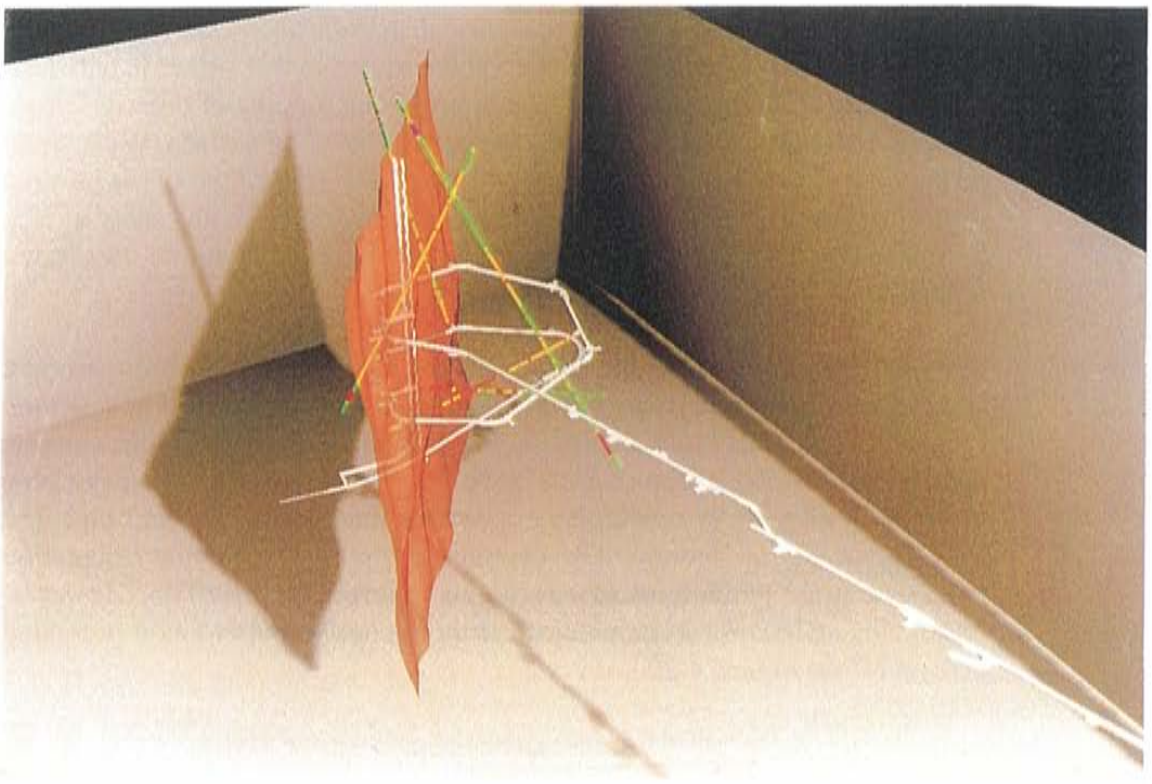

Figure 4-22. *Computer graphics of NE-2, looking NW and down /Munier,1995/.*

Measured strikes in the tunnel vary between N15°E and N36°E measured dips cluster around 65-82°S. However, the width of the most intensively foliated portion of the mylonite varies between 1 and 5 m.

The coordinates of a plane that approximates the zone are presented in *Appendix 2, Table A2-5.*

Observations

NE-2 was indicated geophysically (low-magnetic and decreased resistivity along almost the entire zone). Geological indications were found on surface of the SW part of zone NE-2 (intense fracturing and alteration of outcrops in the trench). Borehole indications in KAS04 (430 m), KAS08 (40-60 m), KAS13 (370-410 m) and HAS16 (20-80 m) of mylonite and crushed and highly altered sections, as well as VSP and borehole radar data indicated the extent of the zone at depth. Hence, fracture zone NE-2 is only locally developed and rather faintly topographically indicated */Wikberg et al, 1991/.*

Intersections of fracture zones mapped in the tunnel, at about 1602 m, about 1844 m and about 2480 m represent one or two branches of NE-2. *(Figures 4-23 and 4-24).* In two percussion boreholes, drilled from the tunnel, penetration rate and borehole TV indications confirmed the zone */Rhén et al, 1995/* at tunnel section 1602 m. An estimated southeasterly dip of NE-2 is supported by the fact that there is no indications of fractured mylonites in core boreholes KA1754A and KA1751A */Munier, 1995/.*

The most prominent structure in the vertical shaft */Munier and Hermansson, 1994/* is an approximately 10 m wide body of mylonite that strikes locally N to NNE and dips 75° towards the E. The inferred outcropping of this significant body of mylonite coincides with the location of NE-2 on surface. What could be interpreted as a branch of NE-2, dips approx. 80° toward the SE as inferred from surface outcropping. It is possible that this mylonite, or any splay of NE-2, rotate or curl with depth towards parallelism with the mylonite intersected in the shaft.

Surface, shaft and tunnel intersections were modelled in three-dimensional space. The observations cannot be uniquely fitted with a single planar structure. However, the undulating nature of the mylonite obvious at the surface, confirmed by various measurements in the tunnel down to about chainage 2480 m are well aligned by a sub-planar structure that strikes 25° and dips 75° towards the SE on average. The natural variability in mylonite orientation makes accurate predictions of any future intersection uncertain. However, reasonable estimates can be obtained from the derived orientation presented here and from *Figure 4-22.*

Figure 4-23. *Fracture zone NE-2 at section 1602 m in the tunnel.*

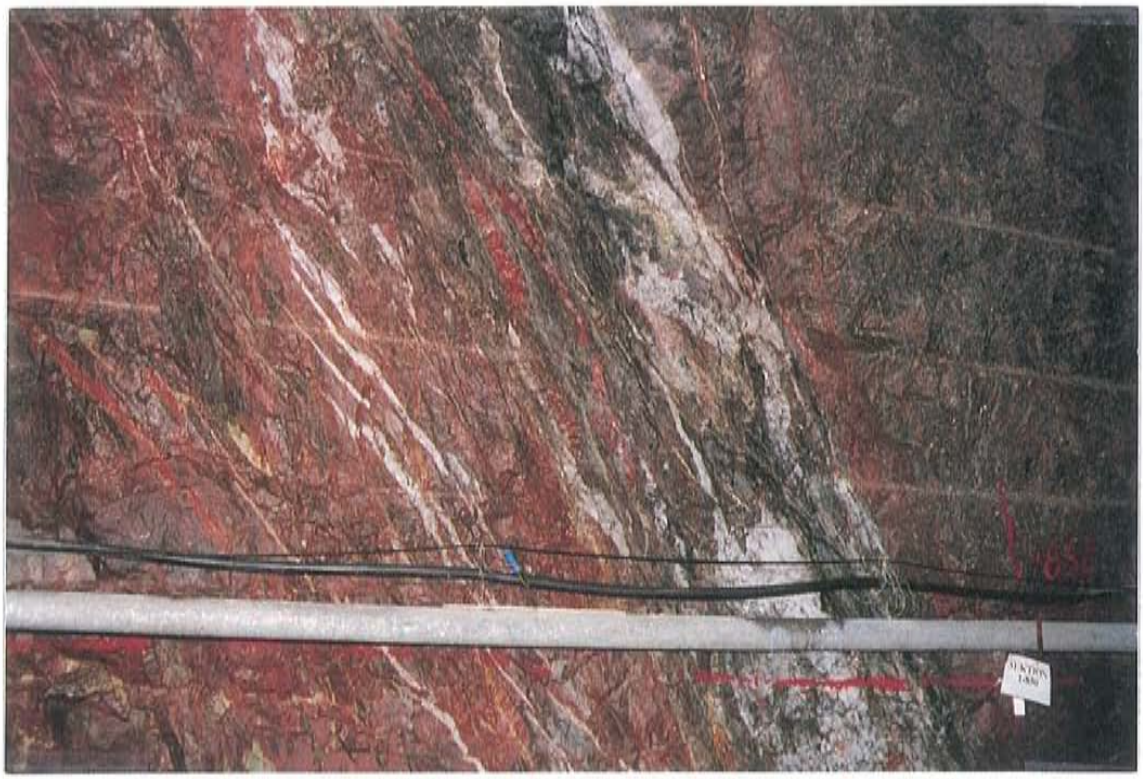

Figure 4-24. *Fracture zone NE-2 at section 1844 m in the tunnel.*

Judgement of reliability

The reliability of the existence (width and properties) of NE-2 in a restricted area of Äspö (surface indications) and in some sections of the tunnel is high but the reliability of geometry and extension is rather low due to the estimated winding extension. Estimated properties of NE-2 are valid only for tunnel and borehole intersections.

Fracture zone EW-1

Geometry and properties

Fracture zone EW-1 can be regarded as a part of the about 300 m wide low-magnetic zone (Äspö shear zone), trending NE, which divides Äspö into two main blocks. EW-1 consists of at least two strands and hydraulic tests indicate that parts of EW-1, as an hydraulic feature, has been approximated with two main hydraulic structures with coordinates as presented in *Appendix 2, Table A2-5*, and within the structure with a hydraulic conductor domain called SRD2, see *Chapter 6*. The hydraulic structures are parallel, strike NE and dip 78° and 88° SE respectively.

Initially the zone was formed by early ductile/semi-ductile deformation. Local development of mylonites and epidotic shear zones controlled the orientation of later brittle deformation in the form of increased fracturing and brecciation. Hydrothermal alteration (oxidation of magnetite to hematite and red-staining of fractures) and formation of different fracture filling minerals probably had an important sealing effect on the main part of the zone. The most conductive parts of EW-1 seem to coincide with some narrow highly fractured sections or single open fractures which are probably not connected along the entire zone.

According to */Munier, 1995/* the ductile precursor of EW-1 was sinistral strike-slip, the latest brittle reactivations appear to have been dextral strike-slip as inferred from fracture geometry and slickenside lines.

Observations

The fracture zone EW-1 was early indicated by the airborne geophysical survey */Nisca, 1987/* and the lineament interpretation */Tirén, 1987/*. Ground geophysical investigation confirmed the extension of EW-1 in more detail. In the first drilling campaign a cored borehole KAS04 (55-70 m and 175-190 m) - inclined 60° SE crossed the zone. EW-1 is also indicated in the percussion boreholes HAS01, HAS05, HAS18, HAS19 and HAS20 by increased fracturing and alteration. EW-1 is schematically visualized by in *Figure 4-25*.

Fracture zone EW-1 is very well documented topographically (50-100 m wide depression in the ground extending many hundreds of metres), geophysically (low-magnetic and low-resistivity zone 200-300 m wide), geologically (outcrops in trench with mylonites and crushed sections) and in boreholes

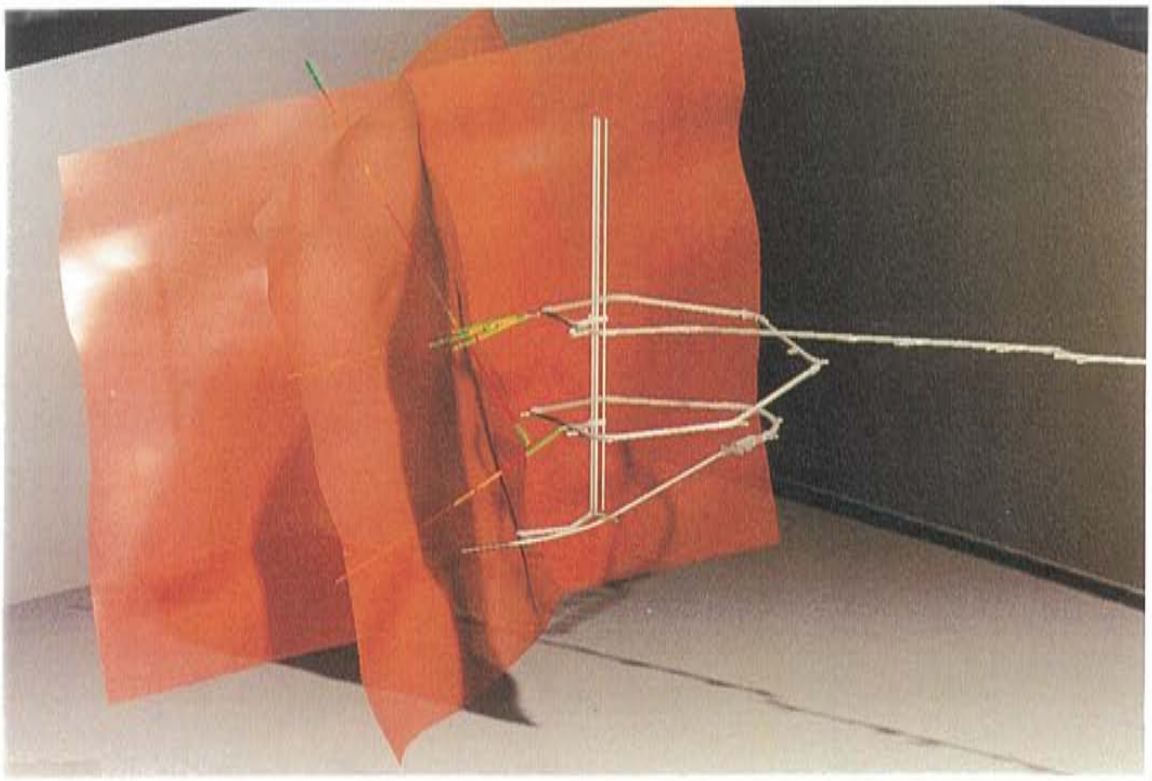

Figure 4-25. *Computer graphics showing the geometry of EW-1 in relation to the HRL. Coloured lines represent boreholes interpreted to be drilled through the structures shown /Munier, 1995/.*

(mylonites and many highly fractured and altered sections in drill cores). EW-1 is also indicated by VSP (Vertical Seismic Profiling) */Cosma, 1990/* and borehole radar */Carlsten, 1990/.*

Core borehole KA1755A (90-100 m and 195-215 m) drilled from the tunnel *(Figure 4-26)* mainly supports the initial model of EW-1 as a complex fracture zone comprising steeply dipping branches in an inhomogeneous rock mass. The rather wide mylonites in the surface trench are found again as narrow veins in the core but the volcanite at the surface is not found again in the core. */Stanfors et al, 1994/.*

An interpretation of EW-1 based on surface geological and geophysical data and information from core borehole KA1755A strongly supports the idea of two main branches - with very intense fracturing, mylonitization and hydrothermal alteration. The rock mass between the two branches is more or less altered, especially at the surface.

Summarized the structural interpretation of EW-1 is based on lineament interpretation, outcrop observations and various boreholes. It has not been possible to find a single plane that uniquely intersects the observations of mylonite, crushed rock and water inflow in the boreholes. Using two faults, the correlation of borehole and surface observations is better constrained. However, additional investigations are necessary to constrain the detailed geometry of EW-1 and its constituent components; alternative models,

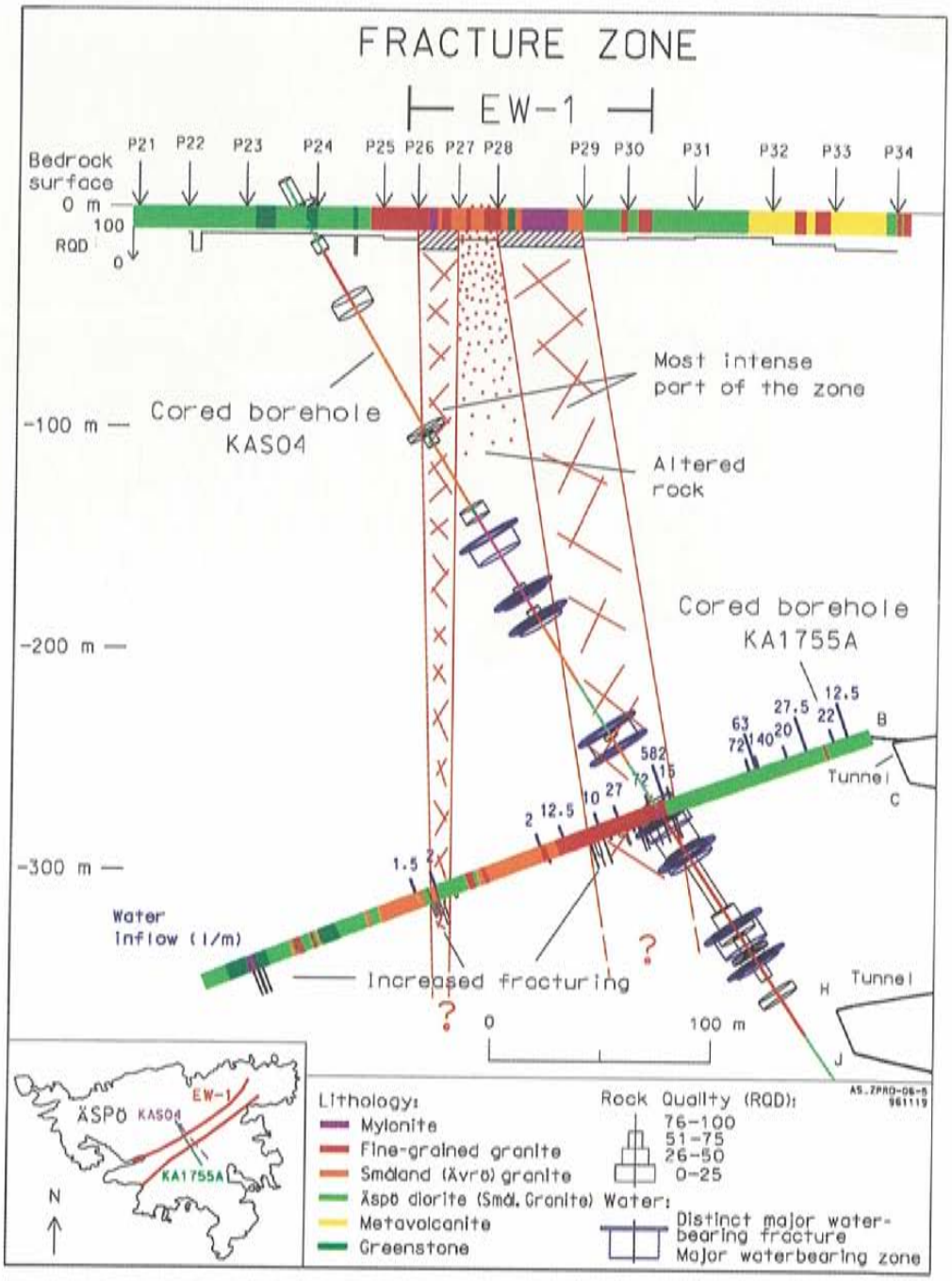

Figure 4-26. *Interpretation of fracture zone EW-1. Section parallel to borehole KA1755A. /Stanfors et al, 1994a/.*

invoking more than two faults, are possible. Using two hydraulic "planes" is probably a too big simplification of a complex zone like EW-1.

Judgement of reliability

The reliability of the existence of EW-1 on the site scale is very high in most of the Äspö island (topography, geophysics and boreholes).

Reliability of properties is high where the zone is penetrated by boreholes. Due to the estimated complicated character of EW-1 the reliability of geometry on a more detailed scale is rather low.

Gently dipping fracture zones and fracture swarms

Geometry and properties

Two well defined gently dipping fracture zones were found in the tunnel. The first one intersects the tunnel at chainage 220 m. It consists of anastomosing fractures striking NW and dipping 25°SW with a spacing of less than 10 cm. The width of the zone is 0.5 m. Parts of the zone consists of calcite-impregnated breccia. Epidote and chlorite fillings are also present */Rhén et al, 1995/.*

The second and most prominent gently dipping fracture zone appears at chainage 1744 m down to 1850 m *(Figure 4-27)*. Intense fracturing trending NE and dipping 32°SE, subparallel to the tunnel for almost hundred metres. The width is less than a metre with mineral fillings of epidote, chlorite and oxide. Parts of the zone contain fault breccia which gradually decreases in intensity to anastomosing fractures with a spacing of 10 cm or more. A minor amount of water inflow (drops) were observed in the brecciated part of the zone.

Except for the two gently dipping fracture zones described many other subhorizontal fractures occur in swarms rather than zones, much like the subvertical NNW hydraulic conductors appear in swarms. The swarms are visible in straight parts of the tunnel, but most detectable in the larger niche corners. *Munier and Hermansson /1994/* defined a 'fracture swarm' as a zone with relatively high fracture frequency, but not so high as a proper 'fracture zone', with fracture orientation essentially parallel to the orientation of the swarm boundary.

Altogether seven subhorizontal fracture swarms have been identified in the HRL. Three of them crosscuts the spiral part of the tunnel at the depths about 220 and 330 m in the two elevator rooms and four swarms in two groups are intersecting the access ramp at around chainage 450 m and 1050 m. Three of the swarms and one gently dipping fracture zone are illustrated in *Figure 4-27*. Details on positions and orientation of the gentle dipping structures are presented in *Munier and Hermansson /1994/, Hermansson /1995/* and *Rhén and Stanfors /1995/.*

Observations

Gently dipping (<35°) fracture zones (GDF) on the surface of Äspö was described by */Talbot and Riad, 1987/* and was interpreted as superficial stress-relief to the surface exaggerated by the retreating Quaternary ice sheets. Further studies of the surface geology revealed the presence of three gentle thrusts on southern Äspö striking E-W and dipping N */Talbot and Munier, 1989/*, all of

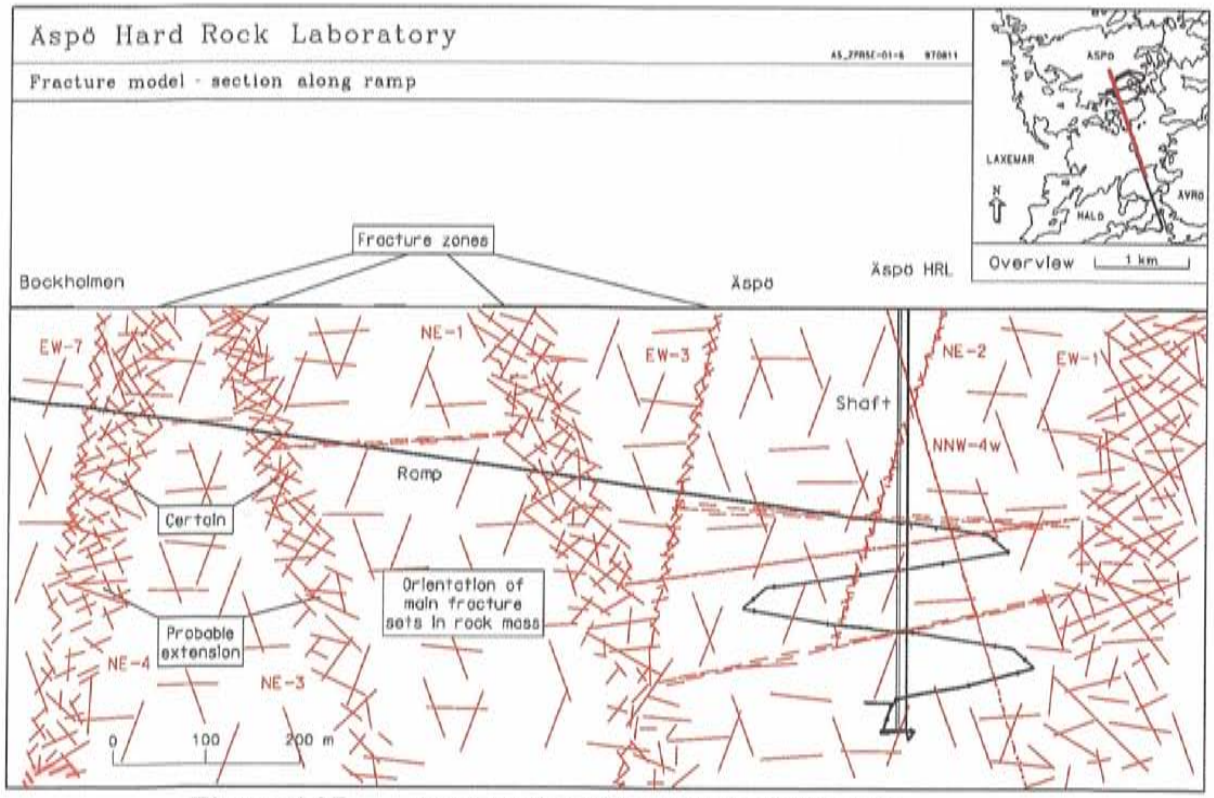

Figure 4-27. *Structural model - section along ramp.*

which appeared to be associated with early gently dipping gneiss zones, thrusts and high fault scarps. Interpretations based on seismic reflections */Ploug and Klitten, 1988/* suggested the presence of gently dipping fracture zones with a 90-133 m spacing at depth */Talbot and Munier, 1989/*. Structural mapping by */Munier and Hermansson, 1994/* in the vertical elevator and ventilation shafts did not reveal any subhorizontal zones or gently dipping gneiss zones. However, occasional gently dipping fractures have been observed both in the shafts and in the tunnel. On stereo plots of the complete fracture pattern there is a clear cluster of subhorizontal fractures scattered over the whole HRL. Radar reflections in borehole KA2048B */Carlsten, 1993/* also reveal a few subhorizontal reflections.

Judgement of reliability

The reliability of existence of gently dipping fracture zones and fracture swarms in the tunnel is high but the reliability of extension, geometry and properties outside the tunnel is estimated to be very low.

Minor subvertical fracture zones

Geometry and properties

Several small-scale fracture zones have been mapped underground. Most of them trend NNE-NE but some WNW-trending zones are also observed. The zones are generally not wider than 1 m and rarely exceed 0.5 m in width. Most

consist of a single or up to a handful of anastomosing faults that generally contain gouge, slickensides or mylonitic fabrics. The host rock is generally mylonitized near faults.

The water-bearing minor subvertical fracture zone NNW-4W is an example of a persistent fracture zone which is confirmed in the tunnel by three intersections at 2020 m, 2120 and 2914 m *(Figure 4-28)* with 5-10 cm wide fractures filled by grout in metre-wide sections of cataclastic granite */Rhén et al, 1995/*. Coordinates for the minor fracture zones judged to be hydraulically important and possible to identify approximately to position and extent are presented in *Appendix 2, Table A2-5* as plane features.

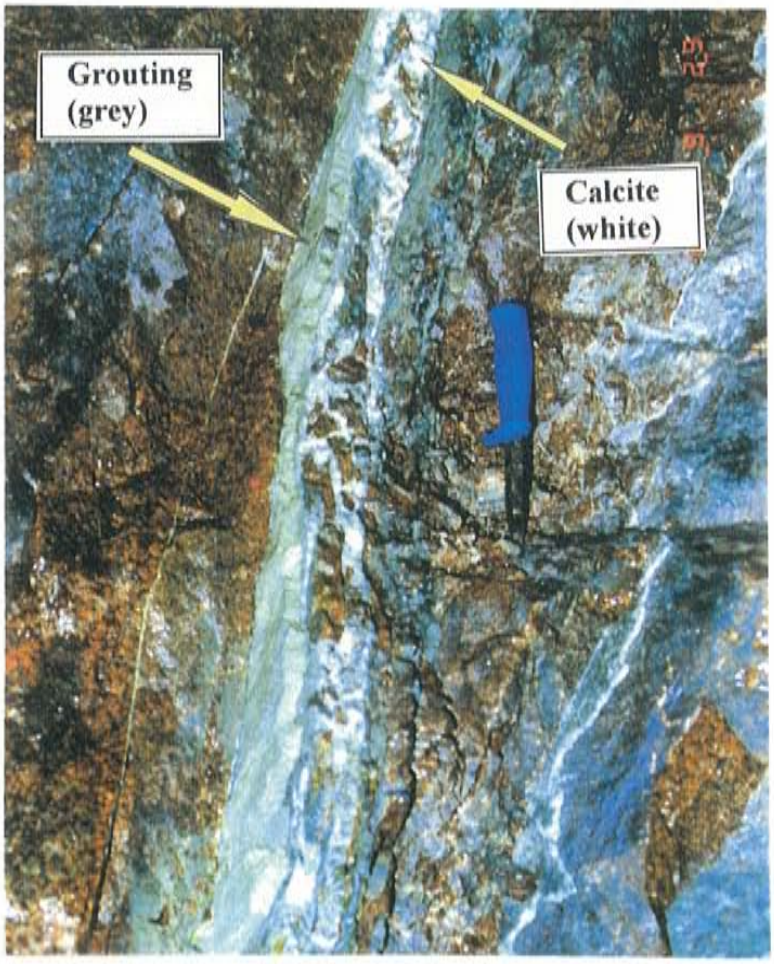

Figure 4-28. *Fracture zone NNW-4W. Intersection in tunnel at 2120 m. White fracture filling is calcite, grey is grouting material /Photo K. Annertz/.*

Observations

A great number of fractures and narrow (decimetre to a few metres wide) subvertical fracture zones striking approximately north have been mapped on outcrops in Äspö. More or less extensive, they seem to branch out in an en-échelon pattern across the island.

Only a few of them are topographically significant but normally too narrow to be geologically unambiguously indicated. Vertical Seismic Profiling and borehole information support the notion of steep, mostly easterly dips. All these fractures and fracture zones were described under the designation 'NNW-system' in the predictions.

Combined results from tunnel mapping and drilling from the tunnel show the characteristic pattern of the small scale structures. They mostly occur in a complex pattern of steeply dipping fractures (fracture swarms) and some decimetre-wide 'fracture zones' trending WNW to NE. Many of the narrow fracture zones are connected to veins or dikes of fine-grained granite. Especially regarding the conductive feature NNW-2 there are a number of a few decimetre-wide fracture zones in the tunnel which seem to be possible to correlate to indications in boreholes, crossing the central part of the spiral, forming a hydraulically active structure trending WNW-NNW, *(Figure 6-31)*. The character of NNW-1 structure as 'fracture zone' is not very evident. NNW-1 should rather be described as a 10-30 m wide swarm of mostly subvertical conductive fractures trending WNW to N, where the WNW-NW trending fractures are normally the most frequent and hydraulically important. According to the structural model *(Figure 4-19)* fracture zone EW-3 acts as a more or less tight barrier between the main water conductor NE-1 and the fractures trending WNW-NW in the western part of the spiral. The highly water-bearing fracture zone NNW-4W is more directly connected to NE-1.

During the course of the investigations for the SELECT Project, the minor fracture zones NW-2 and NW-3 were identified */Winberg et al, 1996/*.

Judgement of reliability

The reliability of the existence and their approximate frequence of the minor zones in the tunnel is high (tunnel mapping and drilling). The reliability of extension, geometry and properties outside the tunnel is estimated to be low.

Small scale fractures in the rock mass

Several authors */Ericsson 1987, 1988, Munier in Stanfors et al., 1993a, 1994a, Munier, 1993a and c, La Pointe et al, 1995, Kickmaier, 1995, Mazurek et al, 1996* and *Poteri, 1995/* have made thorough analyses of the mapped fractures at Äspö which are stored in the SICADA data base. The data base consists of more than ten thousand fracture observations. *Hermansson /1995/* made a special study with the main aim of synthesizing the structural geology of water-bearing fractures.

Regarding fracture frequency (fracture spacing) it is important to make some comments on the different fracture data recorded during the investigations.

During pre-investigation of the Äspö target area a great number of core boreholes were drilled. Most of them are subvertical but one (KBH02) is

subhorizontal. Core mapping of these boreholes recorded 'natural' fractures defined as fractures that have parted the core. Fractures that have not parted the core were recorded as 'sealed' fractures. *Stråhle /1989/.* Fractures induced by drilling were recorded as 'breaks'.

The amount of 'natural' fractures in the surface core boreholes is calculated to be in the order of 3.7 fractures/m for the subvertical boreholes and 3.5 fractures/m in the subhorizontal KBH02 (crush zones, >20 fractures/m, excluded). If we exclude all sections in the core with a fracture frequency >5 fractures/m (fracture zones and increased fracturing) we get 2.2 fractures/m as a mean value for all pre-investigation core boreholes.

To compare core mapping fracture data from surface boreholes, and tunnel mapping data all fractures (>1 m length) intersecting the tunnel axis have been recorded.

For the upper part of the tunnel, down to a level of about -400 m, the mean fracture frequency of natural fractures for a scan line parallel to the tunnel axis is estimated to be in the order of 0.5 fractures/m and below the -400 m level 0.4 fractures/m.

The mean fracture frequency in the hoist shaft is calculated to be in the order of 0.3 fractures/m along a vertical scan line.

The amount of 'natural' fractures in a drill core is normally overestimated due to the fact that many sealed fractures are broken during drilling and handling of the core. These fractures are sealed and tight in the tunnel. The number of 'open' fractures does not match very good between boreholes and tunnel.

According to *Munier /1995/* most fractures mapped at the Äspö HRL (all fractures >1 m in the tunnel except fractures in 'fracture zones') fall into four main clusters *(Figure 4-29).* Three are steep and strike NS, NNW and WNW; a fourth cluster is subhorizontal. *Hermansson /1995/* also describes a less pronounced NE set. The intensity of various clusters varies with the rock type. Fractures in fine-grained granite are typically steep and strike WNW, NS. The subhorizontal cluster is relatively weak *(Figure 4-29b).* The fracture array in Äspö diorite is similar to the array in fine-grained granite but the subhorizontal fractures are more frequent (section 1750-2000 m in the tunnel) in diorite *(Figure 4-29c).* Regarding Småland (Ävrö) granite, the same clusters are present as in Äspö diorite and fine-grained granite, but the clusters striking NNW are more intense in granite samples *(Figure 4-29d).* The fracture array of greenstone samples *(Figure 4-29e)* consists of a single steep cluster striking WNW, which is partly different from other rock types. *Figure 4-12* illustrates the rock distribution of depth in the tunnel.

Figure 4-30 illustrates the cluster orientation at depth. The dominating N-S cluster down to -200 m changes to NW-(WNW) at greater depth. Fracture orientation data from surface mapping in southern Äspö are presented in *Figure 4-31* for comparison.

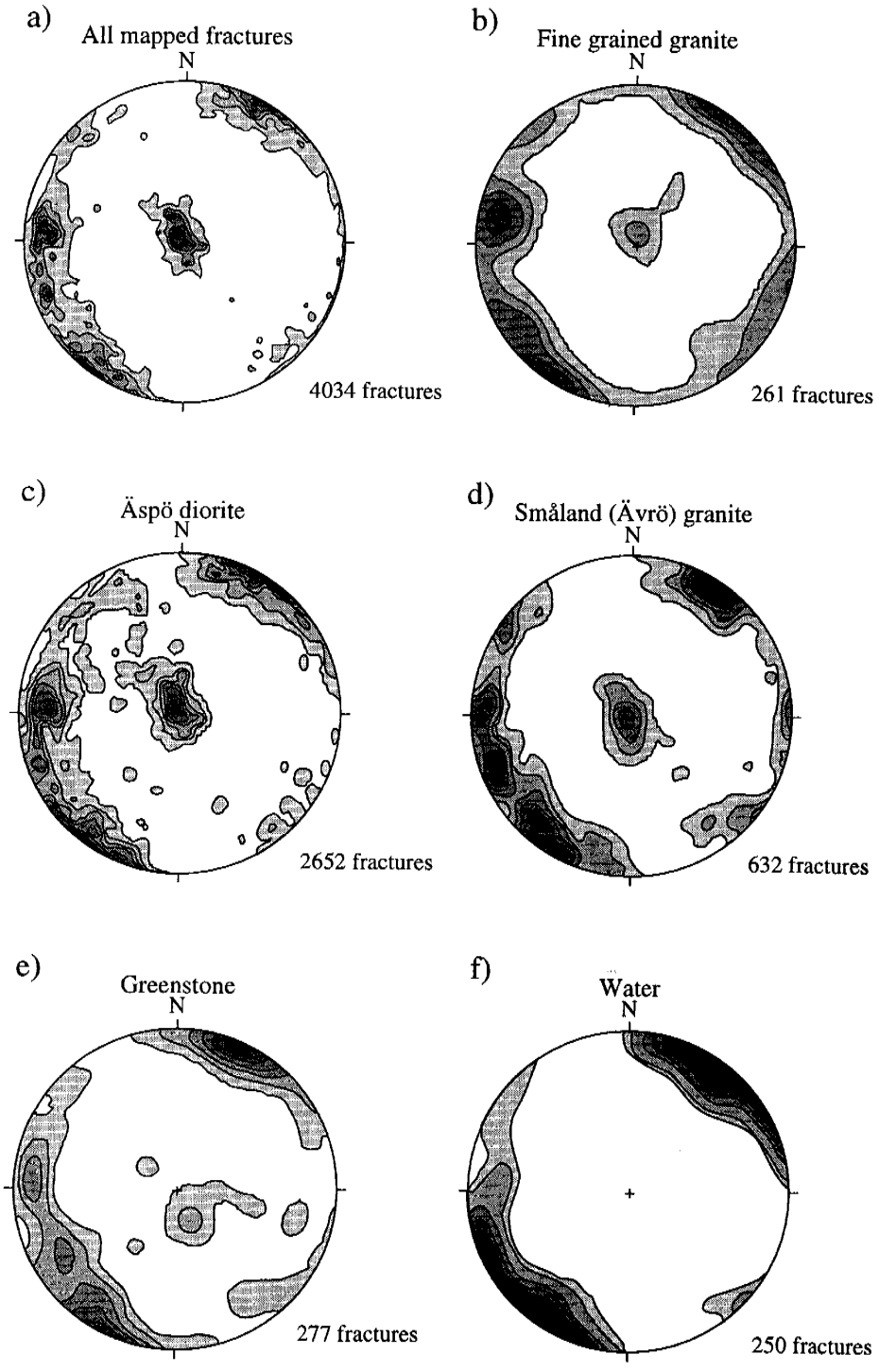

Figure 4-29. *Lower hemisphere, equal area projections of poles to fracture planes contoured according to Kamb. In (a) all fractures sampled in tunnel section 1600-2000 m are treated. The figures (b)-(e) were obtained by sub-dividing the sample represented in (a) into groups of different rock types /compiled from Munier and Hermansson, 1994/.*

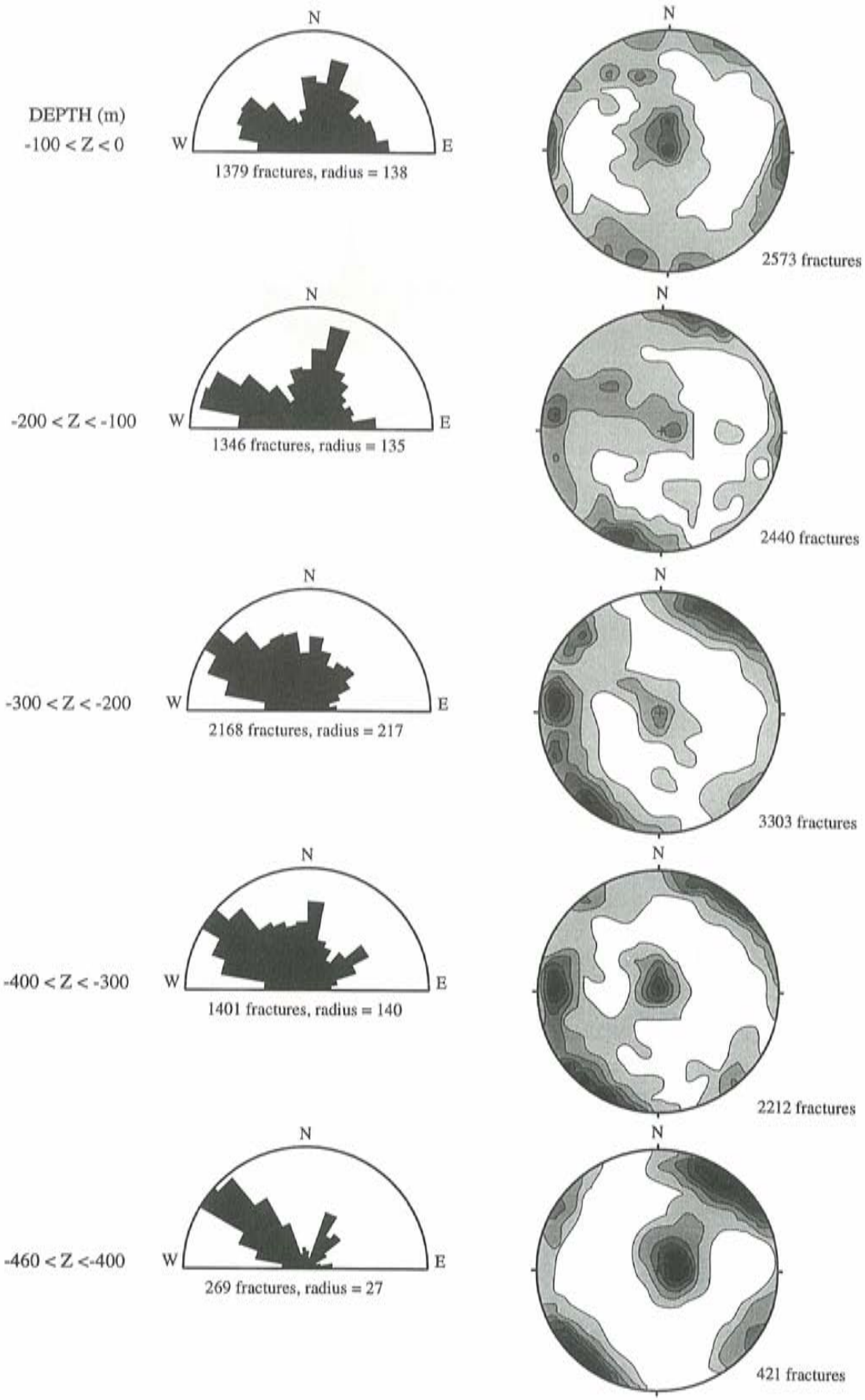

Figure 4-30. *Fracture orientation at different depths in the tunnel. Rosette diagrams for fractures with dips of 70 to 90°.*

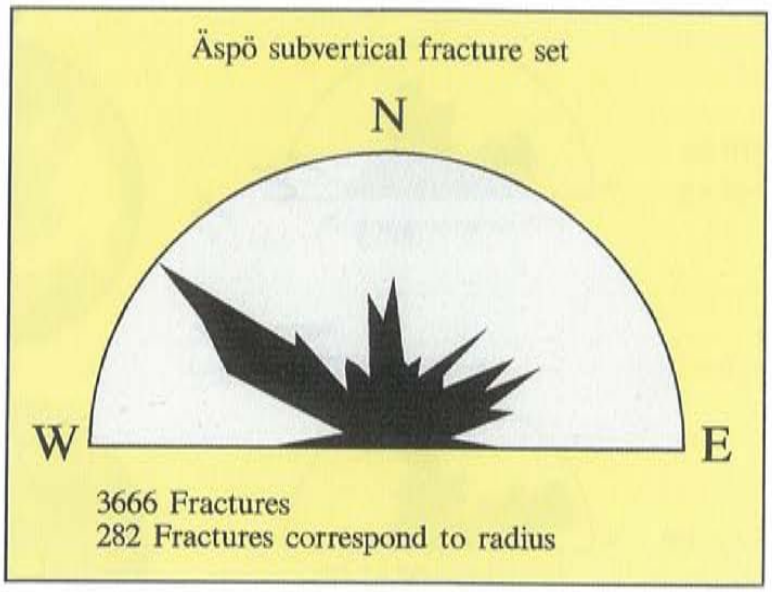

Figure 4-31. *Rosette diagram for all mapped outcrop fractures with dips 70-90 ° in southern Äspö. /Ericsson, 1988/.*

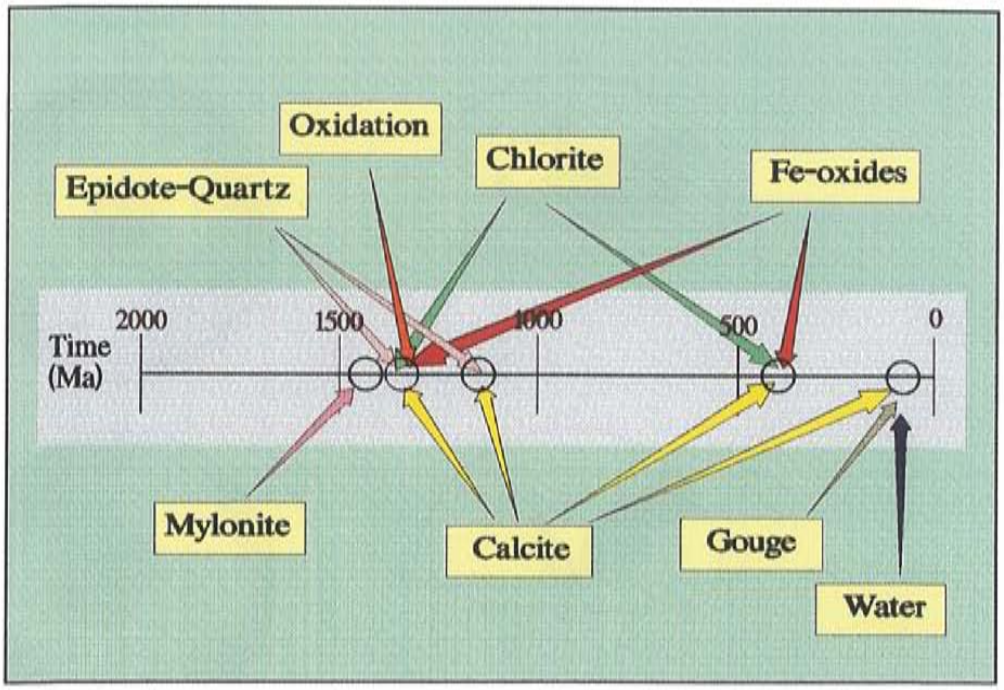

Figure 4-32. *Tentative chronological diagram illustrating main mineral filling episodes.*

Mapped fractures were separated into groups according to their mineralogy and related features */Munier and Hermansson, 1994/*. Fractures coated with epidote and quartz form a single cluster of steep fractures striking NNW. The assemblage of epidote-calcite-chlorite coats steep fractures striking NNW-WNW and forms a single cluster which is wide and diffuse due to the small sample size. Oxidation and red staining occurs on steep fractures striking NS, subhorizontal fractures, and is less obvious on steep fractures striking WNW. Calcite occurs predominantly on fracture surfaces striking WNW. Sub-horizontal and steep fractures striking NE are less prominent. A principal cluster of chlorite fractures is steep and strikes NS-NNE. The subhorizontal cluster and the steep cluster that strikes WNW are weaker. The array of fractures coated with the mineral assemblage chlorite-calcite can be represented by four sets. Three are steep and strike NS, NNW and WNW. A fourth set is subhorizontal. According to *Mazurek et al /1996/*, who investigated water-bearing fractures in the Äspö tunnel, there is no striking relation between fracture infills and fracture orientation.

The relative ages of mineral assemblages filling fractures have been determined by *Tullborg* using intersecting relationships and their formation temperature in *Munier et al /1988/, Munier /1993c/ and Tullborg /1989/*. A succession of fracture fillings of decreasing age has been proposed and includes: quartz, epidote, red staining, chlorite, Fe-oxy-hydroxides and calcite *(Figure 4-32)*. The arrays of mineralized fractures differ considerably with mineral infilling. Younger arrays are more complex due to the superposition of new fracture sets and reactivation of old sets */Munier, 1989, Munier, 1992, 1993c, 1995/*. Repeated and sequential reactivation of the same faults has been demonstrated by superposition of different mineral coatings, each of which displays a characteristic set of slickenside lines */Talbot and Munier, 1989, Mazurek et al, 1996/*.

Fault gouge and water have been treated as fracture fillings. The relative ages of these fractures cannot be deduced by the method applied to other mineral fillings. Most faults with gouge contain most other minerals and apparently have a long history of repeated and sequential reactivations. The relative simplicity of the gouge-filled fracture array implies that only the latest reactivations have been preserved, */Munier, 1995/*.

Fractures containing water have a wide range of orientations but two sets are evident on contoured stereograms; these are steep and strike WNW (most dominant) and NNW *(Figure 4-29f)*. Both sets are present in the arrays of mineralized fractures. It is therefore suggested that the present flow paths are inherited from older structures. Some of these appear to have been repeatedly reactivated ever since at least epidotic times.

Biased mean fracture trace lengths vary with mineralogy and range from 3.4 m (Fe) to 4.57 (quartz) in tunnel section 000-3300 m. */Munier, 1995/*. Pegmatite veins, quartz coated fractures and fractures with fault gouge, are significantly longer than fractures with other mineralogies at the 95% confidence level. The shortest fractures are those coated with Fe-oxides, fluorite, chlorite and calcite.

Mean trace length were calculated for fractures sampled in different rock types. The difference in mean values is not significant at the 95% confidence limit. That is, fracture trace lengths and lithology appear to be uncorrelated at the Äspö HRL.

Due to various sampling bias it is difficult to analyse trace lengths. Here, the difference in biased trace lengths, the relative trace lengths between subsets of the fracture samples is addressed as it is assumed that bias affects all used subsets equally.

Some of the main results of fracture evaluation performed by *Munier /1992, 1993c* and *1995/* are summarized below:

- Fractures sampled at Äspö HRL display an array that consists of four main sets. Three sets are steep and strike WNW, NNW and NNE; a fourth set is subhorizontal.

- The fracture arrays do not differ to a great degree between different rock types. One exception is greenstone that essentially displays steep fractures with WNW strikes.

- The most common fracture coatings are calcite, chlorite and a combination of both. Together, these coat 80% of the mapped fractures.

- Fractures trace lengths are log-normally distributed in all rock types.

- Fracture trace lengths do not vary with rock type.

- Fractures containing water generally have coatings enriched in epidote, quartz and Fe-oxides.

- Fractures with injected grout are steep, strike WNW and are generally longer than other fractures.

An overview of all fracture zones indication and large water-bearing fractures mapped in the tunnel is presented in *Figures 4-33--35.*

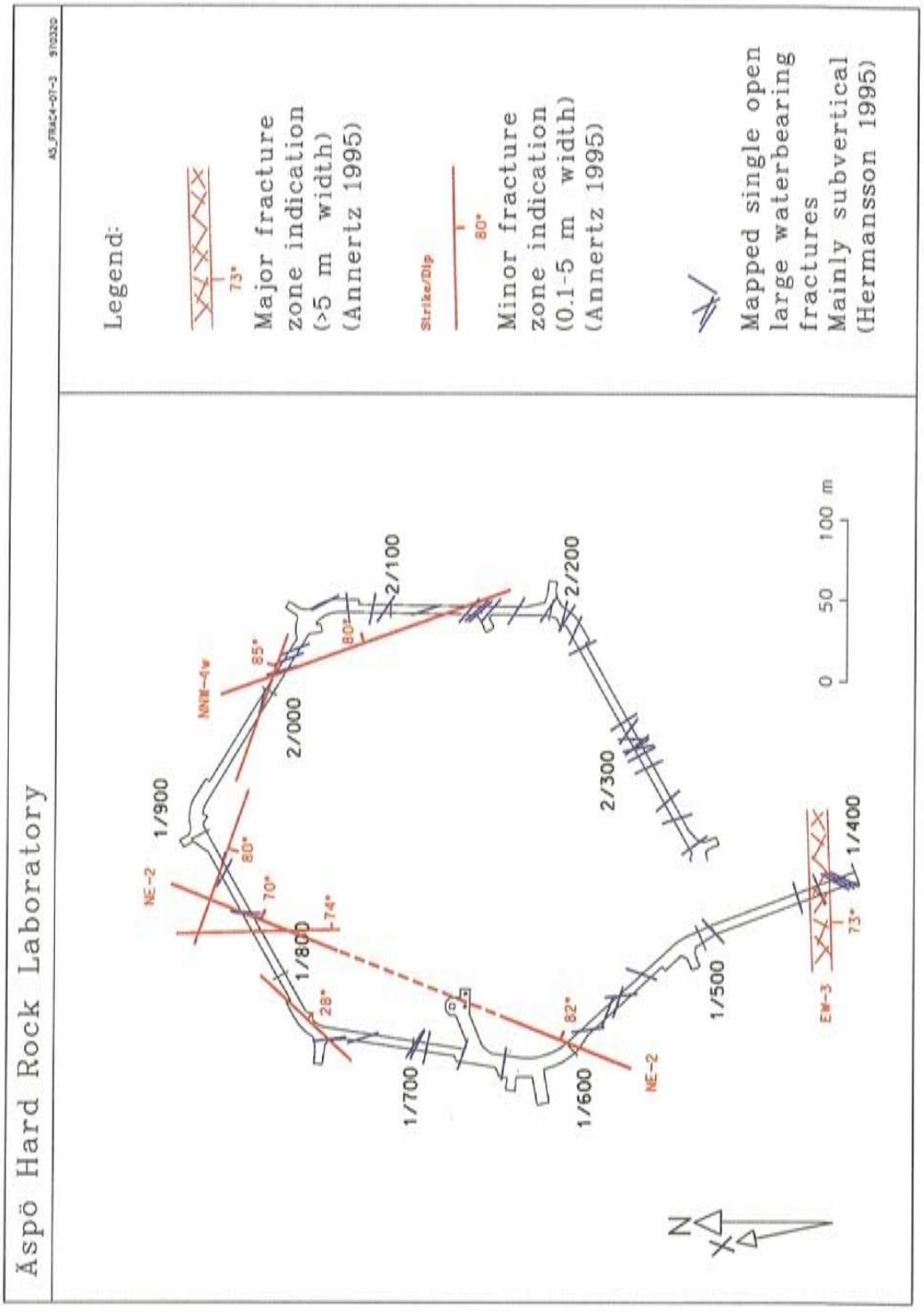

Figure 4-33. *Mapped fracture zones and single open large waterbearing fractures. The fractures are mainly subvertical.*

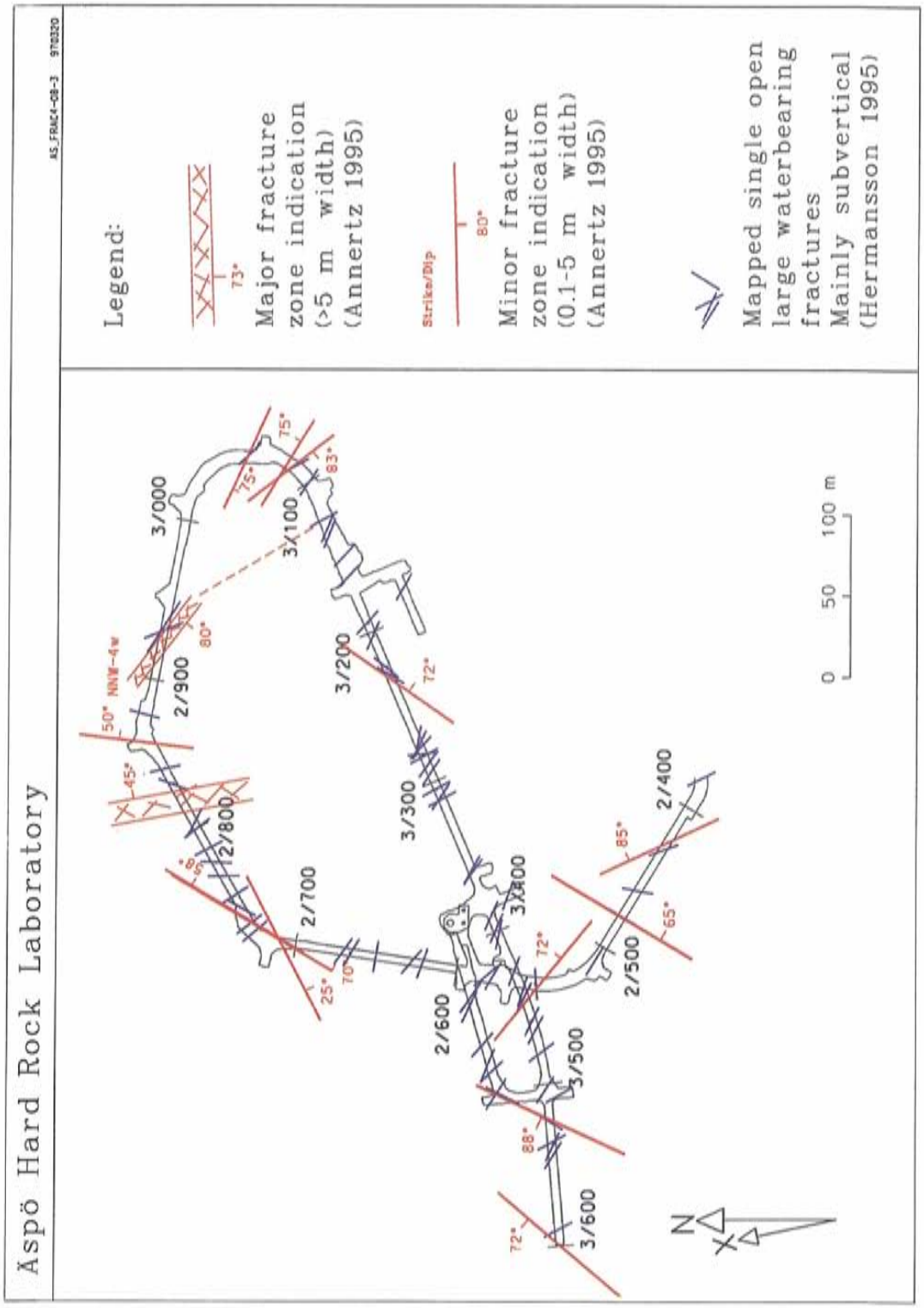

Figure 4-34. *Mapped fracture zones and single open large waterbearing fractures. The fractures are mainly subvertical.*

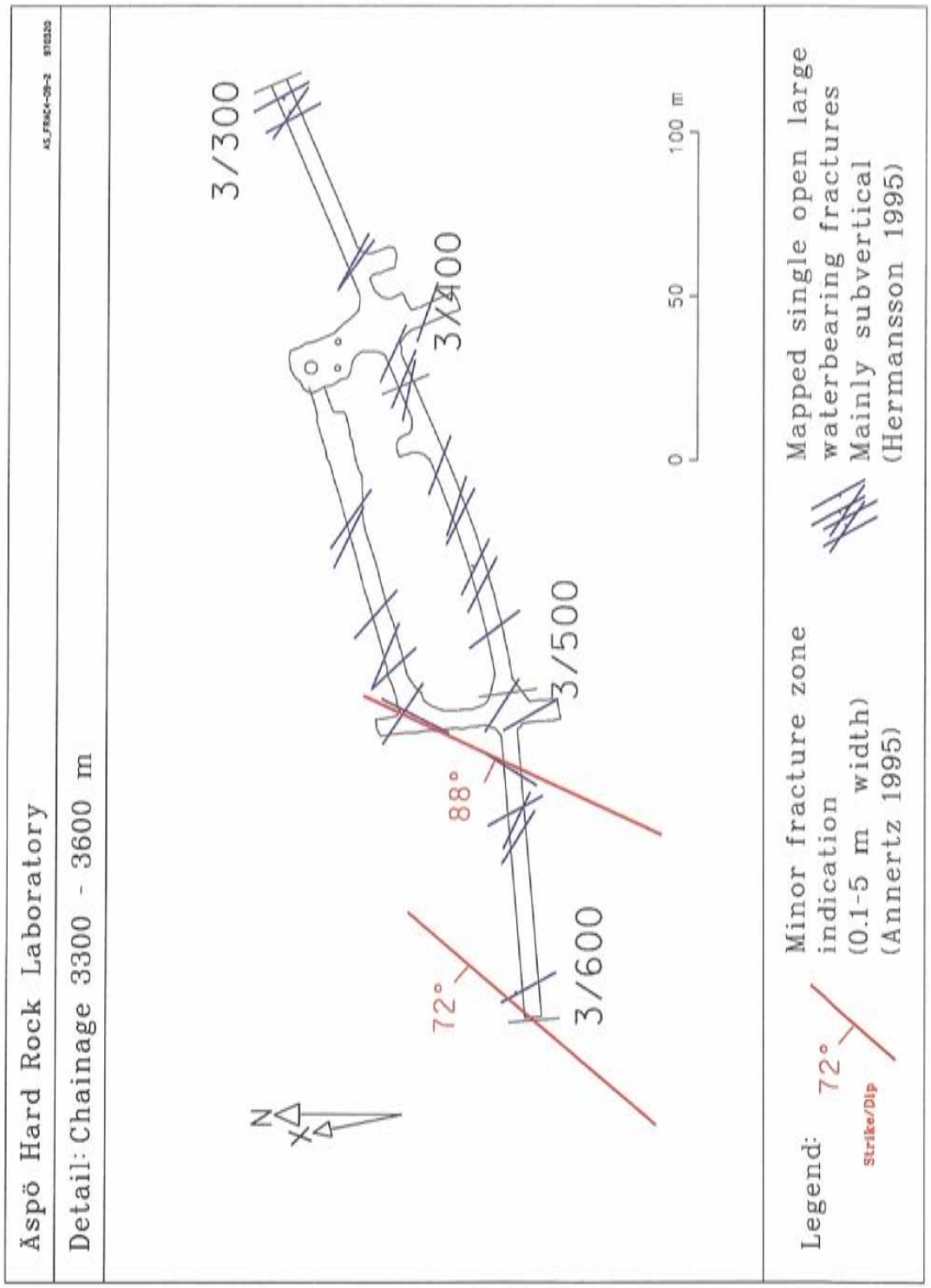

Figure 4-35. *Mapped fracture zones and single open large waterbearing fractures. The fractures are mainly subvertical.*